

FINAL REPORT

NASA CR-72821

APS-5357-R

N-71-24058

**DEVELOPMENT AND TESTING
OF LIQUID METAL FILM THICKNESS
INSTRUMENTATION**

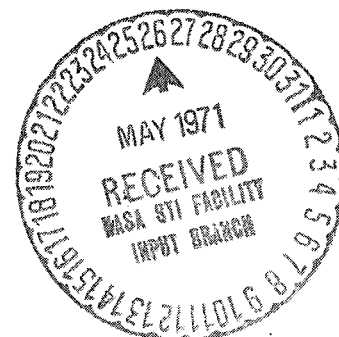
**CASE FILE
COPY**

PREPARED BY

**AIRESEARCH MANUFACTURING COMPANY OF ARIZONA
(A DIVISION OF THE GARRETT CORPORATION)**

**FOR
NATIONAL AERONAUTICS AND SPACE ADMINISTRATION**

**NASA-LEWIS RESEARCH CENTER
CONTRACT NAS3-10611
E. E. KEMPKE, PROGRAM MANAGER**





AIRESEARCH MANUFACTURING COMPANY OF ARIZONA
A DIVISION OF THE GARRETT CORPORATION

NOTICE

This report was prepared as an account of Government sponsored work. Neither the United States, nor the National Aeronautics and Space Administration (NASA), nor any person acting on behalf of NASA:

- (a) Makes any warranty or representation, expressed or implied, with respect to the accuracy, completeness, or usefulness of the information contained in this report, or that the use of any information, apparatus, method, or process disclosed in this report may not infringe privately owned rights; or
- (b) Assumes any liabilities with respect to the use of, or for damages resulting from the use of any information, apparatus, method or process disclosed in this report.

As used above, "person acting on behalf of NASA" includes any employee or contractor of NASA, or employee of such contractor, to the extent that such employee or contractor of NASA, or employee of such contractor prepares, disseminates, or provides access to, any information pursuant to this employment or contract with NASA, or his employment with such contractor.

Requests for copies of this report should be referred to

National Aeronautics and Space Administration
Office of Scientific and Technical Information
Attention: ATSS
Washington, D.C. 20546

FINAL REPORT

DEVELOPMENT AND TESTING OF LIQUID METAL
FILM THICKNESS INSTRUMENTATION

AIRESEARCH MANUFACTURING COMPANY OF ARIZONA
A DIVISION OF THE GARRETT CORPORATION

Phoenix, Arizona

Prepared for
NATIONAL AERONAUTICS AND SPACE ADMINISTRATION

February 1971

CONTRACT NAS 3-10611

NASA Lewis Research Center
Cleveland, Ohio
E. E. Kempke, Project Manager



AIResearch MANUFACTURING COMPANY OF ARIZONA
A DIVISION OF THE GARRETT CORPORATION

DEVELOPMENT AND TESTING OF LIQUID METAL FILM THICKNESS INSTRUMENTATION

ABSTRACT

An existing AiResearch transducer for measuring relative shaft motions, within a 600°F alkali-metal environment, was upgraded to measure potassium films at temperatures from 600° to 1000°F. Various combinations of transducer and journal materials, effects of coil and wire diameters, temperature, frequency, and holder material were investigated to pinpoint key parameters affecting probe sensitivity. Based on these studies, probes were fabricated, tested to 800°F, 14,000 rpm and found to have sensitivities from 0.040 to 0.099 v/mil, using a secondary-to-primary coil-turns ratio of 1.5:1. Al₂O₃ coil cores of 0.46-in. dia were wound with No. 36 Ni-clad silver wire coated with ceramicite insulation. This combination of materials provides stable resistivity with time at high temperatures.



TABLE OF CONTENTS

	<u>Page</u>
1. SUMMARY	1
2. INTRODUCTION	5
3. DISCUSSION OF RESULTS	8
3.1 Task I	10
3.2 Task II	12
3.3 Task III	16
3.4 Task IV	22
4. ANALYTICAL DISCUSSION	24
4.1 Basic Mathematical Model	25
4.1.1 Theory of Operation	25
4.2 Empirical Transducer Study	30
4.2.1 Summary of Basic Trends	30
4.2.2 Description of Static Bench Testing	32
4.2.3 Transducer Design and Fabrication	53
4.2.3.1 Details of Probe Design and Fabrication	60
4.2.3.2 Test Transducer Fabrication	66
4.2.3.3 Material Property Reference for Section 4.2	71
5. CALIBRATION TESTING	72
5.1 Calibration Rig Description	72
5.1.1 Detail Design Considerations	77
5.1.1.1 Calibration Test Rig Motor System Natural Frequencies	77
5.1.1.2 Gas Journal Bearing Design	79
5.1.1.3 Test Rotor Gas Thrust Bearing Design	83
5.1.1.4 Potassium Test Journal Design	84
5.1.2 Calibration Test Rig Thermal Analysis	90
5.2 Calibration Rig Testing and Results	96
5.2.1 Calibration with NaK Film	96
5.2.2 Calibration Testing with Potassium Film	102
5.2.2.1 Terminal Connection Problems	104
6. TURBODYNAMICS TESTING INCLUDING TURBINE AND LOOP MODIFICATIONS	107
6.1 Loop Modifications	107
6.2 Turbine Modifications	111
6.3 Turbine Testing	114



LIST OF FIGURES

	<u>Page</u>
1. Turbodynamic Test Rig Components	7
2. Film Thickness Probe Coil Configuration for 500 Hour Test	9
3. Potassium Film Thickness Probe Assembly	13
4. Potassium Film Thickness Calibration Rig	15
5. Test Journal Specimen	17
6. Coil Sensitivity Versus Temperature	18
7. Film-Thickness Transducer Coils	21
8. Dynamic Bearing Rig	23
9. One-Half of Ideal Film-Thickness Coil Configuration	28
10. Simulated Transducer Setup	33
11. Simulated Transducer Coil Core	34
12. Electrical Resistivity Versus Temperature	35
13. Sensitivity Versus Sleeve Resistivity for Various Sleeve Materials (Standard Transducer, No Window)	38
14. Sensitivity Versus Sleeve Resistivity for Various Sleeve Materials (Standard Transducer, with Window)	39
15. Voltage Output Versus Film Thickness Change for Ti C-10Cb Sleeve	40
16. Sensitivity Versus Film Resistivity for Brass Film (316 SS Window)	42
17. Sensitivity Versus Film Resistivity for Ti Film (316 SS Window)	43
18. Sensitivity Versus K Film Temperature for Several Sleeve Materials (No Window)	44
19. Calculated Sensitivity Versus K Film Temperature for Several Sleeve Materials (316 SS Window 0.010 In.)	45
20. Sensitivity Versus Primary Coil O.D., INCO X Sleeve	49
21. Sensitivity Versus Primary Coil O.D., INCO X Sleeve	50
22. Sensitivity Versus Turns Ratio, INCO X Sleeve	51
23. Sensitivity Versus Turns Ratio, INCO X Sleeve	52
24. Coil Window Configuration Window Thickness for Coil Size	54
25. Sensitivity - Configuration Curves Modified for Window Curvature (Coils M, G, P, S)	55
26. Sensitivity - Configuration Curves Modified for Window Curvature (Coils A, N, I, K)	56



LIST OF FIGURES (Contd)

	<u>Page</u>
29. Insulation Resistance Versus Temperature of No. 38	61
30. Nickel-Clad Silver Wire with "Ceramicite" Insulation	63
31. Coil Stability Study	64
32. Number of Hours at 1000°F Until First Coil-Resistance Change	65
33. Coil Configuration Drawing	67
34. Coil Balance Fixture with Two Coils in Place	68
35. Film-Thickness Transducer Coils	70
36. Liquid-Potassium Calibration Rig	73
37. Potassium Film Thickness Calibration Rig	74
38. Test Journal Specimen	76
39. Potassium Film Thickness Rig Critical Speed	78
40. Potassium Film Thickness Rig Bearing Loads	80
41. Potassium Film Thickness Rig Gas Bearing Geometry	81
42. Potassium Film Thickness Rig Single Pad Load Versus Deflection	82
43. Hydrostatic Thrust Bearing Load Versus Film Thickness	85
44. Crowning of Journal of Various Materials Due to Thermal and Centrifugal Loads	88
45. Temperature Distribution in Film Thickness Calibration Rig - 0.5 Pounds/Minute Cooling Flow	91
46. Temperature Distribution in Film Thickness Calibration Rig - 1.0 Pounds/Minute Cooling Flow	92
47. Temperature Distribution in Film Thickness Calibration Rig - 10.0 Pounds/Minute Cooling Flow	93
48. Journal Bearing Clearance Versus Distance Along Bearing	95
49. Coil Configuration Drawing	97
50. Film-Thickness Transducer Coils	98
51. TZM Sleeve 316 SS Housing NaK Film	100
52. Al ₂ O ₃ Sleeve 316 SS Housing NaK Film	101
53. Coil Sensitivity Versus Temperature	103
54. Sensitivity Versus Temperature and Speed	105
55. Methods of Coil Wire Termination	106
56. Dynamic Bearing Rig	112
57. Turbodynamic Bearing Test Components	113



LIST OF TABLES

	<u>Page</u>
1. Summary of Design Variable Investigation	2
2. Cross Sections of Coil Configurations	45
3. Sensitivity Data from September 4, 1968 to September 13, 1968	99



1. SUMMARY

The primary intent of this program was to upgrade an existing AiResearch-developed device for measuring the relative motion of a journal within a bearing in an alkali-metal system. The transducer set was upgraded to operate under the following conditions:

Lubricant	600° to 1000°F potassium
Turbine speeds	Up to 24,000 rpm
Resolution	0.00005 in.
Materials:	
Housings	Tungsten carbide (K-96) 316 stainless steel T-111 TiC-10Cb
Journals	TZM Tungsten carbide (K-96) TiC-10Cb

During Task I, the transducer was extensively examined using a computer-evaluated mathematic model and later utilizing test transducers and a bench test/calibration rig. Specific conclusions regarding design and operational variables are summarized in Table 1.

The final transducer reflected these conclusions in its design; assuring a reliable device of reasonably optimum sensitivity.

Task II involved design and development of test hardware subjecting candidate probe designs to the following requirements:

- (a) Temperature variation from ambient to 1000°F
- (b) Rotational speed from 0 to 25,000 rpm at temperature

TABLE I

SUMMARY OF DESIGN VARIABLE INVESTIGATION

Design Variable	Range of Investigation	Remarks and Conclusions
Coil Diameter	0.2 to 0.75 in.	Sensitivity improves with diameter with 0.5 in. the near optimum. Optimum secondary-to-primary turns ratio is between 2.1:1 to 2.5 to 1. Sensitivity is a weak function of coil diameter change with high resistivity films, diameter changes create large changes in sensitivity with low resistivity films.
Wire Diameter	0.003 to 0.005 in. (No. 36 to No. 40 ga.)	For high temperature (1000°F or over) resistance stability with time, No. 36 or greater wire diameter must be used. Smaller gage wire (No. 38 and No. 40) showed increased resistivity with time and local hot spotting and deterioration.
Temperature	600- to 1200°F	Number 36 wire wound probes, monitoring a TZM shaft display relatively constant sensitivity with temperature. Potassium increases in resistivity from 10.2 $\mu\text{ohm-cm}$ at 150°F to 55 $\mu\text{ohm-cm}$ at 1230°F.
Applied Frequency	10 to 1000 kHz	Most testing done with 20 kHz. No pronounced effect on sensitivity with frequency variation.
Window Material and Thickness	T-111, SS-316, WC, TiC-10Cb 0.010- to 0.005 in.	Windows were fabricated from 316SST, K-96, T-111 TiC-10Cb all having nominally 0.011 in. thickness. Increasing window thickness reduces sensitivity. The effect is more pronounced with low resistivity films than with high ones.
Sleeve or Journal Material	TZM (6.7 $\mu\text{ohm-cm}$) Ti-6Al-4V (176 $\mu\text{-ohm-cm}$) Insulating sleeves (Al_2O_3) also T-111, TiC-10Cb, Inco X	Within the sample temperature range, (200- to 1100°F) definite trends exist, mostly based on the basic film-to-sleeve resistivity ratio. <u>Low film-to-sleeve resistivity ratios:</u> Sensitivity a function of film thickness changes only <u>High film-to-sleeve resistivity ratios:</u> Sensitivity a function of shaft motions High resistivity sleeve materials (greater than 70 $\mu\text{ohm-cm}$) contribute to 50 percent or less to sensitivity. Increasing resistivity ratio lessens shaft material contribution to sensitivity.



- (c) Measurement of motion of the shaft in two mutually perpendicular planes to an accuracy of ± 0.00005 in.
- (d) Applicability to refractory-alloy material combinations

Final probes designs were calibrated with this equipment to a sensitivity range of 0.040 to 0.099 volts per mil of shaft displacement.

Task III saw the fabrication of four transducer sets for the 500 hr turbodynamic test. The finished coils employed a 1.5:1 secondary-to-primary coil turn ratio, winding No. 36 Ni-clad silver wire with ceramicite insulation, 225 and 150 turns, respectively, around a 90 percent Al_2O_3 core. Approximately 3200 hr total of resistance stability testing at 1000°F temperature indicated that either No. 36 ceramic-insulated Ni-clad silver wire or No. 36 aluminum wire, Al_2O_3 insulated, were sufficiently reliable at the elevated temperatures.

The coil pairs were then balanced electrically at 1000°F temperature by selective turn removal until a null voltage resulted between the two-series-opposed connected secondary coils. The balanced probe sets were then mounted into shielding holders and fitted with connectors for installation and calibration within the turbodynamic test loop.

Task IV was to have been concluded by a milestone-type 500 hr endurance test at 1000°F potassium temperatures. The loop was completely inspected and all questionable components rebuilt or replaced. Portions of the turbodynamic turbine and bearing rig were modified to improve probe reading reliability and accessibility. Four sets of probes were installed and calibrated in the unit. Full steady state boiling conditions were achieved in the loop and testing was begun;



AIRESEARCH MANUFACTURING COMPANY OF ARIZONA
A DIVISION OF THE GARRETT CORPORATION

however, several blockages were experienced in various loop sub-circuits and repeated attempts to clear the lines were unsuccessful. At this point, further tests were deferred by the NASA program manager.



2. INTRODUCTION

The NASA-Lewis Research Center is currently investigating the dynamic characteristics of alkali-liquid-metal-lubricated fluid-film bearings for application in space power turbomachinery. Long life and high reliability in potassium Rankine cycle turbomachinery ultimately depends upon the development of stable rotor bearing systems.

Such development in turn depends upon instrumentation capable of monitoring bearing film thicknesses and shaft motions within a high temperature, alkali metal environment.

Accordingly, this program was intended to design, fabricate, and test a film thickness measuring device for eventual application in space power conversion turbomachinery. The specific requirements of the program involved upgrading an existant AiResearch transducer device such that it would be capable of satisfying the following requirements:

- (a) Operational life of 2000 hr in ambient or liquid potassium environments from 600- to 1000°F
- (b) Frequency response: 0 to 2000 Hz
- (c) Accuracy of measurement: ± 0.000050 in. for film changes up to 0.005 in. at shaft rotational speeds up to 24,000 rpm or ± 1 percent for film changes up to 0.050 in.
- (d) Precision: The calibration of any one instrument within 5 percent of that of any other instrument
- (e) Zero shift: Zero shift with temperature not exceeding 0.01 percent of full scale per degree



AIRESEARCH MANUFACTURING COMPANY OF ARIZONA
A DIVISION OF THE GARRETT CORPORATION

Additional considerations such as compatibility with high strength journal materials, space environmental requirements (high vacuum), and maintainability were to be accounted for.

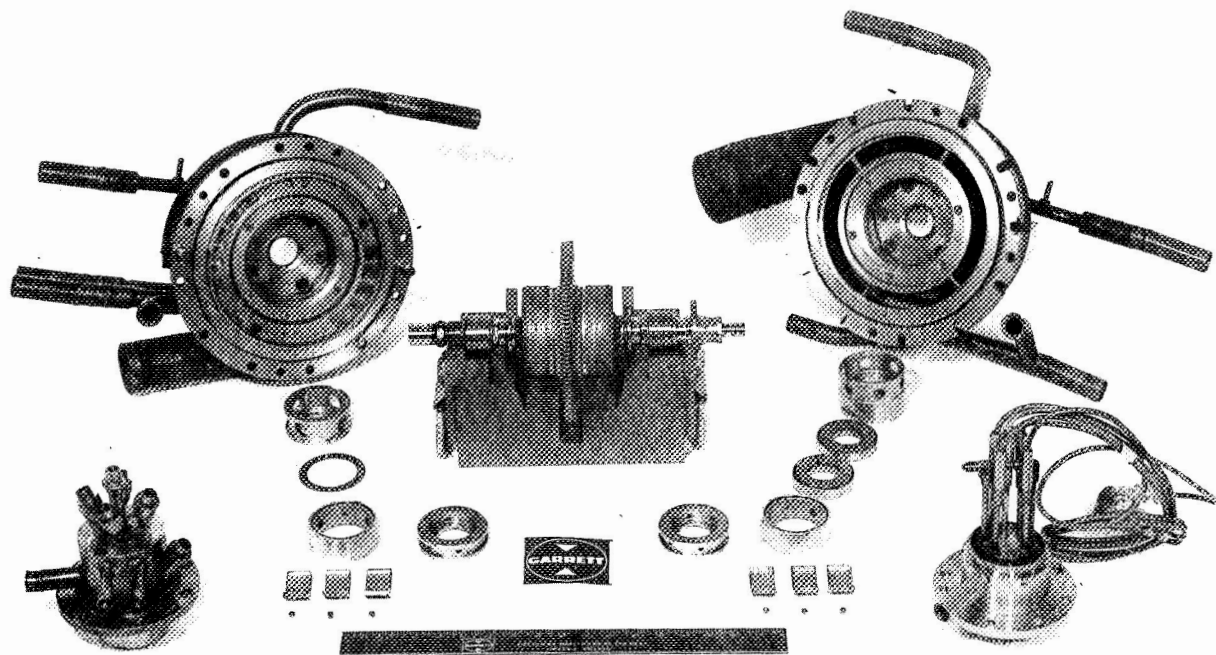
Several geometries, primary-to-secondary coil wire turns ratios, coil-wire and core material variations were to be explored analytically and experimentally in order to achieve a reasonably optimum final configuration.

AiResearch background leading to the current work began in 1964 during the USAF/AEC SNAP 50/SPUR program with the need for a dynamic film-thickness measuring device. This device was used to monitor shaft motions in the 600°F potassium working fluid turbine/bearing test unit shown in Figure 1. Operating this device over a three year period enabled accumulation of extremely useful dynamic performance data on potassium lubricated bearings. Monitoring rotor excursion during all modes of operation could not have been obtained from component inspection before and after the test, or other indirect measurements during the test such as vibration, pressure perturbations, flow rate variations, etc.

Analytical work during the present program was assisted by an AiResearch-modified relaxation solution technique originated by C.V. Dodd in a paper entitled "Solution to Electromagnetic Induction Problems," Oak Ridge National Laboratory (ORNL) Report TM-1842, June 1967.



AIRESEARCH MANUFACTURING COMPANY OF ARIZONA
A DIVISION OF THE GARRETT CORPORATION



TURBODYNAMIC BEARING TEST
COMPONENTS

FIGURE 1



3. DISCUSSION OF RESULTS

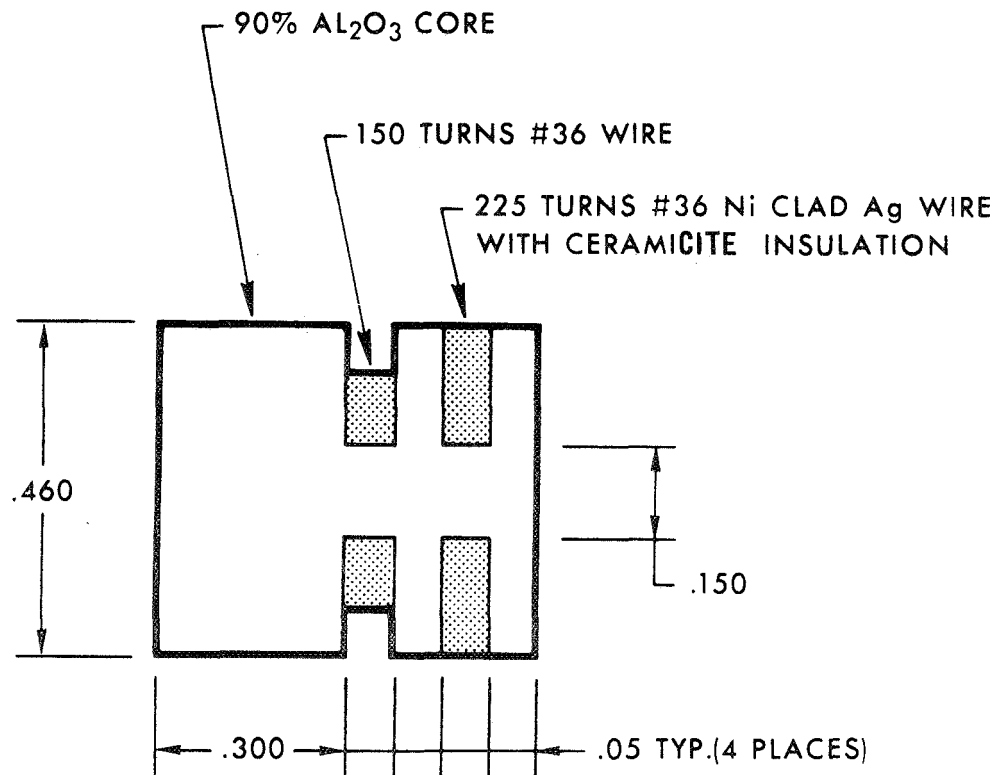
The objective of this program has been to upgrade an existing AiResearch-developed device for measuring the relative motion of a journal within a bearing in an alkali-metal system. The existing device was developed to monitor shaft excursion in a 24,000-rpm 600°F potassium-lubricated-bearing test turbine to a resolution of 0.0001 in. The program has required that the instrument be upgraded to operate under the following conditions:

Lubricant	600 to 1000°F potassium
Turbine speeds	Up to 24,000 rpm
Resolution	0.00005 in.
Materials:	
Housings	Tungsten carbide (K-96) 316 stainless steel T-111 TiC-10Cb
Journals	TZM Tungsten carbide (K-96) TiC-10Cb

The final instrument configuration (Figure 2) is of the eddy-current transducer type. When a coil of wire carrying an alternating current is placed near a conducting material, eddy currents are generated so as to oppose the exciting current in the coil and cause a change in the magnetic field. This change in the magnetic field which is measured by a second coil placed in the field, is a function of the conductivity of the material near the coil, the distance between the material and the coil, and the geometry of the configuration.



AIRESEARCH MANUFACTURING COMPANY OF ARIZONA
A DIVISION OF THE GARRETT CORPORATION



FILM THICKNESS PROBE COIL CONFIGURATION FOR 500 HOUR TEST

FIGURE 2



To facilitate development of the device the program was broken into four basic tasks:

- Task I - Film-Thickness Transducer Analysis
- Task II - Film-Thickness Transducer Bench Testing
- Task III - Final Transducer Fabrication
- Task IV - 500-Hour Potassium Test (including turbodynamic test-turbine and test-loop modification)

3.1 Task I

An existing computer program was modified and checked out for analyzing candidate transducer configurations. The program is based on electromagnetic analysis techniques discussed by C.V. Dodd in a paper entitled "Solution to Electromagnetic Induction Problems," Oak Ridge National Laboratory (ORNL) Report TM-1842, June 1967. Transducer design variables over the ranges shown below were to be analyzed with the intent of identifying the combination providing optimum sensitivity:

TRANSDUCER DESIGN VARIABLES

Coil diameter:	0.2 to 0.75 in.
Wire diameter:	0.003 to 0.005 in.
Temperature:	600 to 1000°F
Applied frequency:	10^4 to 10^6 Hz
Window material:	T-111, SS-316, WC, TiC-10Cb
Window thickness:	0.010 to 0.050 in.
Shaft, bearing and journal or sleeve material:	WC, TiC-10Cb, TZM
Bearing journal or sleeve thickness:	0.1 to 0.5 in.
Fluid:	Potassium liquid and vapor



Unfortunately, extremely long computer run times at each film thickness point precluded extensive analysis. Therefore, the remainder of Task I was supplemented with experimental tests which served to point out the optimum configuration shown in Figure 2. With regard to the design parameters in Table 2 the following trends were observed:

- (a) Coil Diameter and Configuration - An optimized coil configuration was found to be one with a secondary to primary turn ratio of 2:1 or 2.5:1 regardless of the film resistivity. The sensitivity was found to be a weak function of secondary and primary coil diameter changes with a high resistivity film. With a low-resistivity film, however, the sensitivity was found to vary about 10:1 from 0.250 in. diameter to 0.500 in. diameter favoring the larger diameters.
- (b) Wire Diameter - Due simply to durability at temperature, No. 36 wire size was chosen. During extended 1000°F temperature runs, No. 38 and No. 40 wire sizes indicated hot spots and an increased resistivity with time.
- (c) Temperature Effects - Between 600- and 1200°F, transducer sensitivity appeared to be relatively constant when monitoring a TZM shaft.
- (d) Applied Frequency - Since the sensing coils are wired in series opposition and the induced voltages are relative, no pronounced effect of frequency on sensitivity was observed. Most testing was done with an applied frequency of 20 kHz.
- (e) Window Material and Thickness - Final window configurations are nominally 0.011 in. thick and fabricated from 316SST, K-96, T-111 and TiC-10Cb. With a low-resistivity film, an increase in window thickness has a greater effect in reducing the sensitivity than with a high resistivity film.



- (f) Sleeve Material - Data was taken for sleeve resistivities from TZM at 6.7 $\mu\text{ohm-cm}$ to Ti 6Al 4V at 176 $\mu\text{ohm-cm}$. Insulating sleeves were also examined along with T-111, TiC-10Cb and Inco X. Within the temperature range examined, (200 to 1100°F), potassium resistivity varies from 10.2- to 52.0 $\mu\text{ohm-cm}$. Definite sensitivity trends were observed--most based on the film-to-sleeve resistivity ratio.

At low film-to-sleeve electrical resistivity ratios, sensitivity is primarily a function of film thickness changes only. At high film-to-sleeve resistivity ratios, the sensitivity is primarily a function of the sleeve motion with some decrease in sensitivity from coil shielding by the film. Thus, with sleeve resistivities greater than 70 $\mu\text{ohm-cm}$, the sleeve contributes approximately 50 percent or less to the overall sensitivity with high-resistivity films (i.e., high-temperature K) but plays a minor role in affecting sensitivity with low-resistivity films (i.e., low-temperature K).

Based on Task I analysis, probe fabrication and calibration was accomplished under Tasks II and III using the basic probe assembly shown in Figure 3.

3.2 Task II

This task saw the development of transducer hardware and a calibration test rig used to test the transducers under the following operational requirements.

- (a) Temperature variation from ambient to 1000°F
- (b) Rotational speeds from 0 to 25,000 rpm



APS-5357-R
Page 13



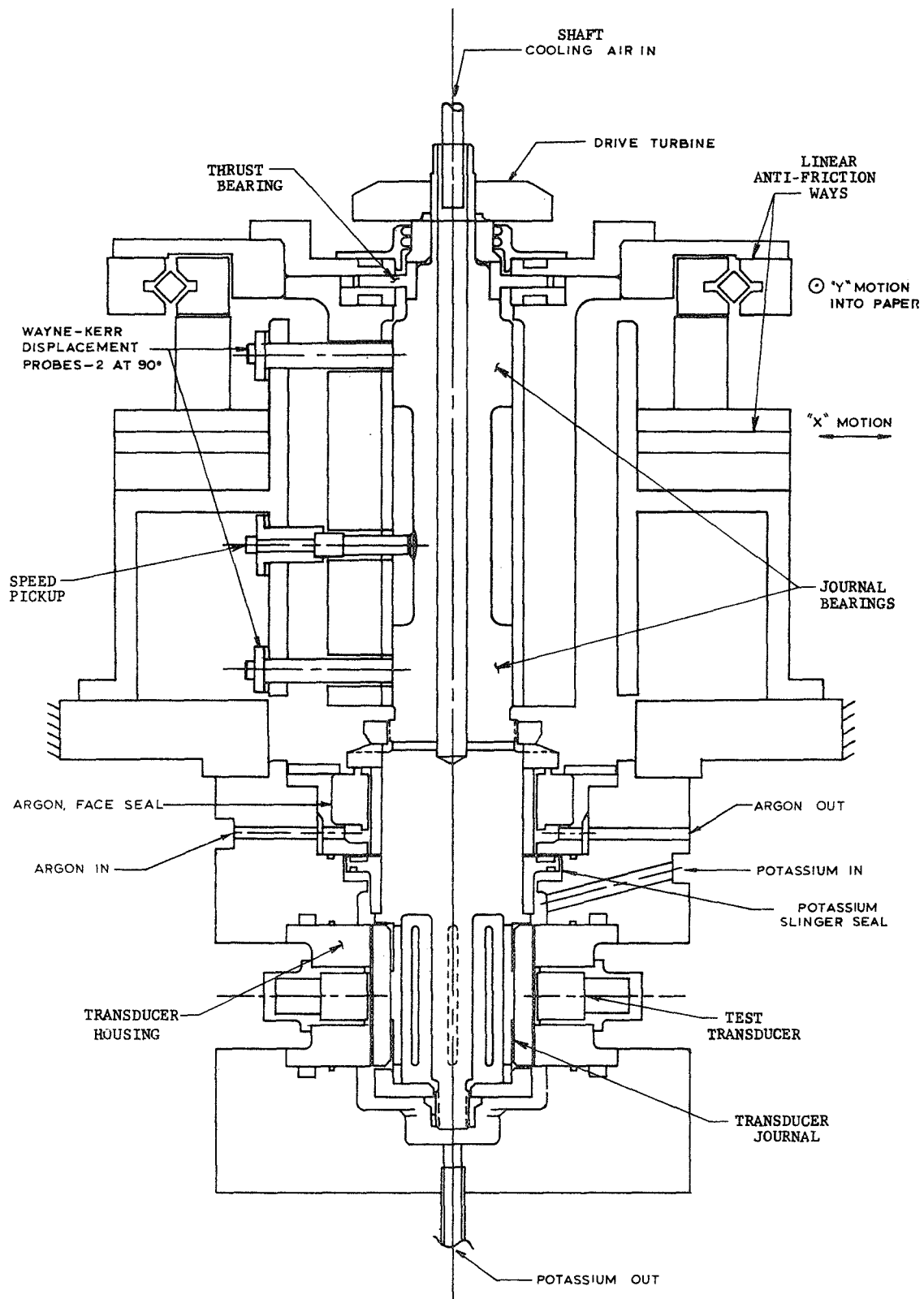
- (c) Measurement of motion of the shaft in two mutually perpendicular planes to an accuracy of ± 0.00005 in.
- (d) Applicability to refractory-alloy material combinations

The rig (Figure 4) consists of a precision rotating spindle mounted in pneumostatic journal bearings. The shaft penetrates the potassium-filled-probe test housing through a combination mechanical face seal and dynamic seal with an argon buffer between. The rotating spindle/bearing assembly is mounted to the base plate through a pair of mutually perpendicular, linear antifriction rollerways. The shaft is driven by a plant-air-activated air turbine.

Radial movement of the precision spindle is measured by two pairs of high-precision capacitance probes mounted in each air bearing. These capacitance probes are calibrated external to the rig with a high-precision absolute calibrating device. Manual movement of the spindle is controlled by precision micrometer heads direct reading to 0.00001 in.

The film-thickness-probe test head consists of a cylinder of the particular housing material of interest, containing the eddy-current coil assemblies and sandwiched between two housings of a material of similar thermal expansion. The assembly is not seal-welded but is statically sealed with metal sealing rings. This design feature allows for the greatest degree of versatility in testing different housing (refractory) materials, various coil configurations, and required window configurations.

The portion of the rotating spindle upon which motion is to be sensed is separate from the basic spindle. It is mounted to the spindle through a slotted shaft arrangement intended to compensate for differences in thermal expansion and yet provide positive register



PREPARED	JFG	10-67	POTASSIUM FILM THICKNESS CALIBRATION RIG	FIGURE — 4 —
WRITTEN				
APPROVED				
			AirResearch Manufacturing Company of Arizona	

FORM P793A-1



with the specimen. This device is shown schematically in Figure 5. The test-coil housing is surrounded by a resistance clam-shell-type heater to provide the required ambient operating temperature. The heater enclosure also serves as a light vacuum or inert-gas chamber to handle potassium leakage and to minimize oxidation in the high-temperature region.

Solid, one-piece instrumentation housings were fabricated for the calibration rig using the following test materials--316 SST, K-96, T-111 and TiC-10Cb. Also tests were conducted using TZM, Al_2O_3 and TiC-10Cb sleeve material.

Eventually, the calibration rig was utilized to calibrate a set of four final design probes for use during endurance testing.

Coil pair sensitivity values of 0.090 volts/mil were recorded for the TZM sleeve and a sensitivity range of 0.090- to 0.099 volts/mil was observed for an Al_2O_3 sleeve using NaK as the fluid film.

Rotational testing at room temperature revealed constant sensitivity with speed.

Calibration of the four probes for the endurance run revealed the sensitivities shown in Figure 6.

3.3 Task III

This task required the design and fabrication of film-thickness probes for use in the 500 hr endurance test. The final probe design employs a 1.5 secondary-to-primary coil turns ratio and was shown in Figure 2. Geometry and dimension evolved from experimental and analytical optimization studies while high temperature resistance stability tests dictated the optimum combination of coil wire material,

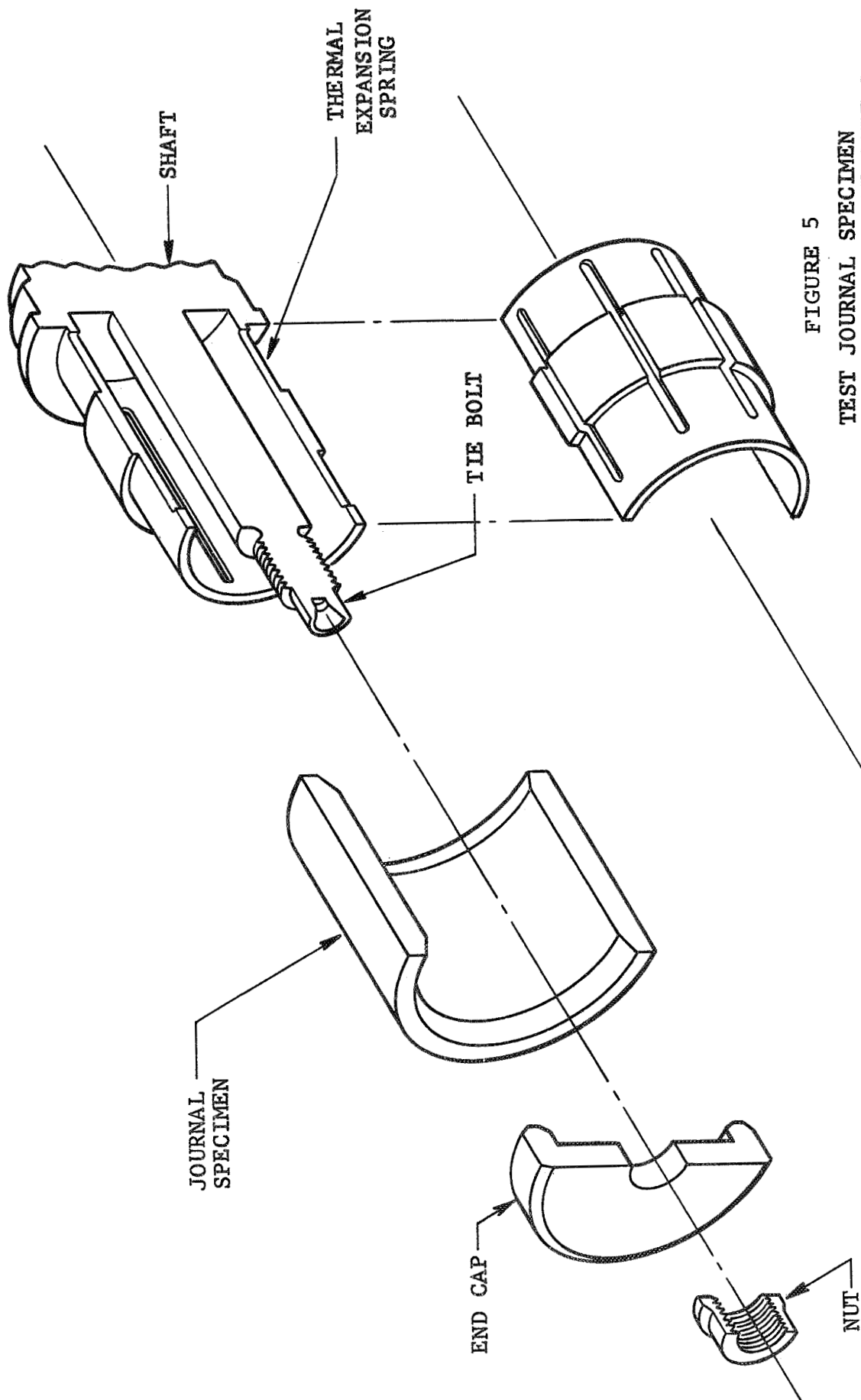
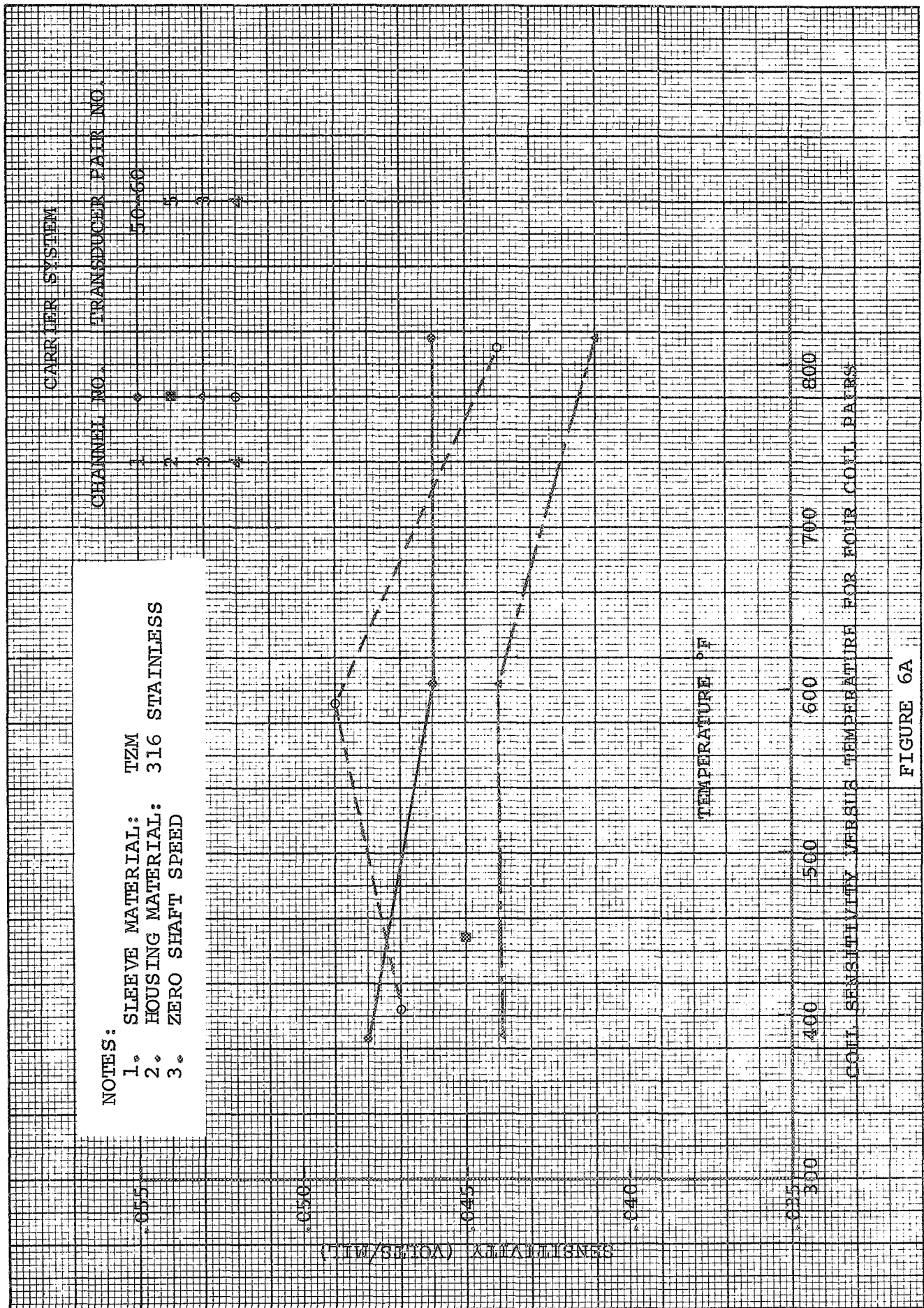
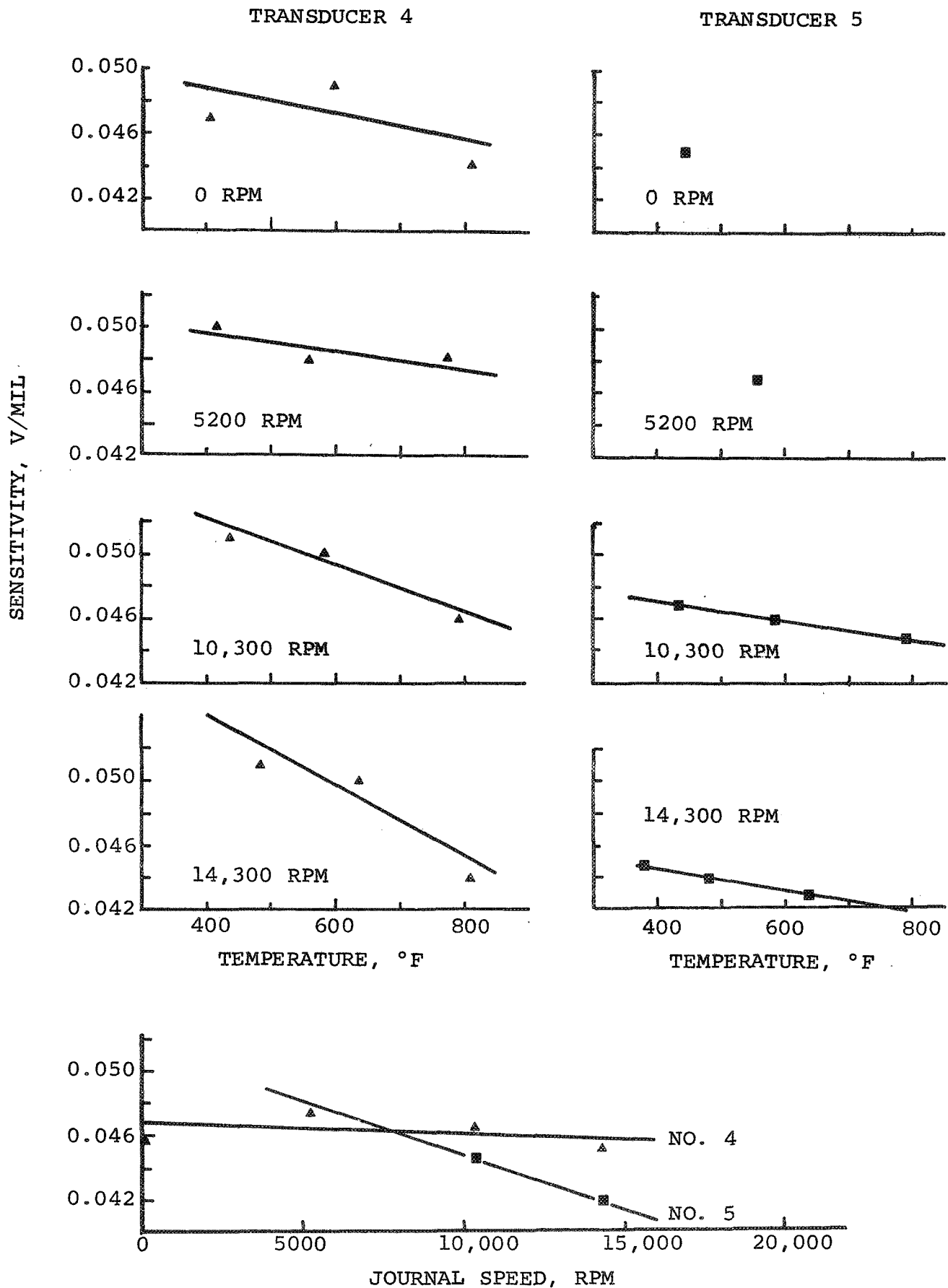


FIGURE 5
TEST JOURNAL SPECIMEN
THERMAL EXPANSION COMPENSATING
DEVICE





TRANSDUCER SENSITIVITY VS TEMPERATURE AND SPEED

FIGURE 6B



gauge, insulation, potting compound and connector design. Number 36 aluminum oxide-coated aluminum wire or Ceramicite-insulated Ni-clad wire both offer high-temperature resistance stability (during 2200 hr of testing at 1000°F) with the aluminum wire slightly more amenable to high temperature conditions. Aluminum, however, may have a tendency to "outgas" in the hard vacuum of space. Therefore all transducers were wound with the Ni-clad silver wire using a 90 percent Al_2O_3 core potted with PBX ceramic cement.

A typical brace of transducers is fabricated by winding the ground Al_2O_3 core with the appropriate number of wire turns then connecting them as follows:

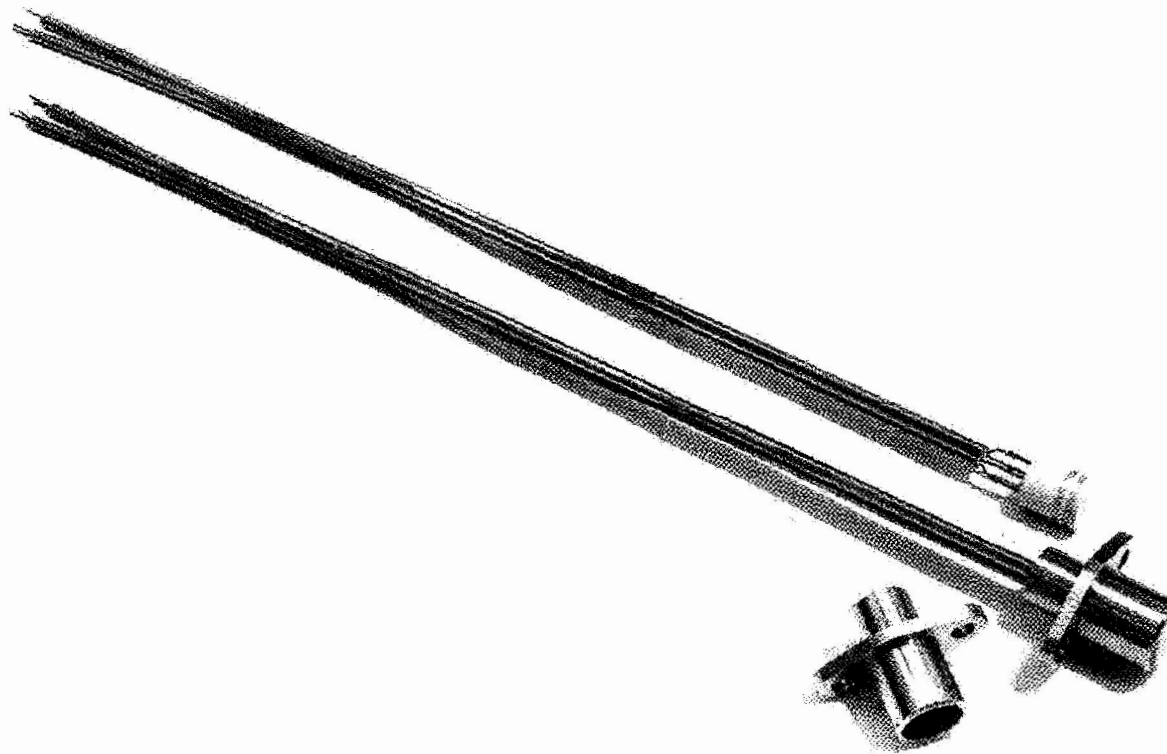
- o 20 kHz primary excitor
- o Primary coils in series
- o Secondary coils in series opposition
- o Digital voltmeter reading net secondary output

The coils are temperature cycled and balanced by selectively removing turns to bring about a null secondary voltage reading. When suitably balanced the coils are placed in holder-lead wire assemblies (Figure 7) and final-calibrated.

Coil sensitivities in the range of 0.090 to 0.10 volts/mil were observed using this process. All coil sets, including the 4 sets calibrated and installed in the turbodynamic loop were fabricated in this manner.



AIRESEARCH MANUFACTURING COMPANY OF ARIZONA
A DIVISION OF THE GARRETT CORPORATION



FILM THICKNESS TRANSDUCER COILS WITH HOLDERS
AND LEAD WIRES

FIGURE 7



3.4 Task IV

The objective of Task IV was a 500-hr verification test of the final film thickness probe configuration resulting from Tasks I, II and III. Part of Task IV involved refurbishing an existant potassium test loop using a 24,000 rpm supersonic potassium bearing test turbine (Figure 8) developed in 1963-64 on the USAF/AEC SNAP 50/SPUR program.

The loop had accumulated approximately 3000 hr with vapor temperatures up to 1350°F and bearing lubricant temperatures up to 600°F. All questionable loop components were replaced and/or rebuilt to provide maximum reliability during the 500 hr test.

Unfortunately, the 500 hr test was not completed although four transducer coil pairs were fabricated, calibrated and installed in the rig. Steady state boiling conditions were established in the loop but soon thereafter the hot trap line and bearing feed lines became plugged and repeated attempts to unplug them were in vain. Shortage of funds affected the cancellation of further testing at this point.

Suitable probes were analyzed, designed and fabricated and lack of a milestone-type test, while unfortunate, should not detract from the significance of these advances.



AIRESEARCH MANUFACTURING COMPANY OF ARIZONA
A DIVISION OF THE GARRETT CORPORATION

DYNAMIC BEARING RIG

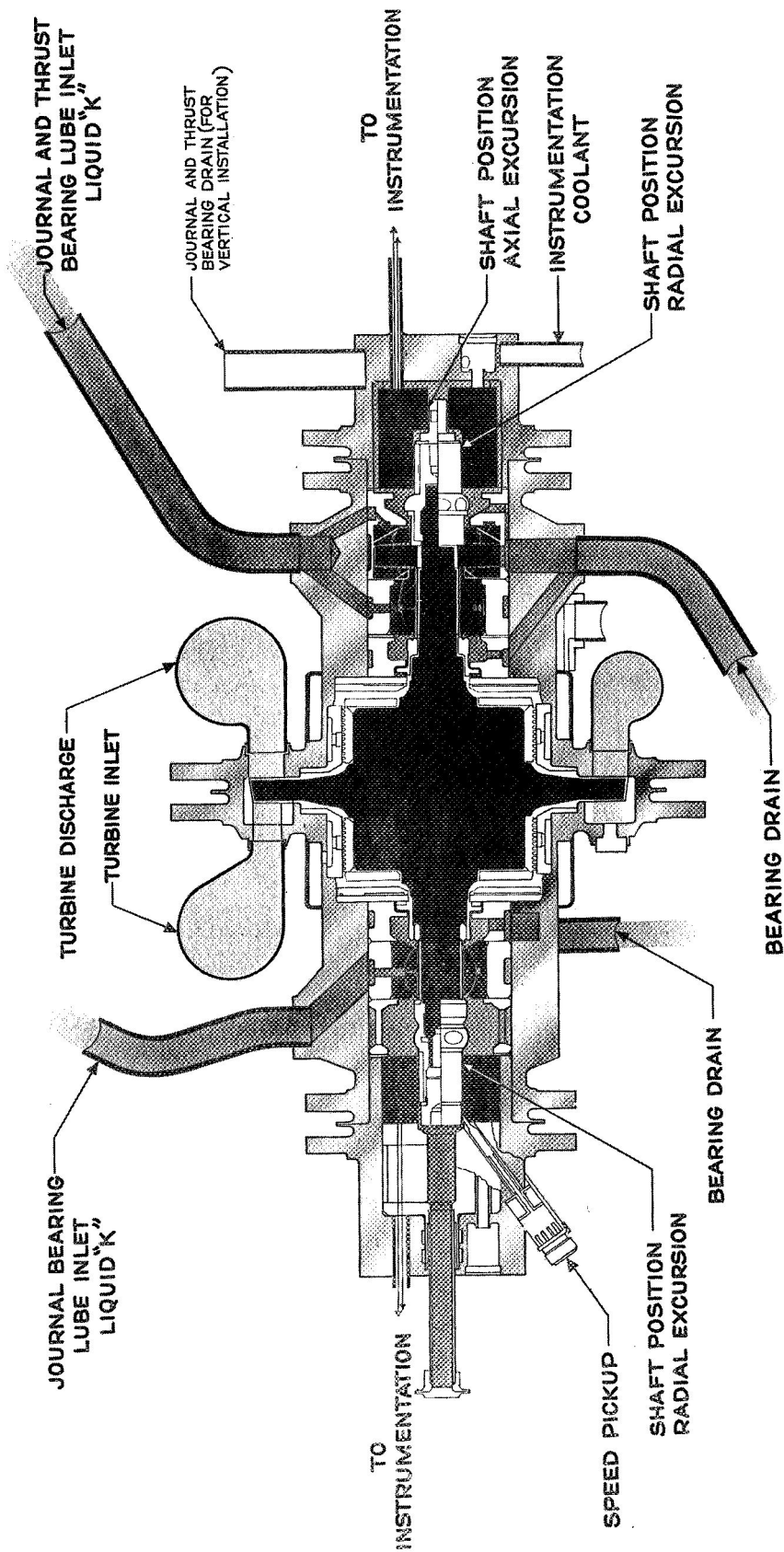


FIGURE 8



4. ANALYTICAL DISCUSSION

During the preliminary design phase of the program, it was decided by NASA to undergo an extensive analytical study of transducer design variables. It was felt that this approach might speed the process of finding the optimum combination of materials and geometry without incurring the time and expense of experimental work. Using computer techniques it would be possible to examine a far wider range of design variables than would be possible with fabricate-then-test techniques.

Therefore, Task I of the program was defined to explore the sensitivity of the transducer device expressed in volts of probe output per microinch of thickness change of the potassium film. Sensitivity variation as a function of the following design parameters was to be explored:

<u>Design Parameters</u>	<u>Range of Investigation</u>
Coil diameter:	0.2 to 0.75 in.
Wire diameter:	0.003 to 0.005 in.
Temperature:	600 to 1000°F
Applied frequency:	10^4 to 10^6 Hz
Window material:	T-111, SS-316, WC, TiC-10Cb
Window thickness:	0.010 to 0.050 in.
Shaft, bearing and journal or sleeve material:	WC, TiC-10Cb, TZM
Bearing journal or sleeve thickness:	0.1 to 0.5 in.
Fluid film:	Potassium liquid and vapor

Also to be explored was the capability of the device for measurement of change in radial clearance of a shaft or in axial clearance of a rotating disk.



4.1 Basic Mathematical Model

4.1.1 Theory of Operation

When a coil of wire carrying an alternating current is placed near a conducting material, eddy currents are induced in the conducting material. These eddy currents are generated so as to oppose the magnetic field. The change in the magnetic field, which can be measured by a second coil in the field is a function of the conductivity of the material near the coil, the distance between the material and the coil, and the shape and size of the material.

The analysis of the instrumentation requires that the functional relationship between the parameters of the coil system--i.e., resistance, inductance, and coil size and the conductivity and permeability of the potassium film, turbine shaft and window material--be determined. A set of equations have been derived that uniquely define the coil parameters as a function of the environment surrounding the coil system.

The solution satisfying that set defines the magnetic field and eddy currents induced in the window and potassium film. The magnetic field is set up by currents residing in the coil. A solution for a given coil and film configuration was derived from Maxwell's equations and Ohm's law. The coil parameters were then determined by integration of the magnetic field over the coil geometry.

The differential equation that determines the magnetic field vector B included in the potassium film is given by the expression:



AIRESEARCH MANUFACTURING COMPANY OF ARIZONA
A DIVISION OF THE GARRETT CORPORATION

$$\nabla^2 B = \sigma \mu \frac{dB}{dt}$$

where

$\nabla^2 B$ = divergency gradient

σ = film conductivity

μ = permeability

t = time

Since the magnetic field will vary sinusoidally with time, the magnetic induction also varies sinusoidally and can be written

$$B = B_o e^{j\omega t}$$

where

B_o = maximum amplitude of B

j = unit vector in the imaginary direction = $\sqrt{-1}$

ω = $2\pi f$

f = frequency

Two approaches may be taken to solve the previous equation. One, a "closed form" solution assumes sinusoidal driving current, linear, isotropic and homogeneous media. These solutions are in the form of Bessel function integrals and while amenable to "first approximation"



type problems, this form did not lend itself to the transducer analysis--largely due to the need for precision and due to the large number of material interfaces inherent in this particular problem.

The second approach, and that selected, is the relaxation method derived in C.V. Dodd's "Solution to Electromagnetic Induction Problems," Oak Ridge National Laboratory Report ORNL-TM-1842, dated June 1967.

The solution for a particular electromagnetic configuration is obtained by deriving the differential equation for the magnetic vector potential from Maxwell's equations. This differential equation consists of several terms that are approximated by finite-difference equations. These approximations provide a means for expressing the magnetic vector potential at a given point in terms of the vector potential at several nearby points. The computer program is written to solve for the vector potential by a relaxation method. From the values of the vector potential at the location of the film-thickness transducer, the induced voltage in the transducer coils can be calculated.

The computer model transducer configuration consists of two coaxial coils--one positioned adjacent to the other, and both positioned adjacent to several layers of materials with various electrical conductivities, as shown schematically in Figure 9. The transducer cross section as positioned in the turbine is obtained by passing a plane through the axis of the transducer and the rotational axis of the turbine shaft. It is identical to the actual transducer configuration.

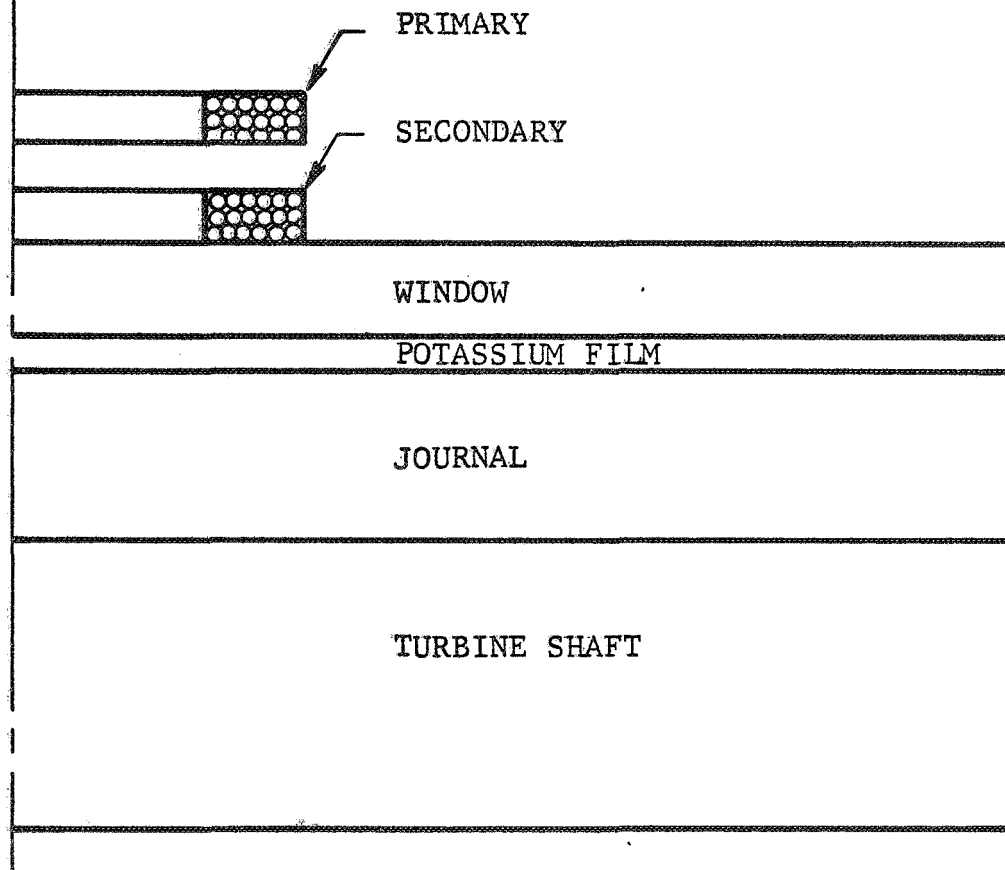
The various mesh sizes were used in the relaxation procedure to provide more accuracy in simulating the variation of the potassium film as a function of journal motion in the bearing. A very coarse



AIRESEARCH MANUFACTURING COMPANY OF ARIZONA
A DIVISION OF THE GARRETT CORPORATION
PHOENIX, ARIZONA

COIL AXIS

CUTOFF POINT--
WHERE MAGNETIC-
FIELD STRENGTH
HAS DROPPED TO
5% OF ITS ORIGINAL
VALUE



ONE-HALF OF IDEAL FILM-THICKNESS COIL CONFIGURATION

FIGURE 9



mesh (50 x 50) was formulated. A very satisfactory convergence was obtained with this mesh. A computer subroutine was written to stretch the 50 x 50 mesh to a 250 x 250 mesh keeping the configuration boundaries proportional. The results from the 50 x 50 mesh were then used as initial estimates for the 250 x 250 mesh. A tape overlay method was developed for cascading the arrays making possible operation on the CDC 3400 computer without overflowing the storage capacity.

Versions of the program (up to 100 x 100 mesh array without external tape storage) were used to calculate the induced transducer voltages for 600°F film thickness of 0.010-, 0.020-, and 0.030-in. Two sleeve materials were explored--tungsten-carbide with cobalt binder (Kennametal K-96) and Ti-6Al-4V.

In each case calculations were run to the point where error between the last two computer iterations was 0.01 percent or less. These computer calculated induced primary voltages were then used to calculate the induced voltages in the secondary coil of the transducer using the mutual inductance coupling.

For the tungsten-carbide case, the induced secondary voltage remained constant for the three film thicknesses. For the Ti-6Al-4V case, there was an increase in voltage of 0.6 mv/mil over the range of thicknesses investigated.

A comparison was made of calculated and experimentally determined values of voltage sensitivity for a transducer configuration with Ti-6Al-4V as the sleeve material. The computer-determined (calculated) value was 0.6 mv per mil, where the experimental value obtained from data generated during the SPUR bearing test program was found to be 1.7 mv per mil. The difference could be caused by differences in geometry and can only be resolved by further computer calculation.



Due to the large computer time expense inherent in the long (4 to 5 hr) convergence times required for each film thickness change, additional computer runs were suspended by the NASA Program Manager.

Further efforts to select and optimize transducer configurations were diverted into an experimental channel using simulated transducers as described in the next section.

4.2 Empirical Transducer Study

Task I originally entailed the use of a mathematical model to analyze film thickness transducer sensitivity as a function of changes in the film thickness. This program proved economically unfeasible to operate for extensive transducer analysis. Extremely slow convergence times caused principally by discontinuities along material interfaces resulted in computer run times on the order of 4 to 5 hr for each film-thickness change point. Therefore, the Task I phase of the program was rechanneled toward an empirical approach. This approach involved static bench tests varying the parameters of interest, and observing their effect on transducer sensitivity.

The variables investigated included sleeve material, window thickness, temperature, coil diameter and configuration, and window curvature. Rotational effects were investigated using the calibration test rig. This is essentially the same variable set which would have been examined analytically were it not for the inordinate amount of computer expense.

4.2.1 Summary of Basic Trends

Data taken using the static bench tests reveal the following trends:



- (a) Sleeve Material - At low film-to-sleeve electrical resistivity ratios, the sensitivity is primarily a function of film thickness changes only. At high film-to-sleeve resistivity ratios, the sensitivity is primarily a function of the sleeve motion with some decrease in sensitivity from coil shielding by the film. Thus, with sleeve resistivities greater than 70 $\mu\text{ohm-cm}$, the sleeve contributes approximately 50 percent or less to the overall sensitivity with high-resistivity films (i.e., high-temperature K) but plays a minor role in affecting the sensitivity with low-resistivity films (i.e., low-temperature K).
- (b) Window Thickness - With a low-resistivity film, an increase in window thickness has a greater effect in reducing the sensitivity than with a high resistivity film.
- (c) Temperature - The sensitivity with a TZM shaft should be relatively constant with temperature between about 600° and 1200°F.
- (d) Coil Diameter and Configuration - An optimized coil configuration was found to be one with a secondary to primary turn ratio of 2:1 or 2.5:1 regardless of the film resistivity. With a high resistivity film, the sensitivity was found to be a weak function of secondary and primary coil diameter changes. With a low-resistivity film, however, the sensitivity was found to vary about 10:1 between coil diameters of 0.250- to 0.500 in.
- (e) Window Curvature - By introducing a calculation technique to correct the foregoing results for window curvature, no deviation from the above-mentioned trends was evident.



- (f) Rotational Effects - Utilizing the calibration test rig, a limited amount of testing with NaK was conducted using a baseline transducer with a 0.500 nominal OD and a 1:1 turns ratio. These were tested in housings machined from solid billets of material. The minimum window thickness through which the instrument senses is 0.011 in. Data taken at room temperature with a Type 316 Stainless-Steel housing and a TZM sleeve indicates constant transducer sensitivity with speed.

4.2.2 Description of Static Bench Testing

In order to investigate the film thickness transducer sensitivity over a wide range of variables, a simple static bench test rig (Figure 10) was designed and fabricated. The basic transducer consists of two coil cores, each wound with two coils of fine magnetic wire. Typical coil dimensions are shown in Figure 11.

The two coil sets are mounted in the test fixture facing each other with colinear axes. Between the faces of the transducer coils are mounted layers of various materials simulating a window, a liquid metal (or other fluid) film, and the shaft (sleeve) material. The thicknesses of the various strata may be changed by moving or changing the sheets of material. For instance, a 1-mil movement of the shaft is simulated by moving a 1-mil sheet of the fluid-film simulating material from one side of the simulated shaft to the other.

In order to determine the materials suitable for the simulation, the values of electrical resistivity versus temperature were plotted in Figure 12 for the candidate materials. From these plots the following materials were selected for simulating the potassium film at various temperatures:

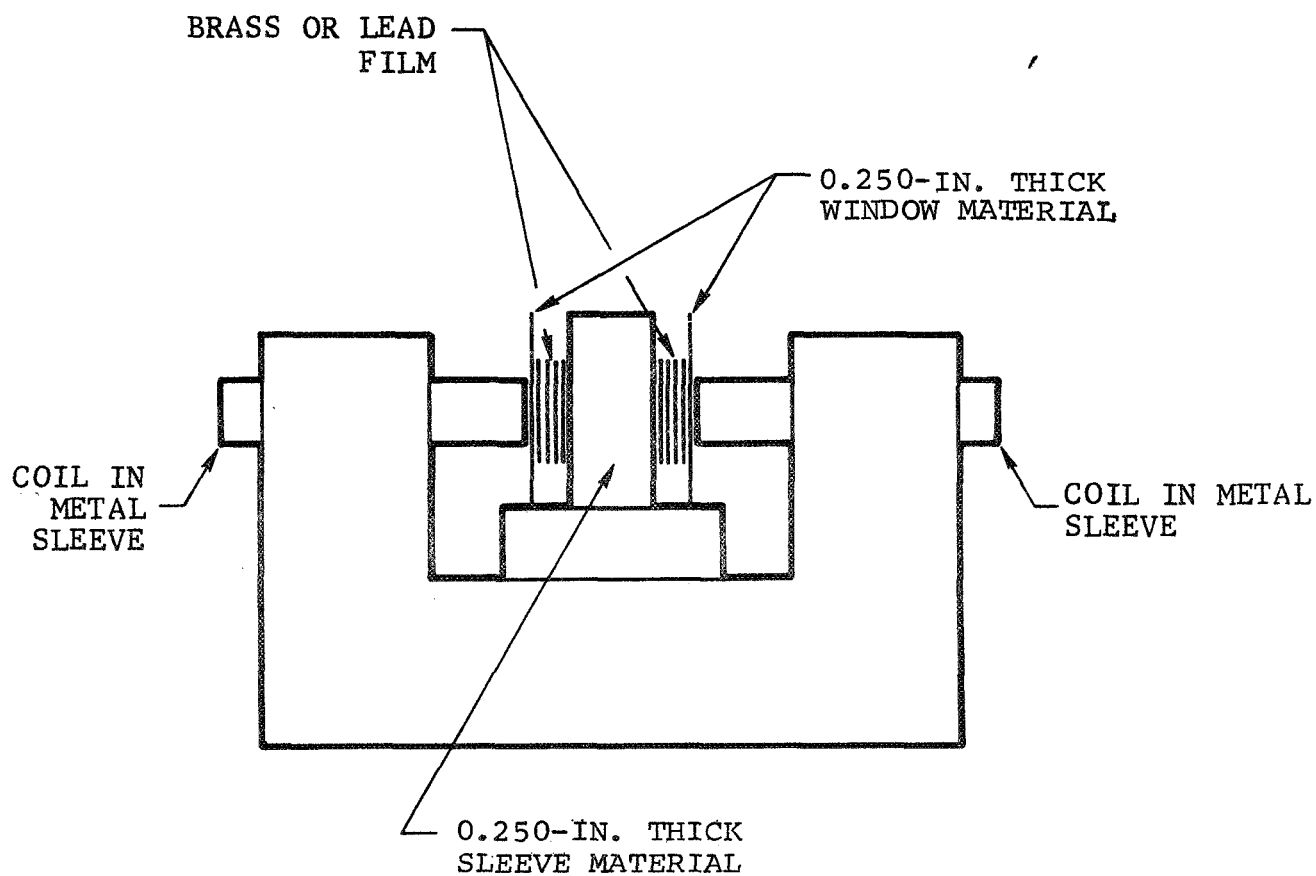
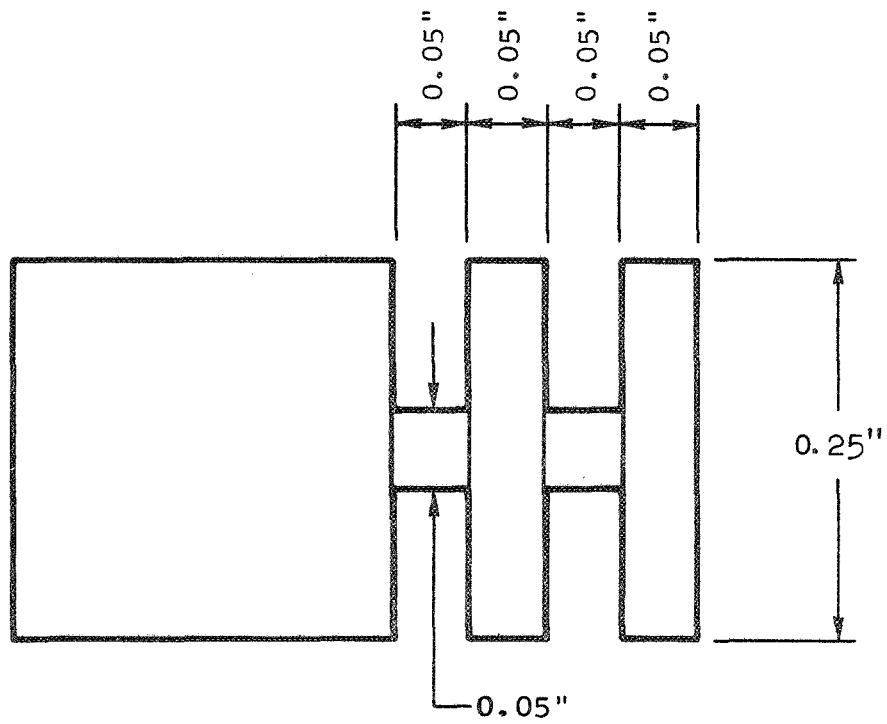
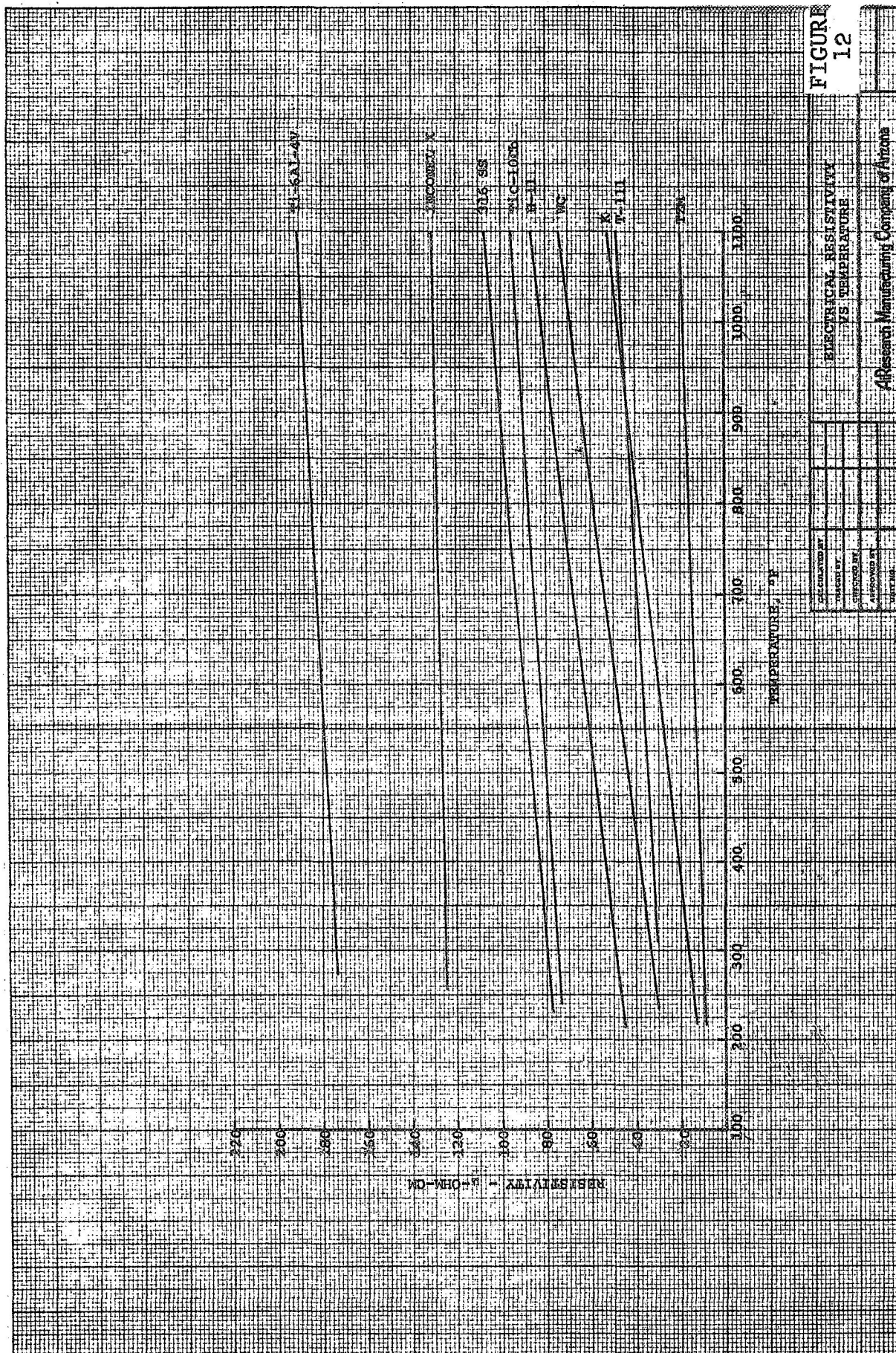


FIGURE 10
SIMULATED TRANSDUCER SETUP



COIL CORE-FABRIC FILLED
PHENOLIC

FIGURE 11
SIMULATED TRANSDUCER COIL CORE





<u>Material</u>	<u>Simulated Potassium Temperature, °F</u>	<u>Resistivity μohm-cm</u>
Brass	105	10.2
Cupro-nickel No. 710	550	27
Cupro-nickel No. 715	700	34.4
Titanium	1120	55

The pertinent parameters influencing transducer sensitivity are sleeve material, window thickness, temperature, coil diameters, configuration, and window curvature. The following paragraphs give brief descriptions of how each parameter and its effect on sensitivity was examined.

- (a) Effects of Sleeve Material - To simulate the sleeve, various metals were selected and fabricated into blocks 0.75 x 0.75 x 0.25 in. These blocks covered the electrical resistivity range from TZM at 6.7 μohm-cm to Ti-6Al-4V at 176 μohm-cm. Al₂O₃ and phenolic blocks were also fabricated and used to simulate an insulator (very high resistivity) as the sleeve material.

The sensitivity measurements were performed with the standard transducer configuration previously discussed. Each coil set has two windings of 120 turns each of No. 36 Formvar covered wire.

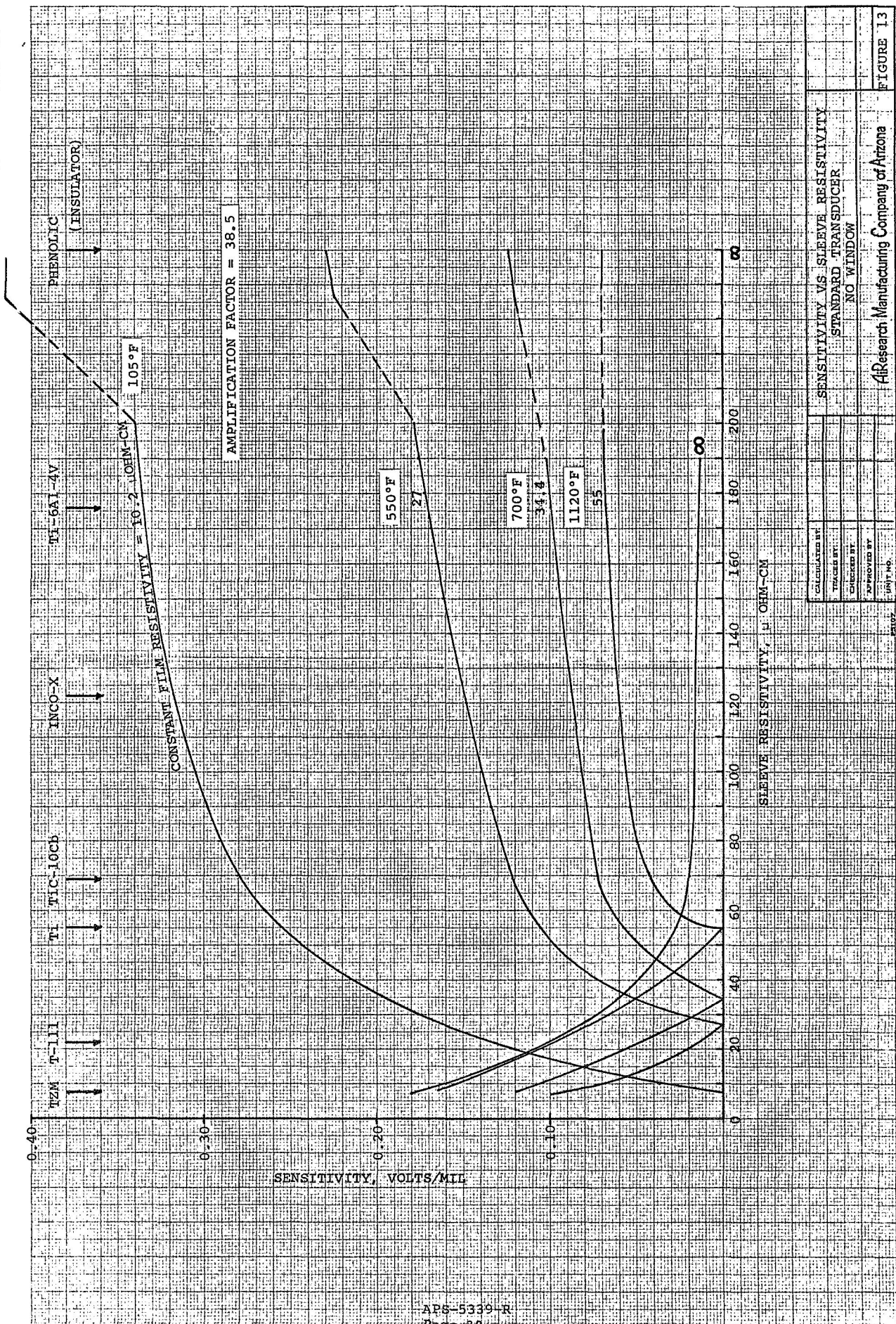
The transducer was placed in the fixture with a nominal film of 0.016 in. between each coil and the sleeve material. The coils were excited electrically with a Consolidated Electrodynamics Corp. 20-kHz carrier amplifier Type 1-127. The



carrier amplifier was adjusted to balance the coils electrically. The film was varied in known amounts on each side of the sleeve material and the resulting imbalance indicated on a digital voltmeter.

Data have been obtained over the sleeve electrical resistivity range from 6.7 to 176 $\mu\text{ohm-cm}$ and for an insulator (Figures 13 and 14). In each case the sensitivity in volts per mil has been plotted versus sleeve resistivity for a given film. The sensitivity figures shown for the curves include an amplification factor of 38.5, as supplied by the carrier amplifier. A sample of the raw data taken with a TiC-10Cb sleeve and with the film represented by the materials shown is presented in Figure 15.

To determine the effect on the sensitivity of the sleeve material alone, (i.e., no film present) a series of tests were conducted using paper as the simulated film. Since the paper is a nonconductor, the coil output will only be affected by the motion of the sleeve material. The data generated during these tests are also plotted on Figures 13 and 14 and are indicated by the lower curve (paper film). By comparing these data, it can be seen that a low-sleeve resistivities (i.e., below 40 $\mu\text{ohm-cm}$), the sensitivity is mainly a function of sleeve motion for high-resistivity films. As the film resistivity is decreased, however, the film tends to shield the coils from the sleeve, and there is a decrease in sensitivity. At the lowest film resistivity, the sensitivity has increased greatly due to the film. But as the sleeve resistivity is decreased below 20 $\mu\text{ohm-cm}$, the film again shields the sleeve from the coils and the sensitivity decreases. At sleeve resistivities greater than



CALCULATED BY	SENSITIVITY VS SLEEVE RESISTIVITY
TRACED BY	STANDARD TRANSDUCER
CHECKED BY	NO WINDOW
APPROVED BY	
DATE	

AI Research Manufacturing Company of Arizona

FIGURE 13

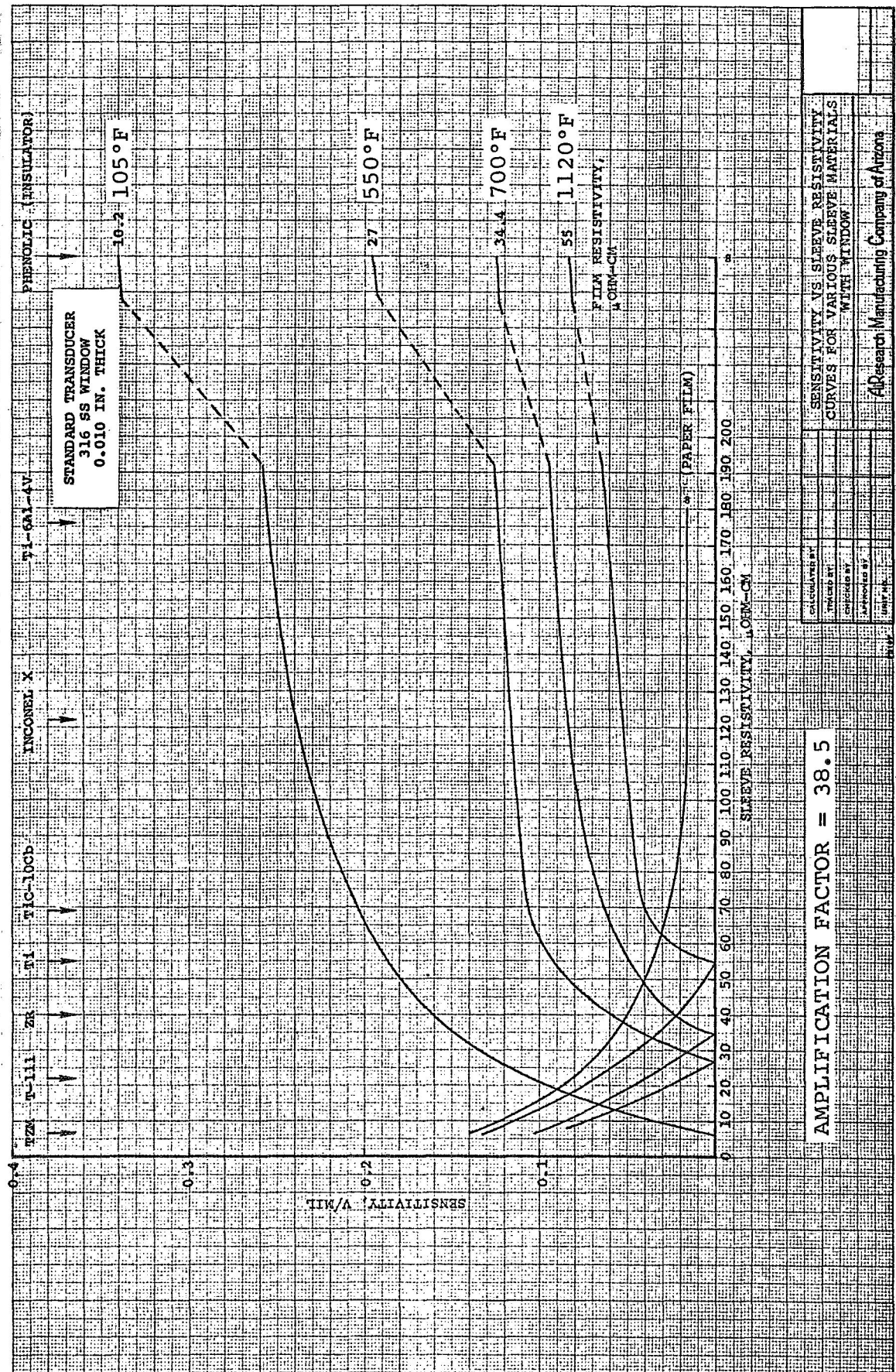


FIGURE 14
APS-5339-R
Page 39

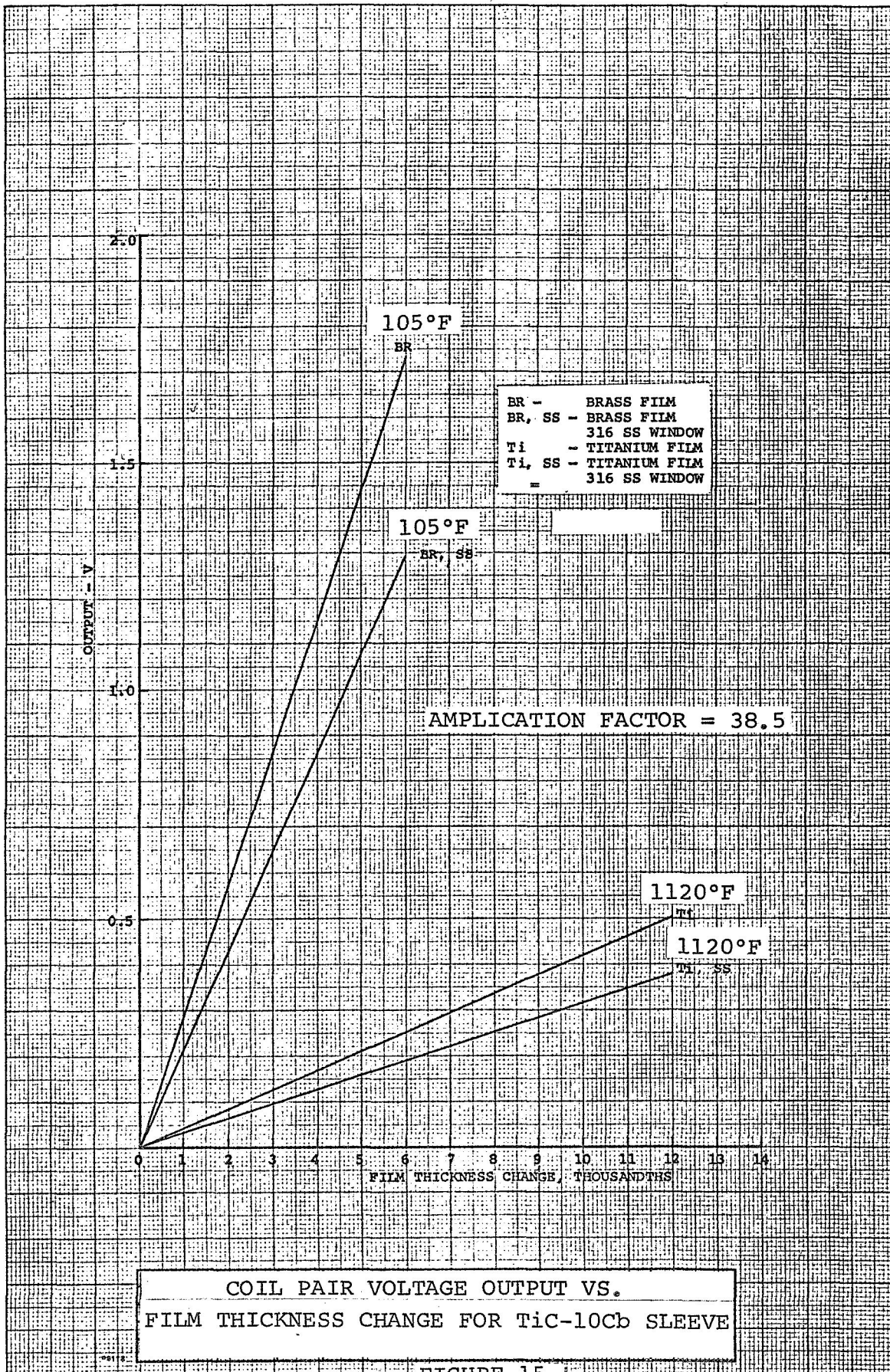


FIGURE 15
APS-5339-R
Page 40



70 $\mu\text{ohm-cm}$, the sleeve contributes approximately 50-percent to the overall sensitivity for the highest film resistivity but plays only a very minor role in affecting the sensitivity with low-resistivity films. In the sleeve resistivity region between 40 and 70 $\mu\text{ohm-cm}$, the low resistivity film is the dominant contributor to the sensitivity while the high-resistivity films do not contribute greatly to the sensitivity until the sleeve resistivity has increased to 70 $\mu\text{ohm-cm}$.

- (b) Effects of Window Thickness - The effect of changes in window thickness was determined by using several pieces of stainless steel sheet between the coils and the film. These data (Figures 16 and 17), indicate a fairly uniform change in sensitivity with an increase in window thickness. It is apparent that the increase in window thickness has a greater effect on the sensitivity with a low-resistivity film than with a high-resistivity film.
- (c) Effects of Temperature - To obtain some idea of how the temperature would affect the transducer sensitivity, a series of calculations were performed using the sleeve material data. The values of sleeve material resistivity corresponding to the four temperatures previously listed were obtained for TZM and TiC-10Cb. The potassium film for these four temperatures was simulated by the materials listed in Section 4.2.2. Using Figure 13, a sensitivity for each simulated film combination and sleeve resistivity was determined. Sensitivity versus temperatures were plotted as in Figure 18 for a range of potassium film temperatures. In the case of the data taken with a stainless steel window, the sensitivity data were taken into account the temperature effect on window resistivity. These data were then plotted in Figure 19.

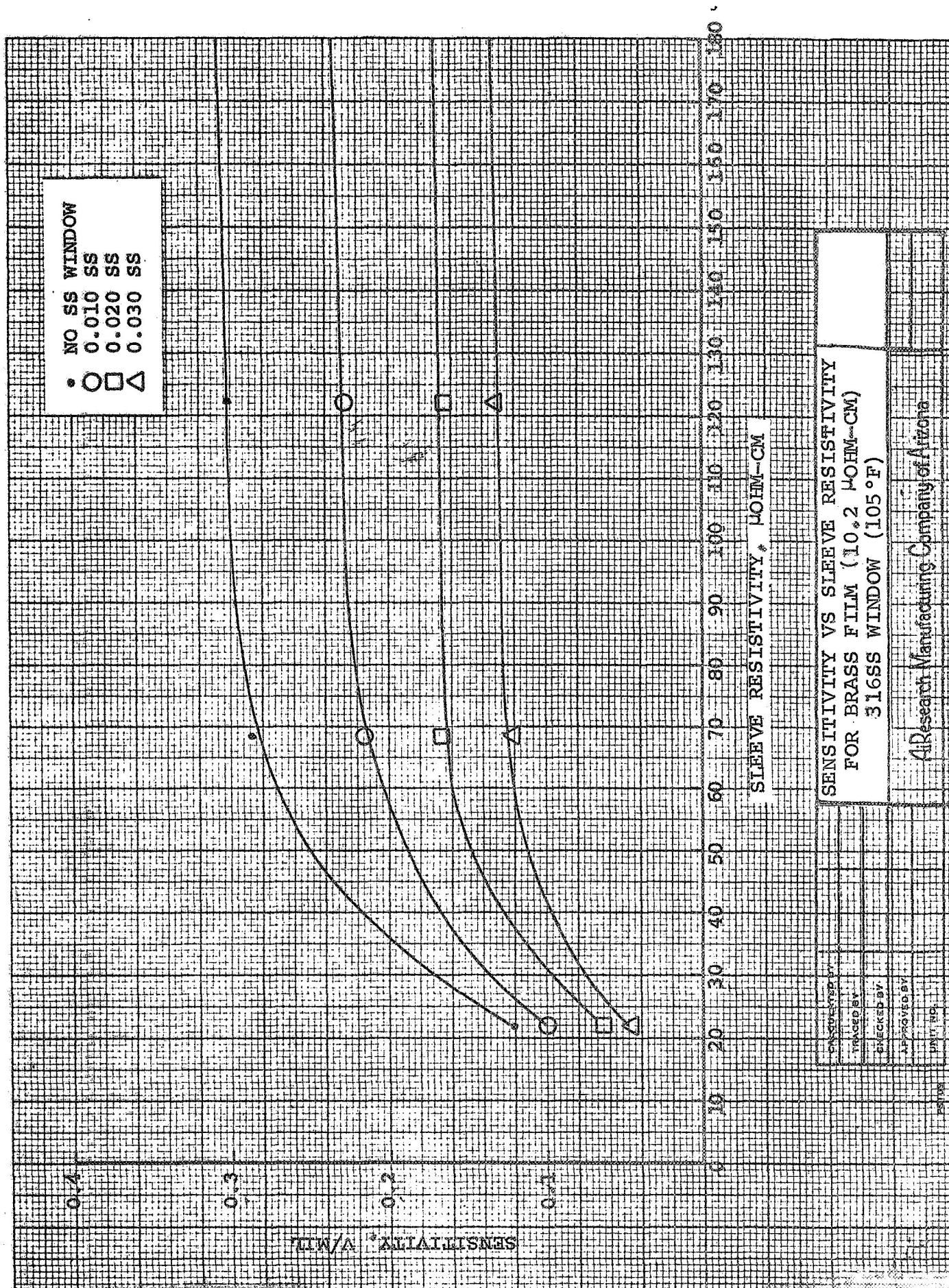


FIGURE 16

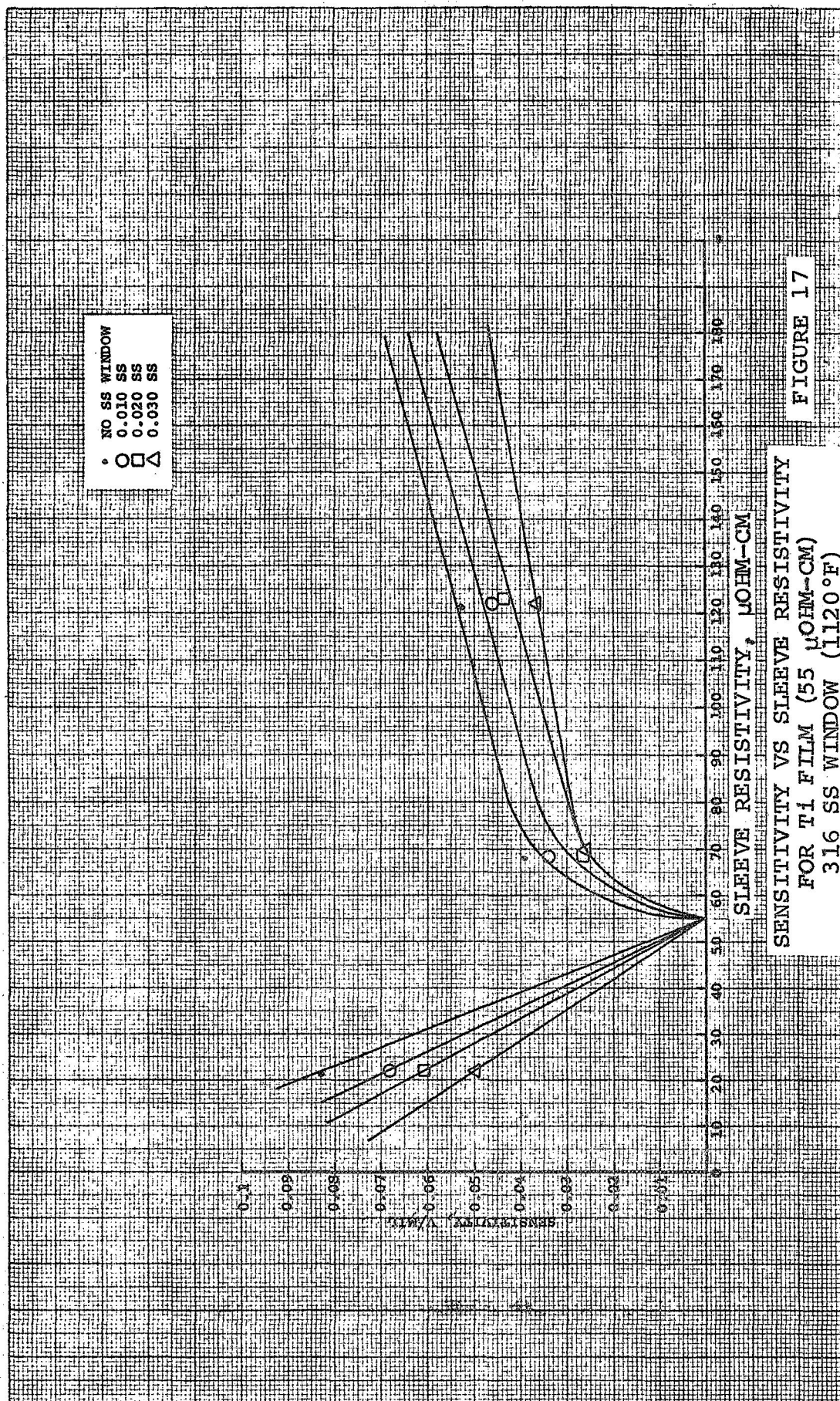
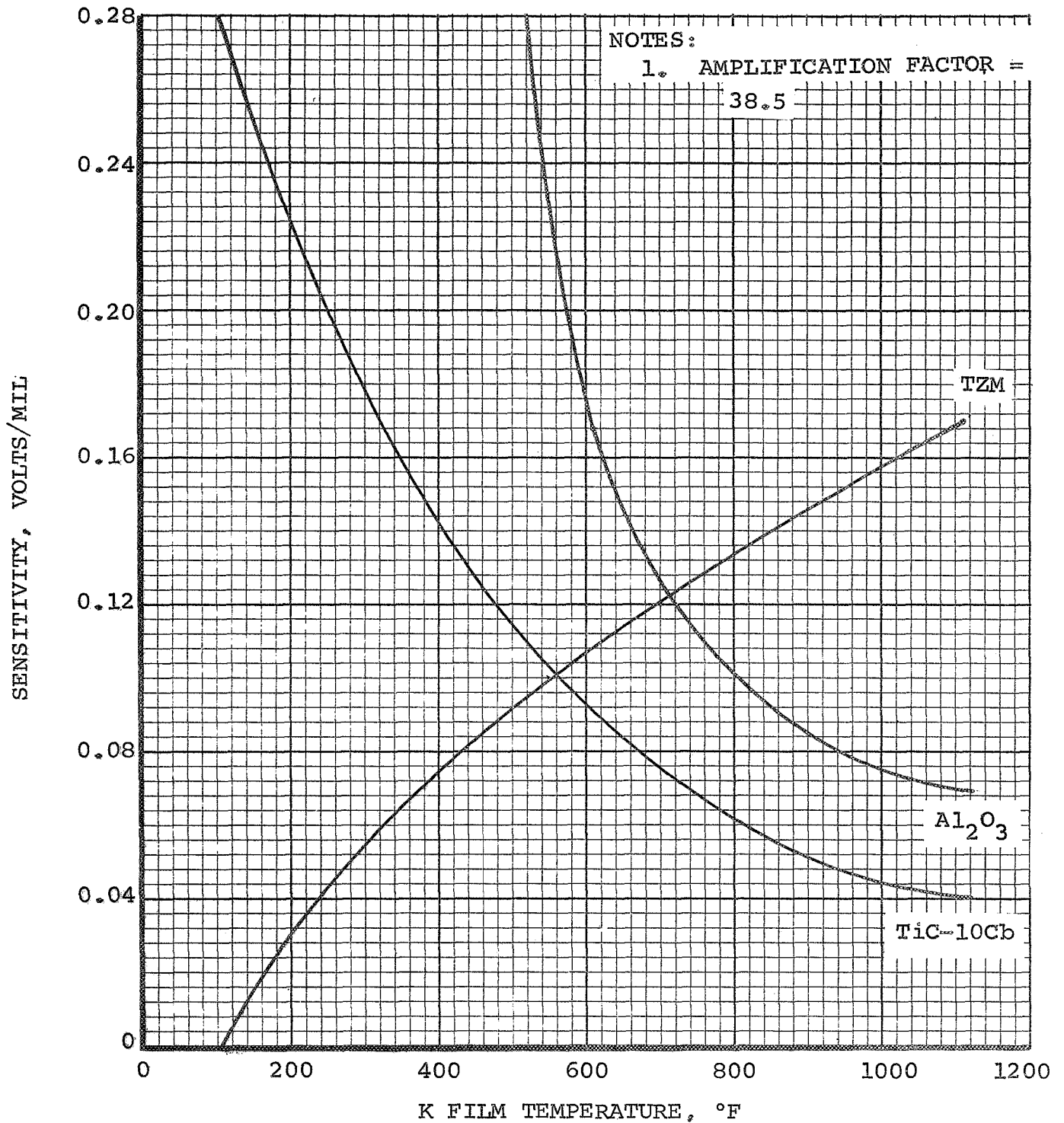
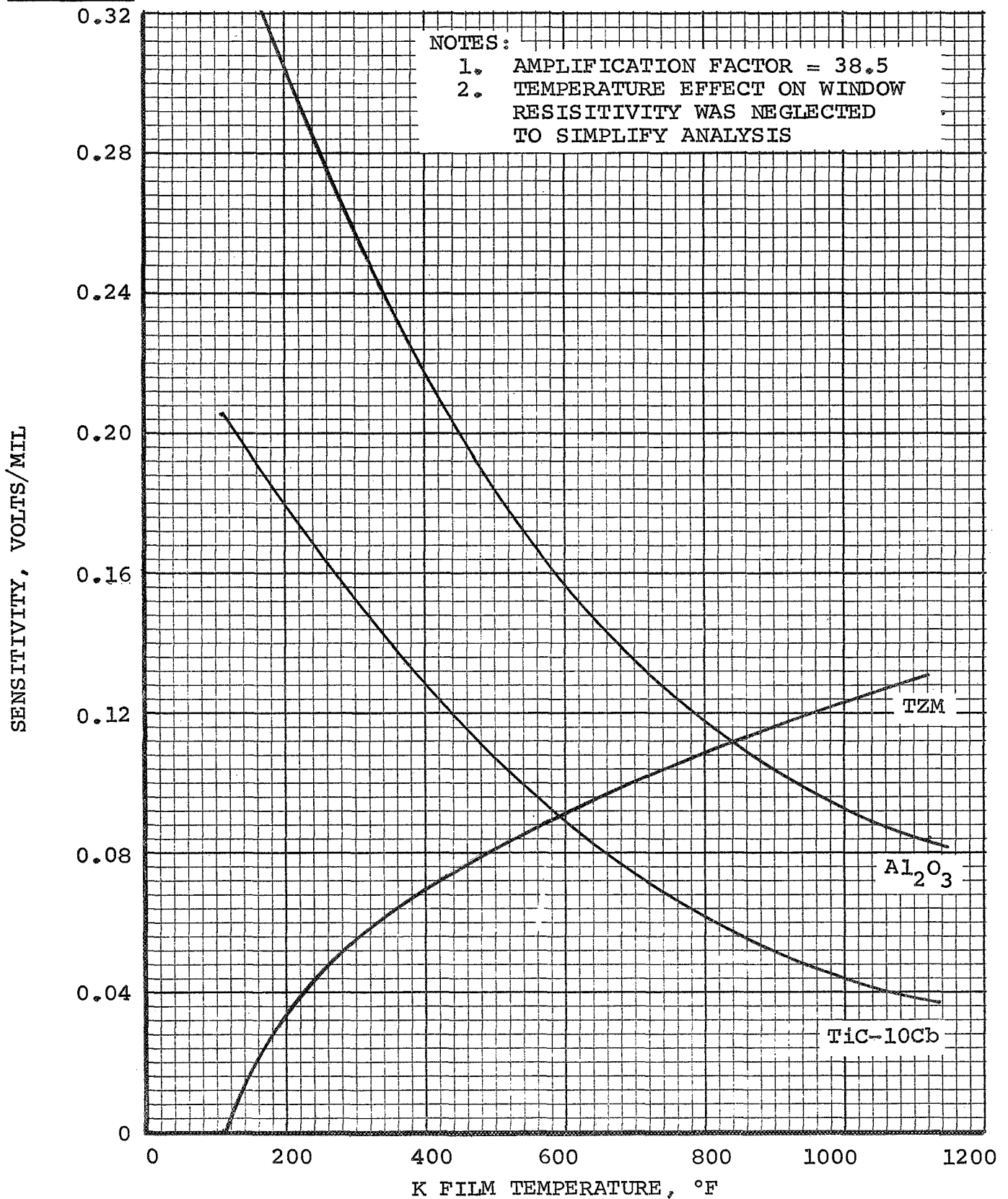


FIGURE 17



CALCULATED SENSITIVITY VS K FILM TEMPERATURE
FOR SEVERAL SLEEVE MATERIALS - NO WINDOW

FIGURE 18



CALCULATED SENSITIVITY VS K FILM TEMPERATURE
FOR SEVERAL SLEEVE MATERIALS - 316SS WINDOW (0.010 IN. THK.)

FIGURE 19

APS-5367-R

Page 45



- (d) Effects of Coil Diameter and Configuration - Changes in coil configurations have a marked effect on the transducer sensitivity. In order to study these effects, several transducers were fabricated and tested in the bench rig. These transducers incorporated changes in the turns ratio of the primary and secondary windings, and variations in the diameters of the windings. Table 2 depicts the cross sections of these various transducers and lists turns in the windings and windings diameters.

The test results covering these transducers have been combined to show the effect on transducer sensitivity when one parameter is varied. In Figure 20, the effect of changes in the primary coil outer diameter, keeping the number of turns on the primary and secondary constant, is shown. Figure 21 shows a similar condition with the secondary coil outer diameter being the variable. To study the effects of changes in the number of turns on the primary and secondary windings, Figures 22 and 23 were generated. These show first the variation in primary turns and then the variation in secondary winding turns.

From these curves, it can be seen that the optimum configuration in the range of variables tested is the one with a secondary to primary turns ratio of 2:1 or 2.5:1. This is the optimum case for either low- or high-resistivity film. These cases were run with a fairly high-resistivity sleeve.

TABLE II
CROSS SECTIONS OF COIL CONFIGURATIONS











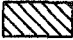

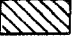






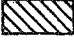


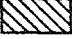

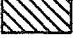
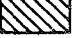



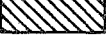
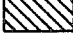
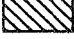
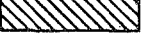
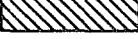
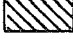
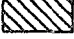
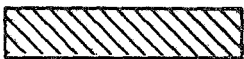





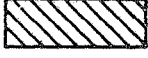
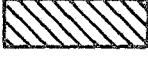
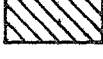
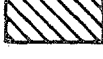
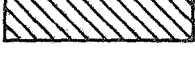
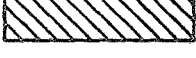
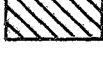
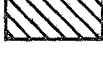
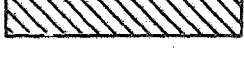

CONFIGURATION NUMBER			PRI. (UPPER WINDING)		SEC. (LOWER WINDING)	
			ID	OD	ID	OD
A			0.050	0.250	0.050	0.250
						
M			0.150	0.350	0.050	0.250
						
H			0.250	0.450	0.050	0.250
						
J			0.350	0.550	0.050	0.250
						
N			0.050	0.250	0.150	0.350
						
I			0.050	0.250	0.250	0.450
						
K			0.050	0.250	0.350	0.550
						
F			0.050	0.350	0.150	0.350
						
O			0.050	0.450	0.150	0.350
						

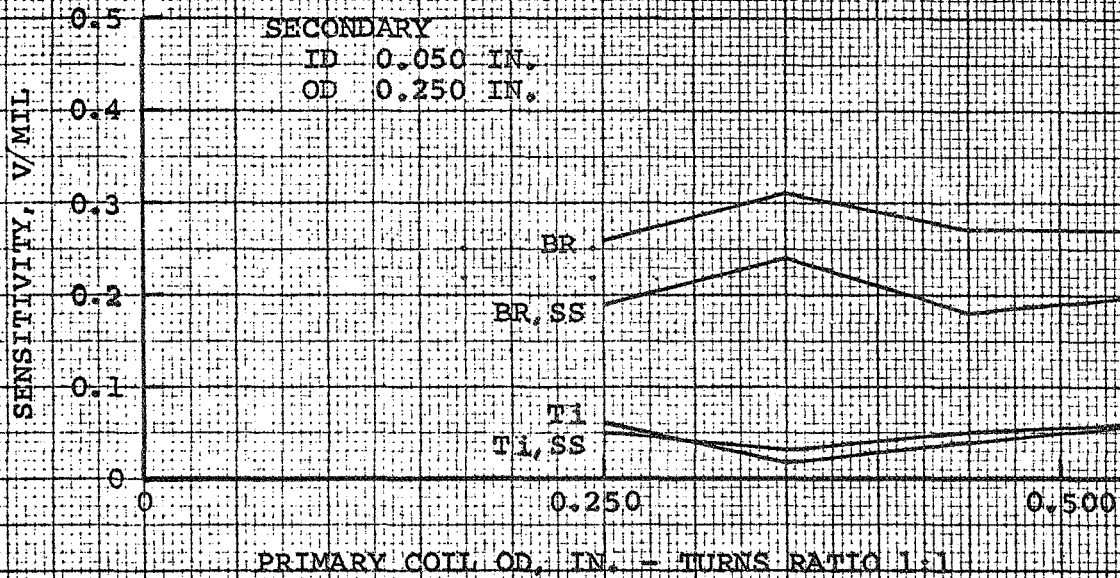
TABLE II (Contd.)

CROSS SECTIONS OF COIL CONFIGURATIONS

CONFIGURATION NUMBER			PRI. (UPPER WINDING)		SEC. (LOWER WINDING)	
			ID	OD	ID	OD
R			0.050	0.550	0.150	0.350
						
G			0.150	0.350	0.050	0.350
						
P			0.150	0.350	0.050	0.450
						
S			0.150	0.350	0.050	0.550
						

COILS - A
M
H
J

BR - BRASS FILM
BR, SS - BRASS FILM
SS WINDOW
Ti - TITANIUM FILM
Ti, SS - TITANIUM FILM
SS WINDOW



CALCULATED BY

TRACED BY

CHECKED BY

APPROVED BY

UNIT NO.

INCO X SLEEVE

AirResearch Manufacturing Company of Arizona

FIGURE 20
APS-5357-R
Page 49

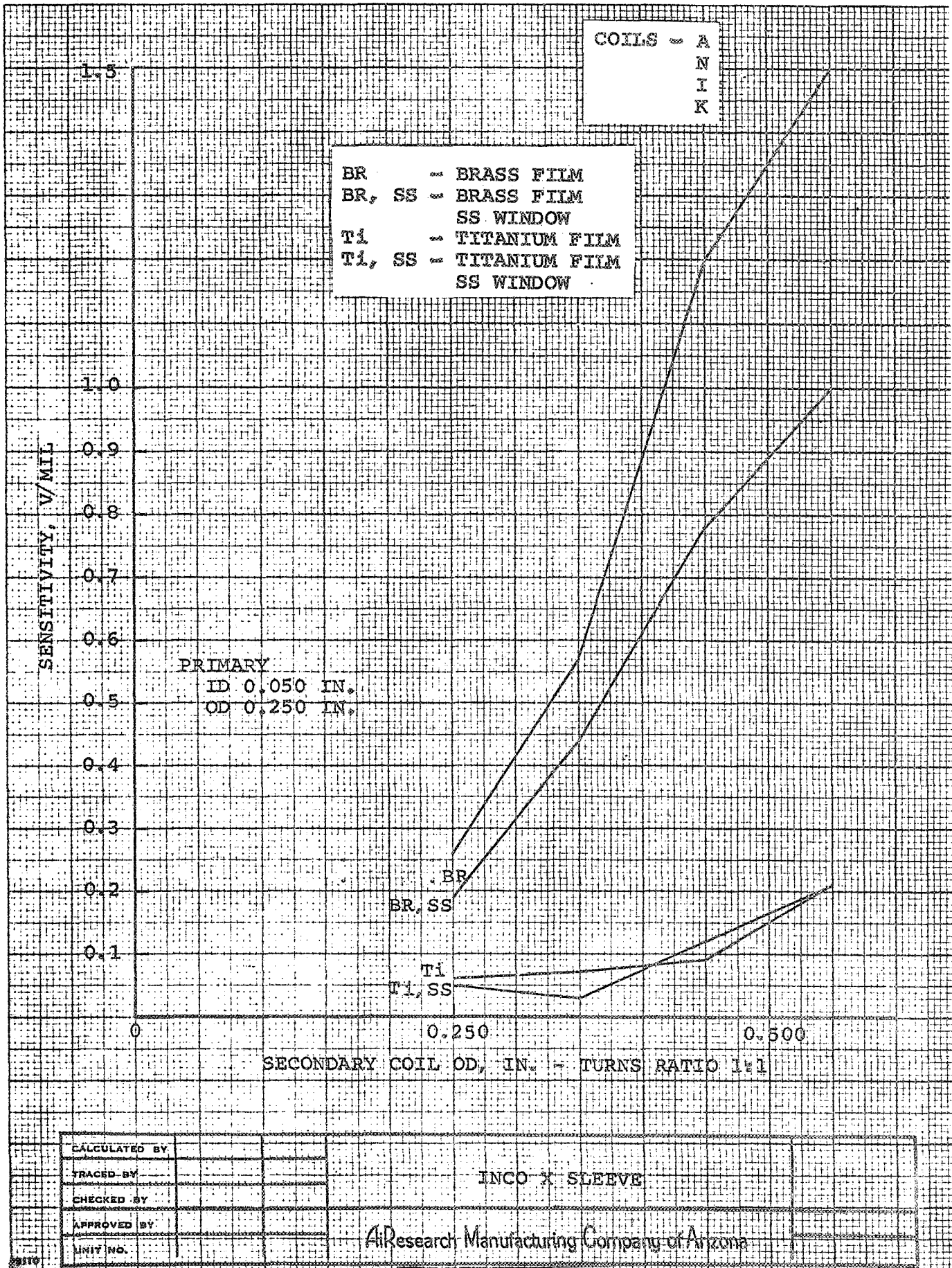


FIGURE 21

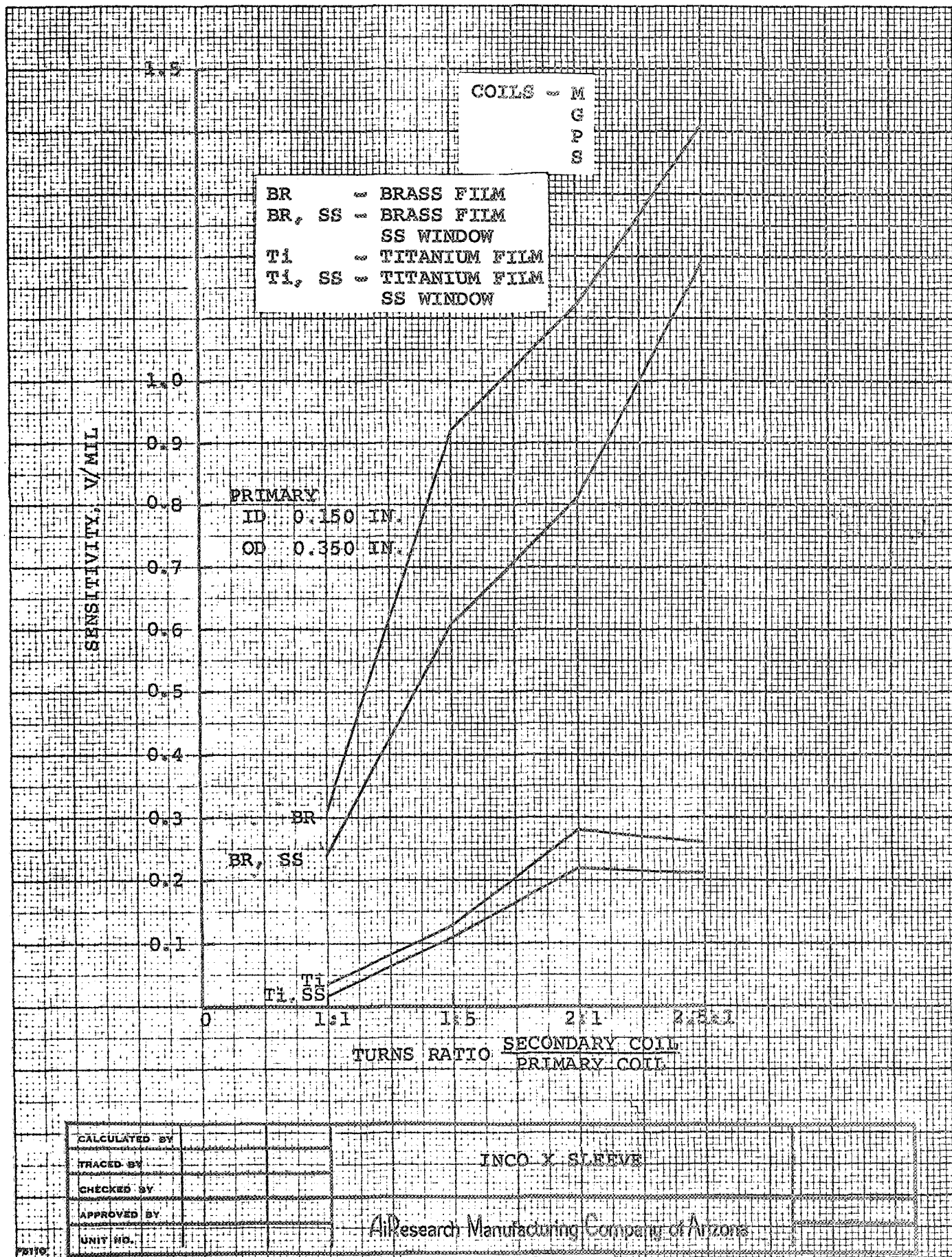


FIGURE 23



- (e) Effects of Window Curvature - Since the actual window in the bearing housing of the turbine is not flat but has a curvature on the journal side, calculations were made to take this window thickness variation into account. The technique used to perform the calculations is shown in Figure 24. The coil configurations were drawn on a large scale model of the window cross section and an average window thickness for each coil determined. The sensitivity was then modified by this increase in thickness and replotted on Figures 25 and 26. The results are essentially the same as those presented in Figures 20 through 23.

4.2.3 Transducer Design and Fabrication

This section details Task III--the design and fabrication of film thickness probes for use in the 500-hr endurance test. The final probe design employs a 1.5 secondary-to-primary coil turns ratio and is shown in Figures 27 and 28. The design shown evolved from optimization studies using analytical and empirical techniques. Several transducers were fabricated for base-line test purposes and for use in high temperature (1000°F) resistance stability tests.

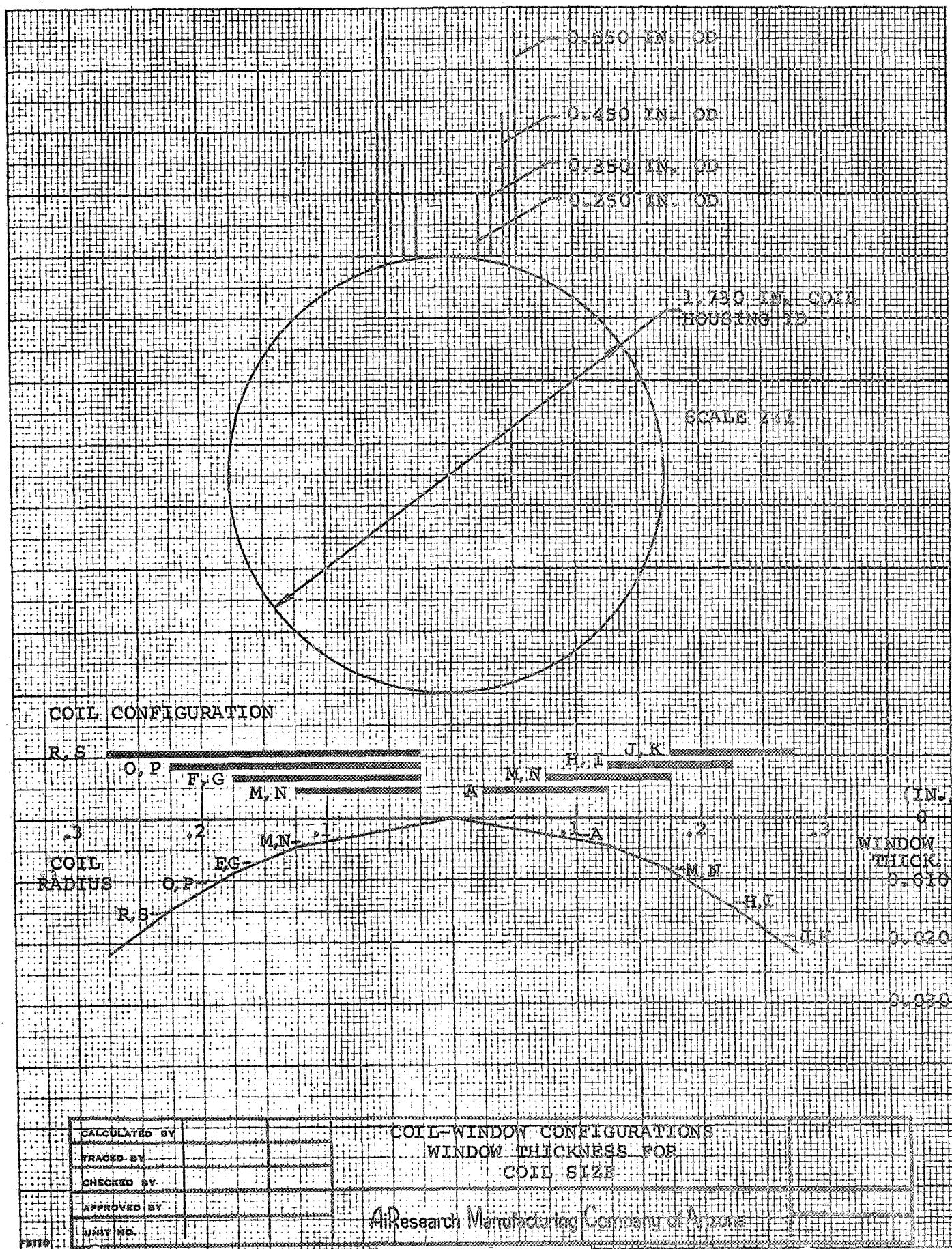


FIGURE 24

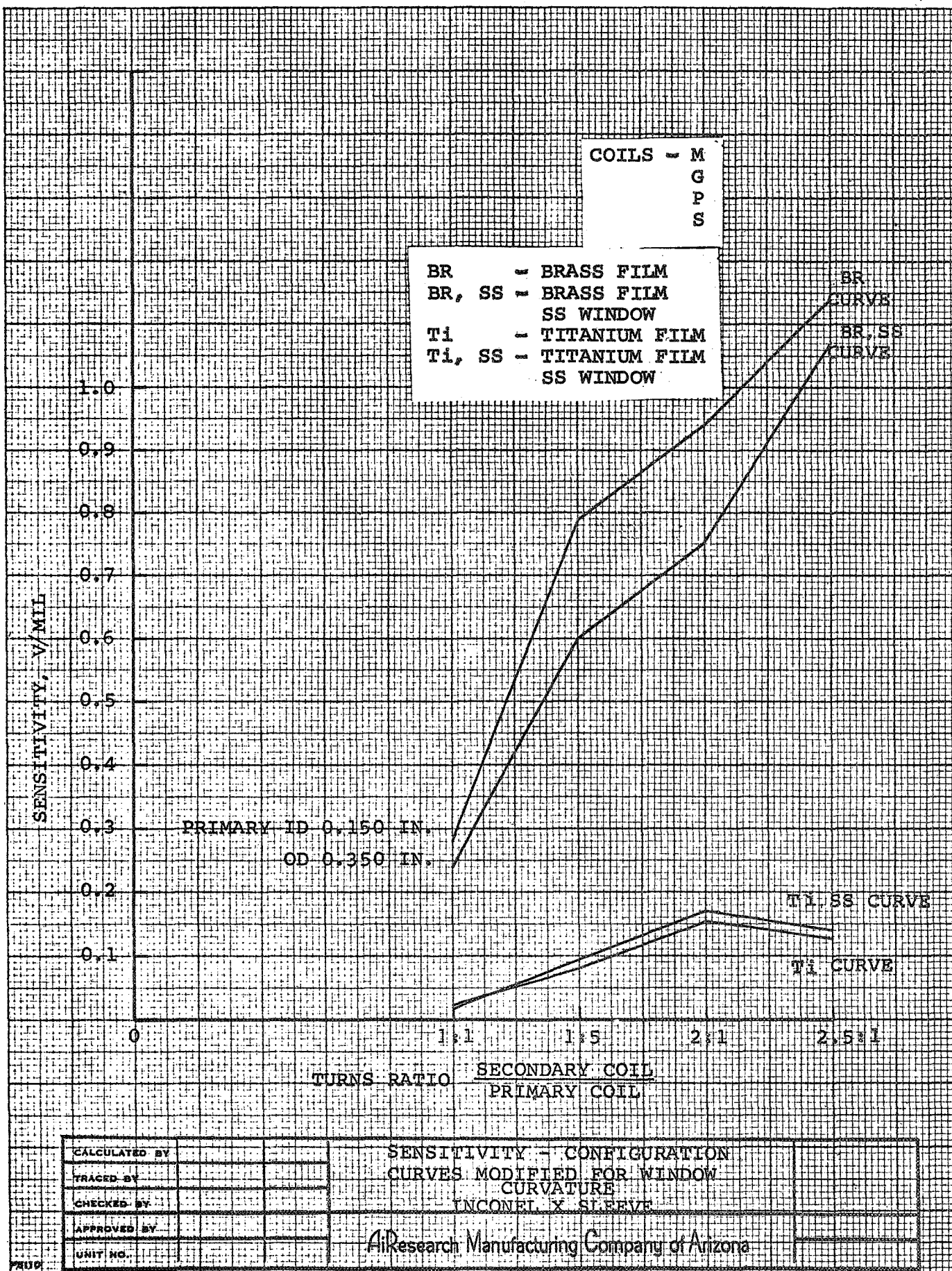


FIGURE 25

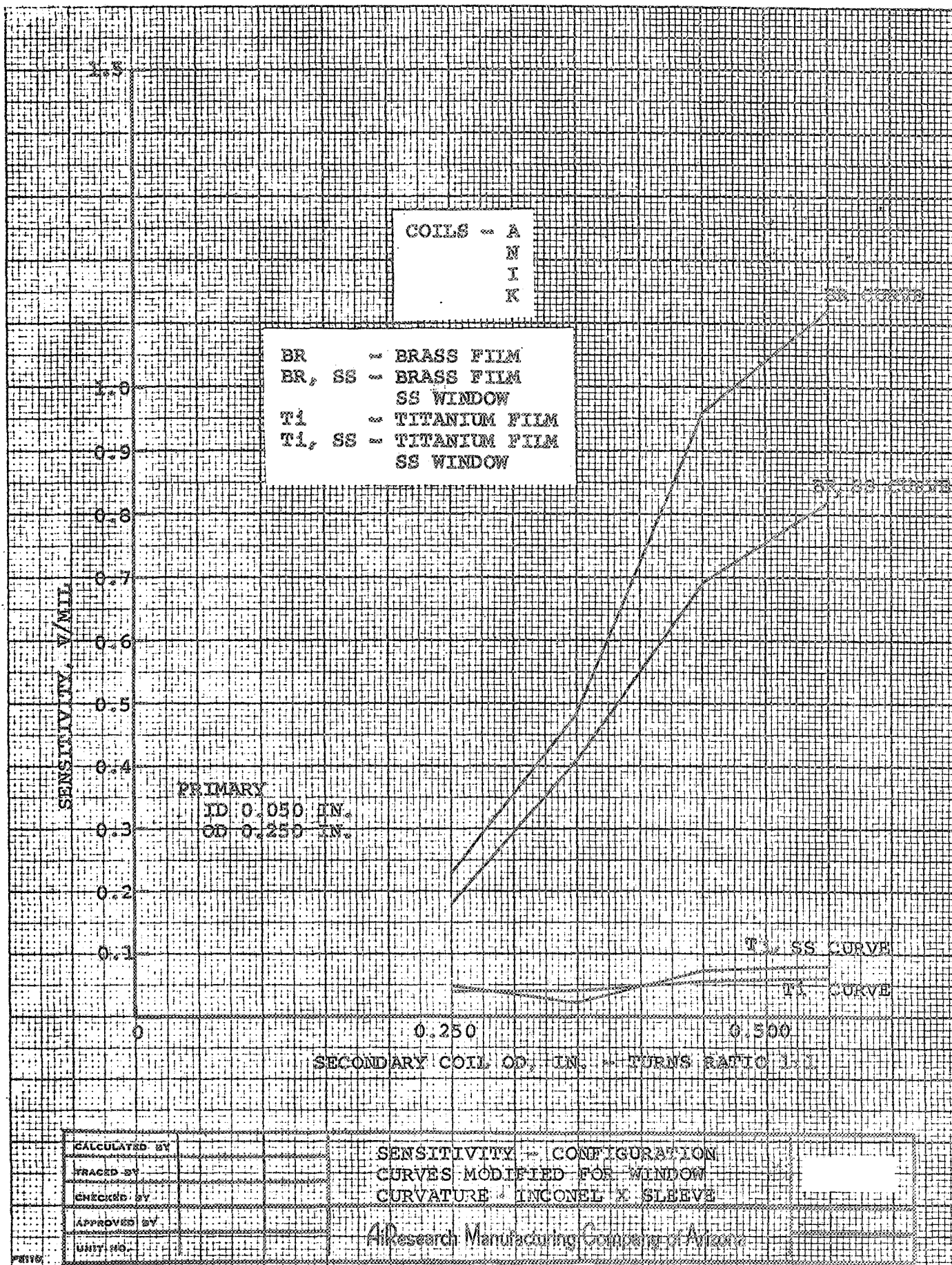
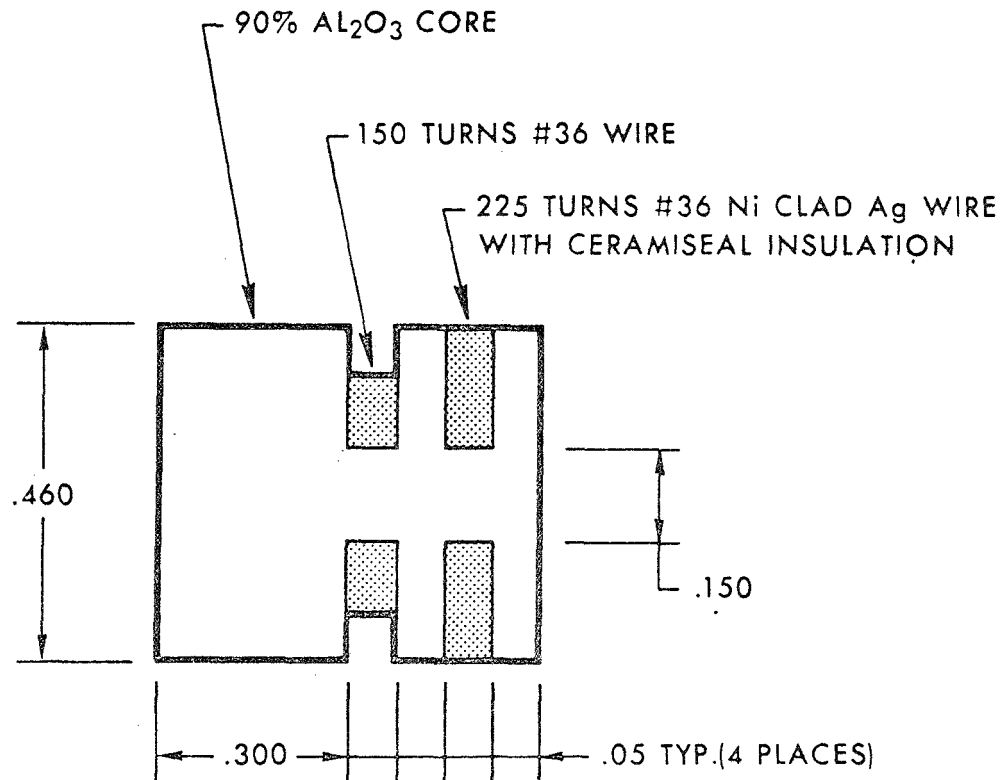


FIGURE 26

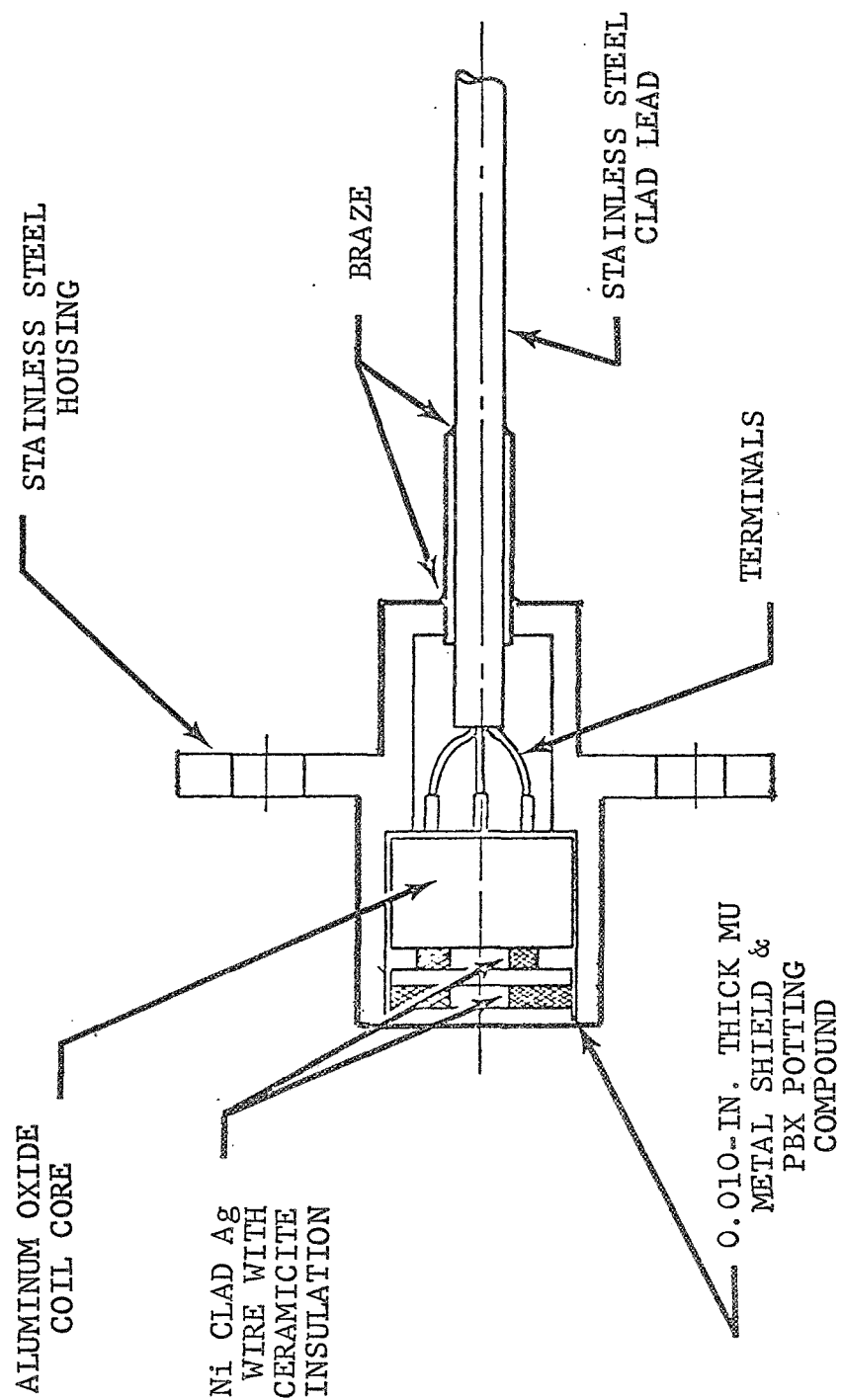


AIRESEARCH MANUFACTURING COMPANY OF ARIZONA
A DIVISION OF THE GARRETT CORPORATION



FILM THICKNESS PROBE COIL CONFIGURATION FOR 500 HOUR TEST

FIGURE 27



POTASSIUM FILM THICKNESS PROBE ASSEMBLY

FIGURE 28



Eventual selection of coil wire material, wire gauge, insulation, potting compound, and connector design was made on the basis of two high temperature (1000°F) tests. The first test (approximately 1000 hr) was made to select the most durable material-gauge combination from a set of 36-, 38- and 40 ga wire coils. Of the two material configurations tested, (nickel-clad silver wire with Ceramicite coating versus aluminum wire with Al_2O_3 coating) the 36 ga aluminum wire appeared the least sensitive to time-temperature effects. Therefore, a second 2200 hr test was made comparing 12 sets of Ni-clad silver wire coils with 12 sets of aluminum wire coils, both of 36 ga diam wire. All 12 aluminum wire coils were unchanged in resistance after the tests, while several of the Ni-clad silver wire samples showed evidence of burn spots on the wire or an increase in resistance over the initial values.

Superior performance of the aluminum wire was overridden by additional considerations relating to eventual transducer application; namely,

- (a) It was suspected that the aluminum might have an adverse effect on the NASA selected potting compound
- (b) There was some apprehension over the possibility of aluminum evaporation ("outgassing") in the hard-vacuum space environment.

Therefore, 36 ga Ni-clad silver wire was selected for the final transducer test configuration using PBX Ceramic Cement as the potting compound.

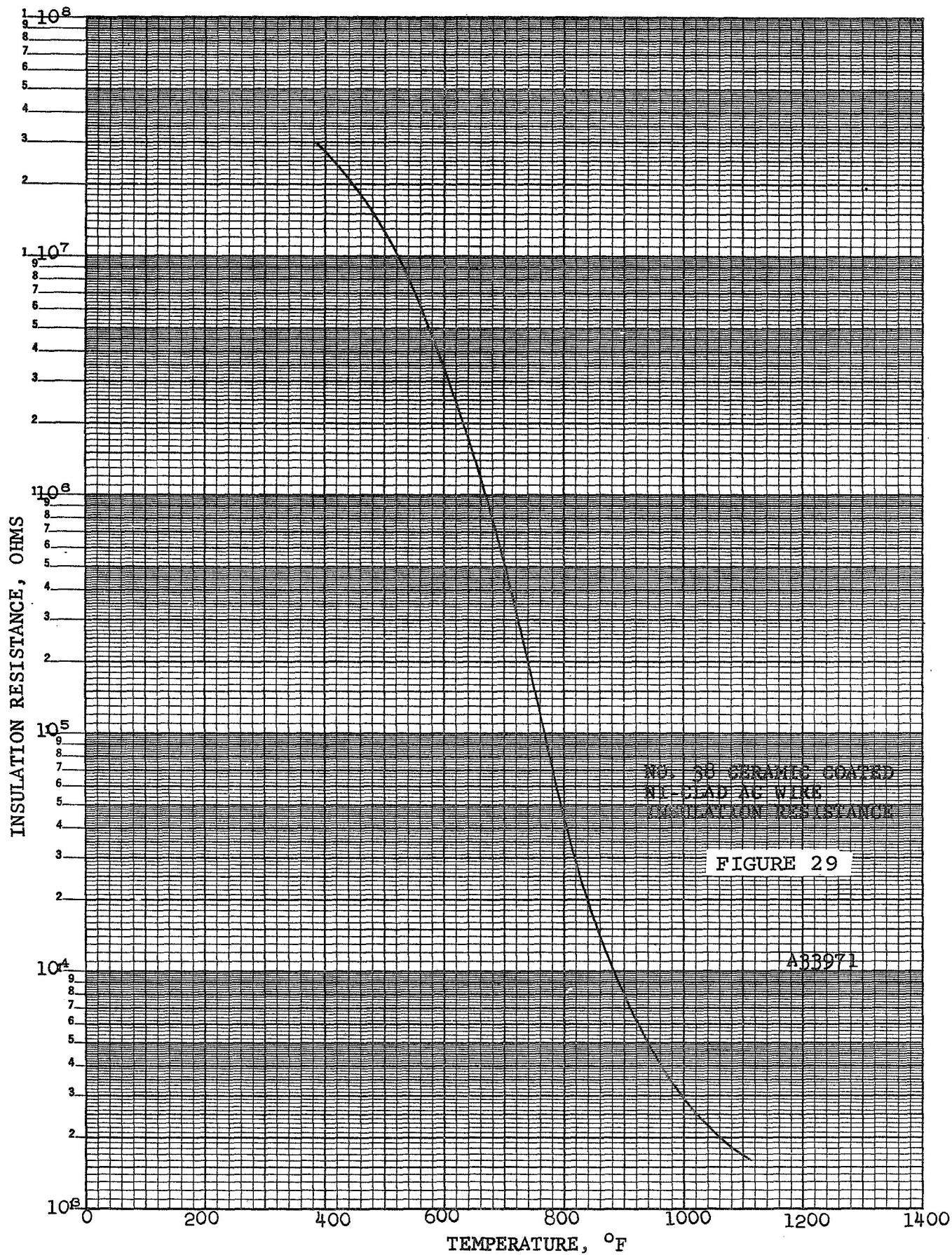


4.2.3.1 Details of Probe Design and Fabrication

- (a) Wire Selection - Two candidate wire materials were considered, Ni-clad silver and aluminum coated with Al_2O_3 . The silver wire composition is as follows:

<u>Element</u>	<u>Percent In Core</u>	<u>Percent In Cladding</u>
Silver	99.95 Min	
Nickel	0.001	99.65
Copper	0.05	0.03
Iron	0.002	0.05
Manganese	0.001	0.10
Silicon	0.001	0.03
Carbon		0.05
Sulfur		0.005
Arsenic	0.00	
Phosphorus	0.00	
Oxygen	0.00	0.05
Nitrogen	0.00	0.05

Initial samples of the ceramicclad insulated Ni-clad silver wire were tested for insulation breakdown at the elevated temperature and voltages. The resistance testing was done by twisting together two wire lengths and measuring the resistance between them with a General Radio Impedance Bridge. Figure 29 shows the insulation resistance as a function of temperature. A voltage breakdown of 23 vdc was measured at 1100°F; the nominal transducer operational voltage is about 5 vdc.





A comparison was also made of the wire resistance before and after ceramic coating. The calculated resistance was 0.765 ohms/ft. Measured values were for the uncoated wire--0.773 ohms/ft and for the coated wire--0.810 ohms/ft. The coated wire undergoes a curing process at 1900°F during the insulating process.

The ceramic coated wire was sectioned and photographed at 500X magnification in the etched and unetched condition as shown in Figure 30. The section clearly shows a uniform cladding thickness but the insulation is largely invisible. The large axe-shaped piece in the upper photograph is a portion of the cladding that was peeled away. After initial tests indicated satisfactory wire properties, several coil sets were prepared with 36-, 38- and 40 gauge sizes tested at 1000°F for approximately 1000 hr. Coil resistance versus time at temperature is shown in Figure 31. The coil wound with No. 36 aluminum wire showed no degradation with time.

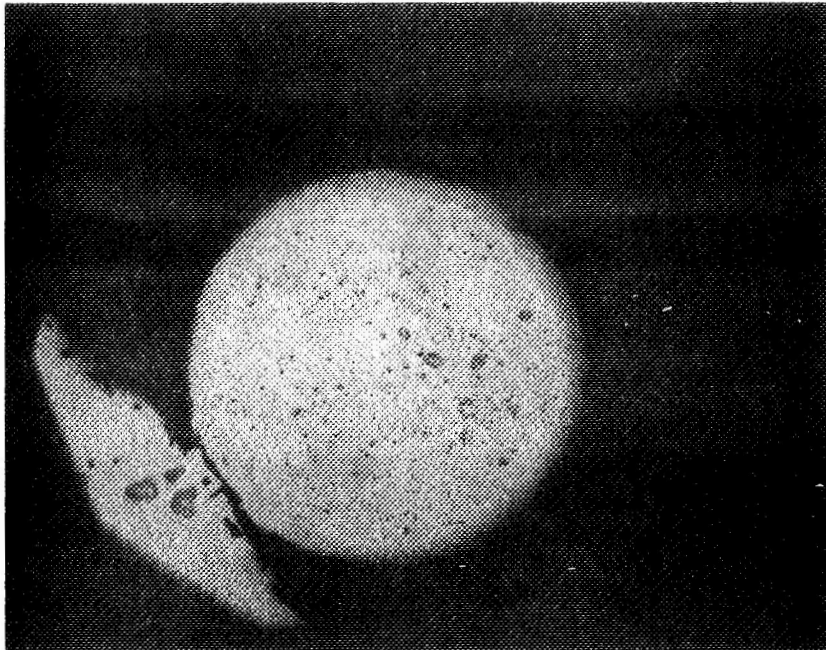
Three of the four coils wound with No. 36 nickel-clad silver wire also showed no change in resistance. The fourth coil experienced a mechanical failure at the wire termination post on the coil. The coils wound with the smaller sizes of nickel-clad silver wire showed various stages of deterioration. From the early start of these tests, it was evident that only the largest wire, No. 36 gauge, should be used for high temperature transducers.

Based on the results of the first test, a second coil stability test was made. This test consisted of 24 coils, 12 wound with No. 36-gauge nickel-silver wire and 12 wound with No. 36-gauge aluminum wire, placed in an oven and a means provided for monitoring the electrical characteristics from outside the oven. The test was terminated at 2200 hr. Figure 32 shows the stability of each coil as a function of time at temperature.

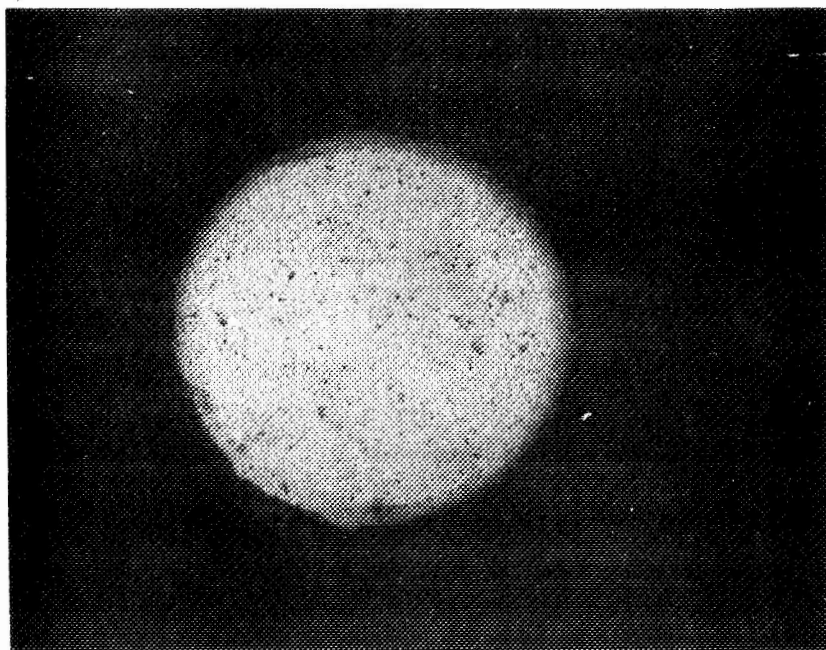


AIRESEARCH MANUFACTURING COMPANY OF ARIZONA
A DIVISION OF THE GARRETT CORPORATION
PHOENIX, ARIZONA

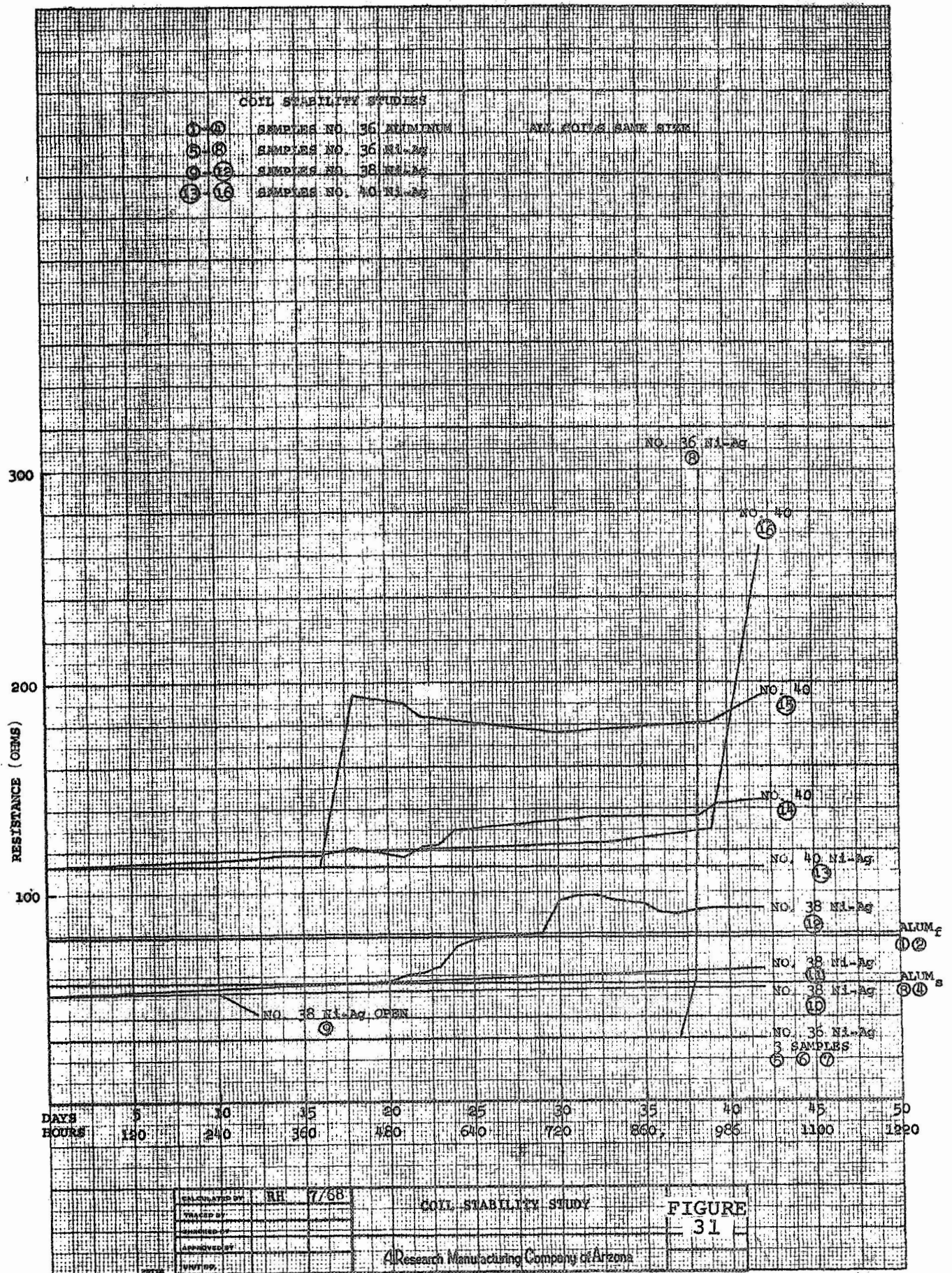
WIRE DIAMETER - 0.0045

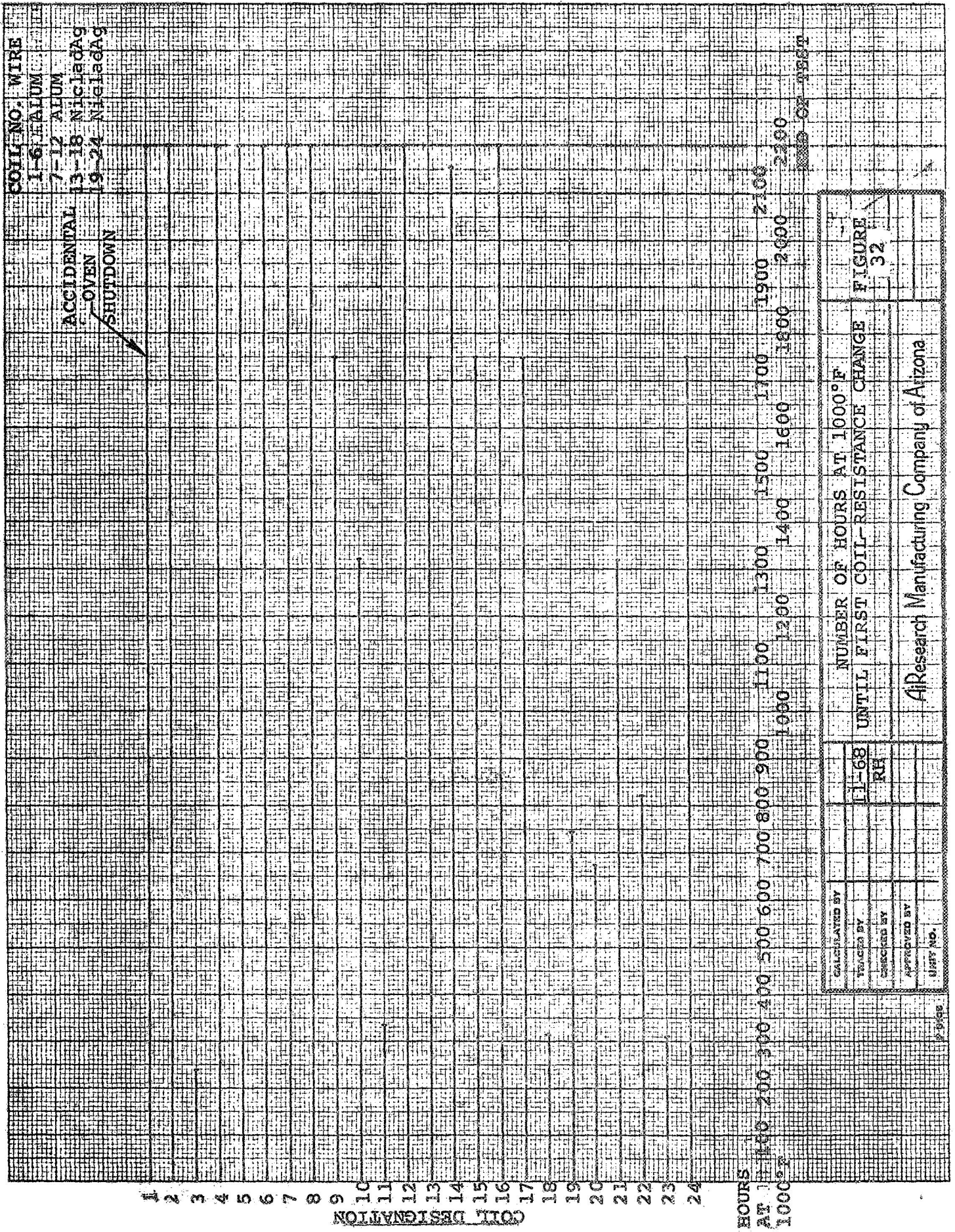


UNETCHED - 500X MAG



ETCHED - 500X MAG
NICKEL-CLAD SILVER WIRE WITH "CERAMICITE"
INSULATION CURED AT 1900F
FIGURE 30







Inspection of the coils after removal from the oven revealed the following results. All 12 coils wound with No. 36 aluminum wire were intact and had not changed in resistance. However four of these were open where the wires joined the terminal pins of the coil. The 12 coils wound with No. 36 nickel-clad silver wire were either open and showed evidence of burn spots on the wire or showed an increase in resistance from the initial resistance values. Seven of the 12 were also open at the terminal pins on the coil forms.

Two types of potting compound were used in the coils--Technical G Copper Cement, and PBX Ceramic Cement. The PBX cement held up very well during the 2200 hr, while the Technical G changed color and cracked away from the terminal pins and wires. It also had a crumbly appearance.

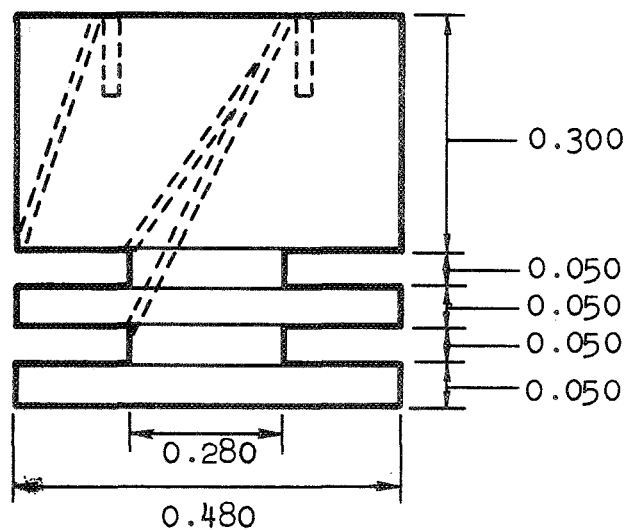
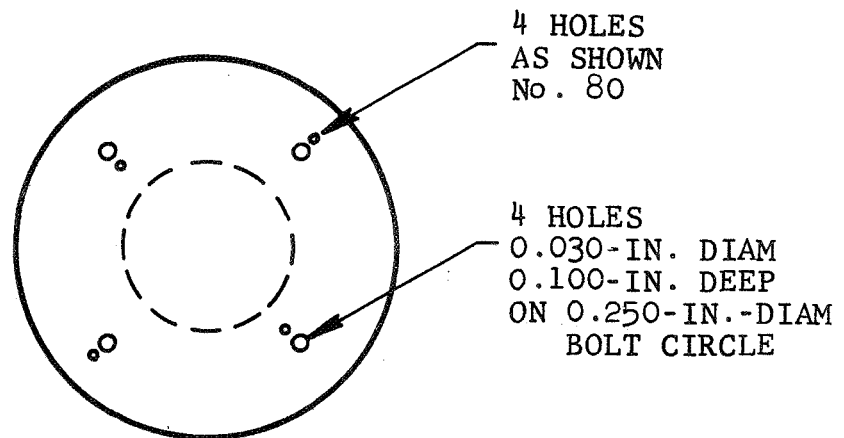
4.2.3.2 Test Transducer Fabrication

Probes were fabricated for use during the static bench tests, calibration test rig development and, of course, for the final endurance testing.

Several steps are required to complete the fabrication of coil assembly for the film-thickness transducer. The first step involves making the coil form itself (Figure 33). If made from Lava it is machined to shape on a lathe and then fired to form a dense ceramic structure. If the form is made from Al_2O_3 as were all final configurations, it is ground to the appropriate shape. Next, the primary and secondary coils are wound with the appropriate number of turns of ceramic insulated core. After a pair of coils is wound they are connected together and balanced electrically on the fixture shown in Figure 34. The primary windings are joined in series and connected to



AIRESEARCH MANUFACTURING COMPANY OF ARIZONA
A DIVISION OF THE GARRETT CORPORATION
PHOENIX, ARIZONA



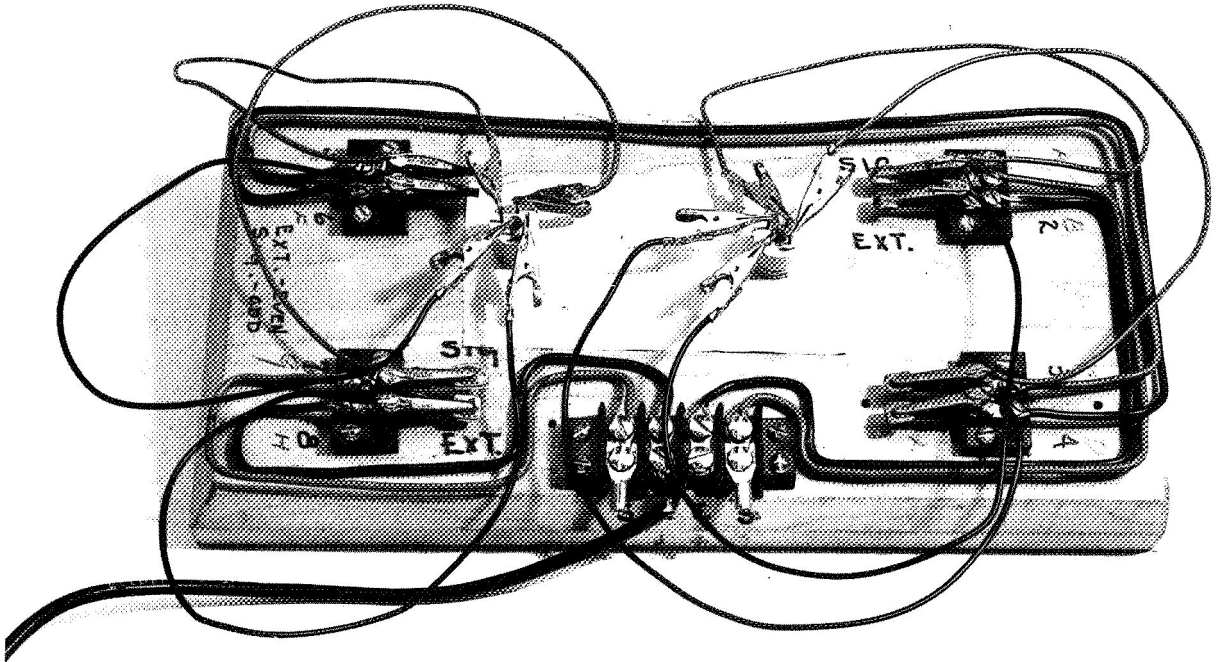
MATERIAL:
CERAMIC

COIL CONFIGURATION DRAWING

FIGURE 33



AIRESEARCH MANUFACTURING COMPANY OF ARIZONA
A DIVISION OF THE GARRETT CORPORATION



COIL BALANCE FIXTURE
WITH TWO COILS IN PLACE

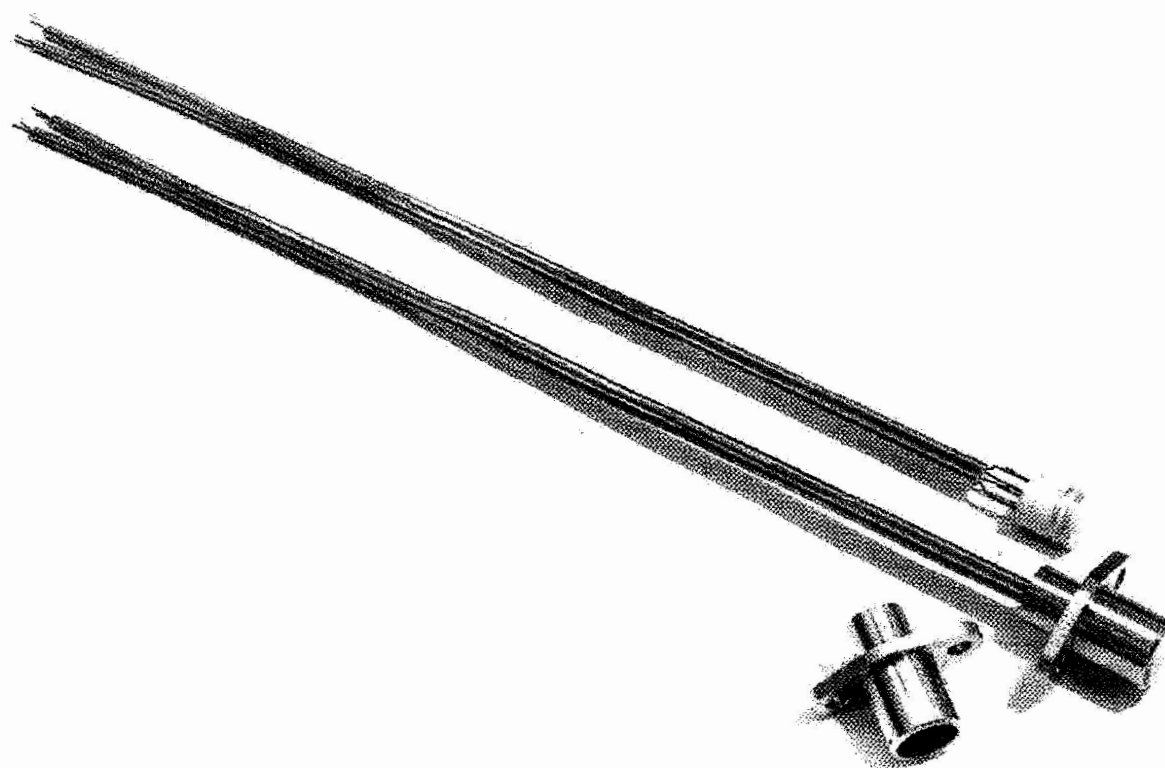
FIGURE 34



a 20-k-Hz oscillator. The oscillator output is 5 volts rms. The secondary windings are connected in series opposition such that the output of one coil cancels the output of the other coil. The resultant output is displayed on an oscilloscope and/or a digital voltmeter. In order to keep the unbalance at a reasonable value, turns of wire are removed from one secondary coil to lower the unbalance to at least 5 mv peak-to-peak. After initial balancing the coils are heated to 1000°F for about one hour. They are rechecked for balance, turns removed as necessary, and the coils reheated. Usually two or three heating cycles are sufficient to stabilize the coils. Leads are fastened to the coil pins and the coils assembled in the coil holders. Temperature cycling is again performed to insure system stability. The coils are then permanently fastened in the holders and connectors attached to the coil leads. A completed transducer set is shown in Figure 35.



AIRESEARCH MANUFACTURING COMPANY OF ARIZONA
A DIVISION OF THE GARRETT CORPORATION



FILM THICKNESS TRANSDUCER COILS
WITH HOLDERS AND LEAD WIRES

FIGURE 35



4.2.3.3 Material Property References for Section 4.2

1. TZM data - Climax Molybdenum Co. of Mich. Huron Pkwy., Ann Arbor, Mich.
2. T-111 data - Aerospace Structural Metals Handbook, ASD-TDR-63-741, Vol. II, Mar. 1965.
3. Tungsten carbide data - Thermal Properties of 26 Solid Materials to 5000°F, ASD-TDR-62-765, Jan. 1963.
4. Potassium data - Liquid Metals Handbook, Revised Ed. 1954, Oak Ridge Nat. Lab.
5. H-11 data - Westinghouse Elec. Corp., Aerospace Elec. Div., Lima, Ohio, Mats, Eng. Lab. Rept.
6. 316 stainless steel data - Aerospace Structural Metals Handbook, ASD-TDR-63-741, Vol. I, Mar. 1965.
7. Inconel X data - Materials Lab., AiResearch Mfg. Co.
8. Ti-6Al-4V data - Aerospace Structural Metals Handbook, ASD-TDR-63-741, Vol. II, Mar. 1965.
9. TiC-10 Cb data - NASA Lewis.
10. Zirconium, Titanium, Al_2O_3 and Phenolic data - Materials engineering, Materials Selector Issue, Oct. 1967.



5. CALIBRATION TESTING (TASK II)

The intent of Task II was to provide a calibration test rig capable of verifying the analytical and empirical studies of Task I, and providing in-place calibration of the selected transducer design. The calibration test rig met the following requirements:

- (a) Temperature variation from ambient to 1000°F
- (b) Rotational speeds from 0 to 25,000 rpm at temperature
- (c) Measurement of motion of the shaft in two mutually perpendicular planes to an accuracy of ± 0.00005 inch
- (d) Applicability to refractory-alloy material combinations

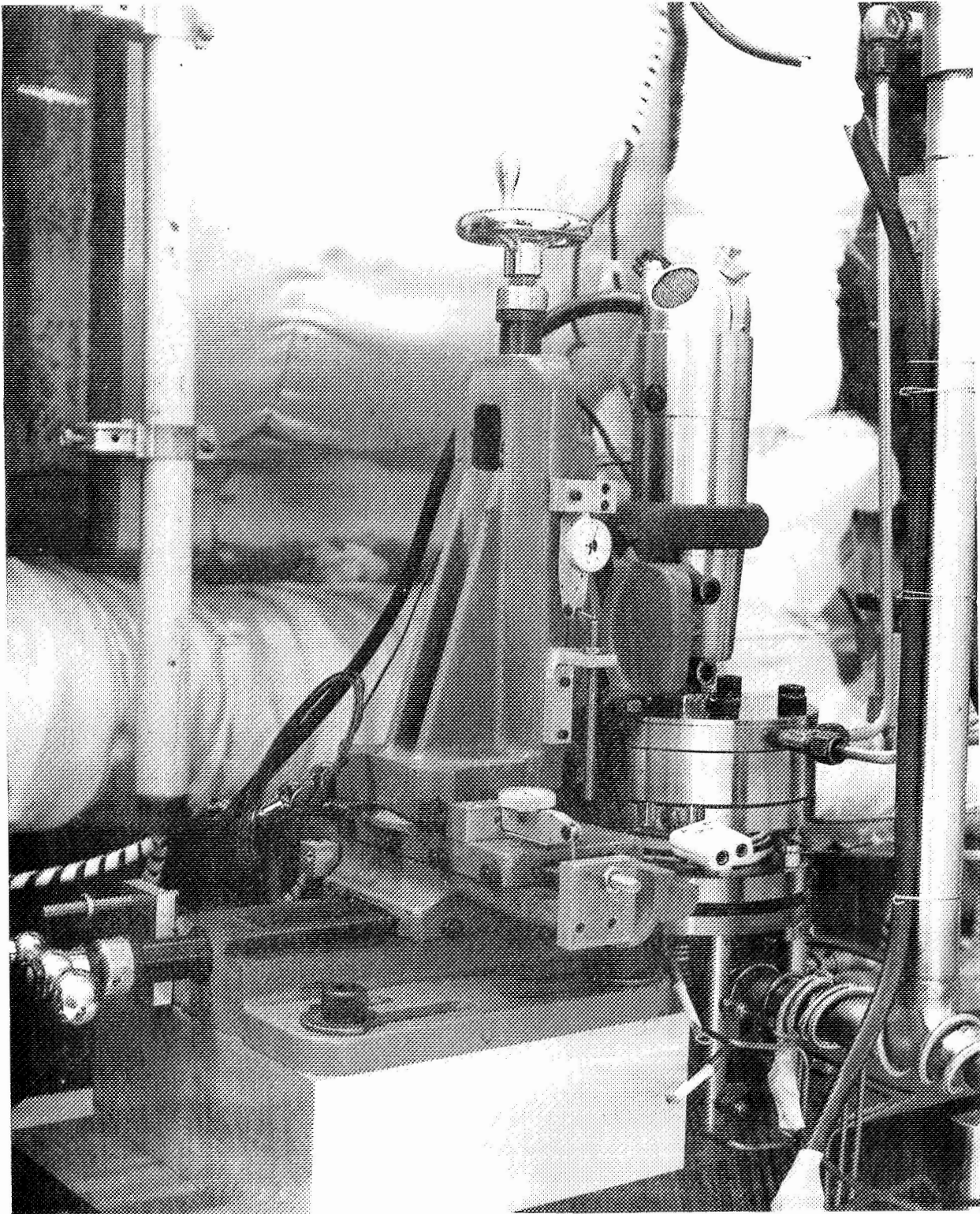
Final hardware evolved from an existant AiResearch calibration test rig shown in Figure 36.

5.1 Calibration Rig Description

The rig (Figure 37) consists of a precision rotating spindle mounted in pneumostatic journal bearings. The shaft penetrates the potassium-filled-probe test housing through a combination mechanical face seal and dynamic seal with an argon buffer between. The rotating spindle/bearing assembly is mounted to the base plate through a pair of mutually perpendicular, linear antifriction rollerways. The shaft is driven by a plant-air-activated air turbine. Manual movement of the spindle is controlled by precision micrometer heads reading directly to 0.00001 in.

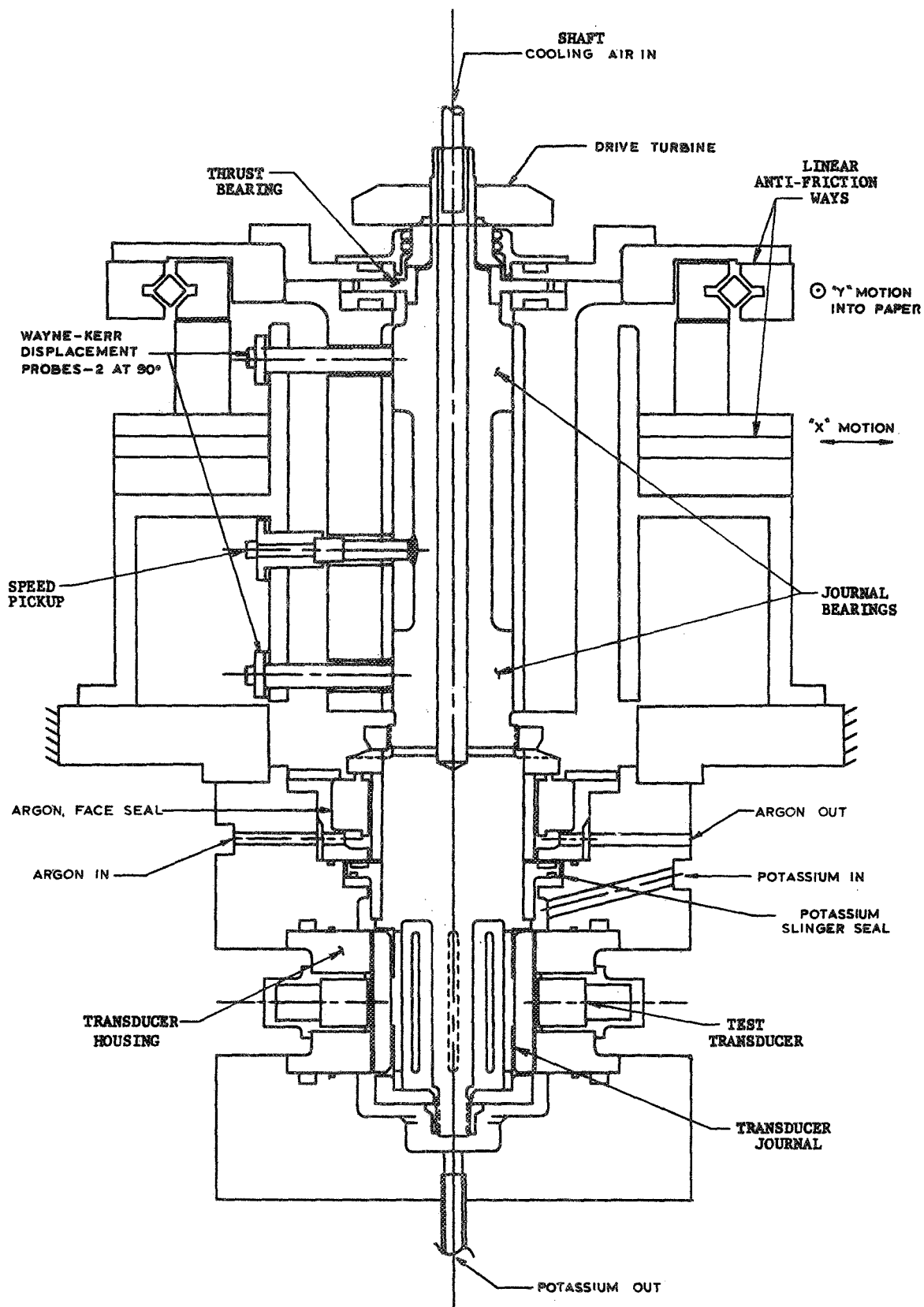


AIRESEARCH MANUFACTURING COMPANY OF ARIZONA
A DIVISION OF THE GARRETT CORPORATION



FILM THICKNESS PROBE CALIBRATION TEST RIG

FIGURE 36



PREPARED	JFG	10-67	POTASSIUM FILM THICKNESS CALIBRATION RIG	FIGURE 37
WRITTEN				
APPROVED			AlResearch Manufacturing Company of Arizona	

FORM 1705A-1



Radial movement of the precision spindle is measured by two pairs of high-precision Wayne-Kerr capacitance probes mounted in each air bearing. These capacitance probes are calibrated external to the rig through direct mechanical measurement of specimen movement with a Model 21-4000-00 Micro-Displacement Calibrator manufactured by Clevite Corporation. This device is capable of rendering a probe calibration accuracy of about ± 5.5 microinches for the range of movement of interest (0.015 inch). The minimum dial graduation on this device is 20 microinches with a digital readout device available to half that dimension.

The film-thickness-probe test head consists of a cylinder of the particular housing material of interest, containing the eddy-current coil assemblies and sandwiched between two housings of a material of similar thermal expansion. The assembly is not seal-welded but is statically sealed with metal sealing rings. This design feature allows for the greatest degree of versatility in testing different housing (refractory) materials, various coil configurations, and required window configurations.

The portion of the rotating spindle upon which motion is to be sensed is separate from the basic spindle. It is mounted to the spindle through a slotted shaft arrangement intended to compensate for differences in thermal expansion and yet provide positive register with the specimen. This device is shown schematically in Figure 38. The test-coil housing is surrounded by a resistance clam-shell-type heater to provide the required ambient operating temperature. The heater enclosure also serves as a light vacuum or inert-gas chamber to handle potassium leakage and to minimize oxidation in the high-temperature region.

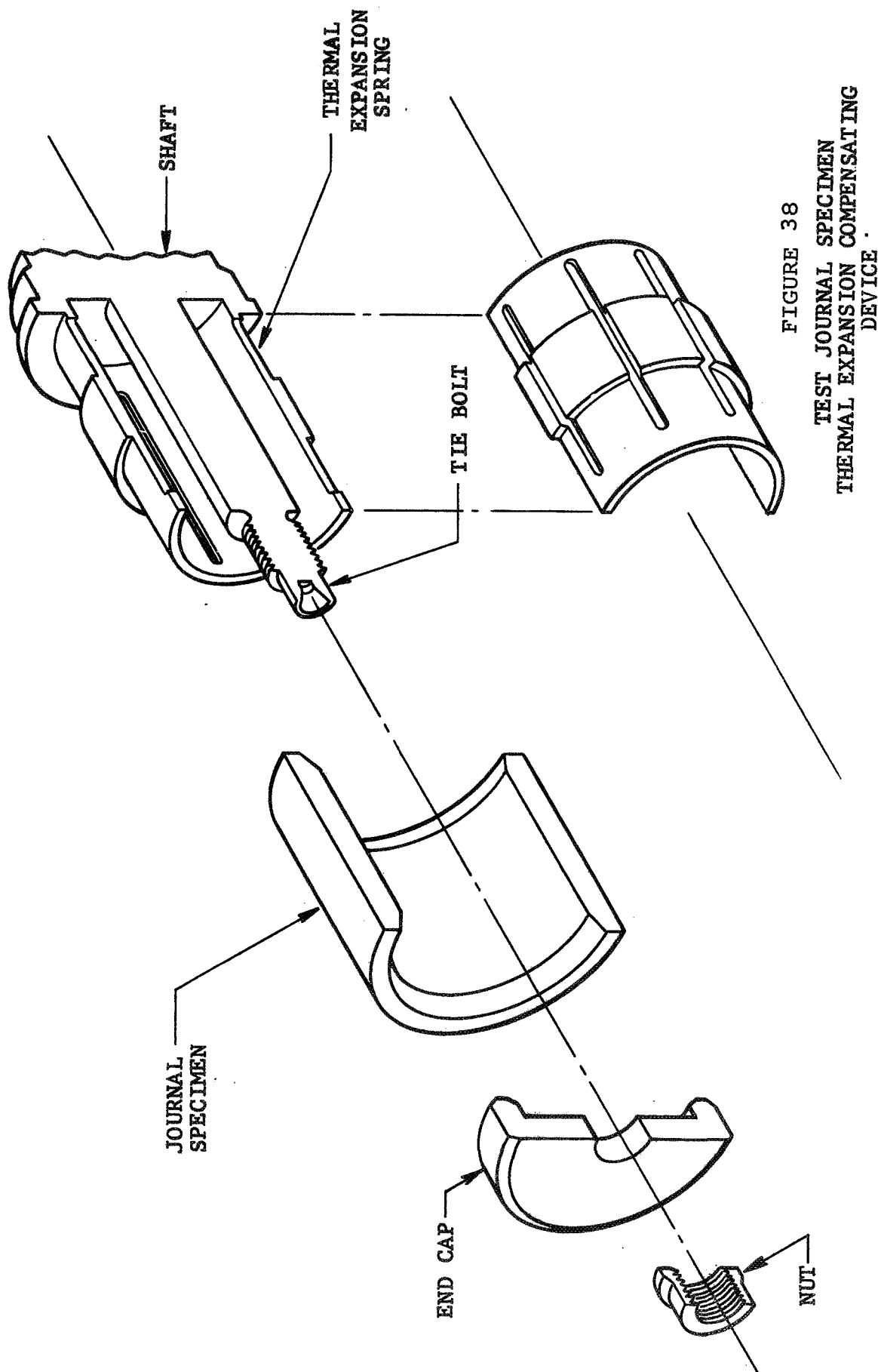


FIGURE 38

TEST JOURNAL SPECIMEN
 THERMAL EXPANSION COMPENSATING
 DEVICE



5.1.1 Detail Design Considerations

A number of detailed changes and modifications were incorporated into the design of the existent calibration rig. The following improvements were added:

- (a) The x-y cross-slide system support ring was made completely symmetrical, and a feature was added to allow it to flex thermally without distorting the cross-slide assembly.
- (b) A pneumostatic thrust bearing replaced the anti-friction thrust bearing.
- (c) The heater enclosure around the instrumentation section was modified to serve as a light vacuum or inert-gas (argon) chamber to handle potassium leakage and minimize oxidation in the high-temperature region.

In addition, extensive studies were made of the rotor suspension system (journal and thrust bearings) together with a complete thermal analysis of the unit to determine how expansion and vibration would effect measurement sensitivity.

5.1.1.1 Calibration Test Rig Rotor System Natural Frequencies

Critical-speed and bearing-load considerations were major factors in the design of the test rotor. In order to minimize shaft eccentricity under operating conditions, the rotor geometry and bearing stiffnesses were examined together. The dependence of critical speeds of the rotor upon the bearing stiffnesses is presented in Figure 39. Practical bearing stiffnesses, based upon bearing design considerations, dictate operation between the first and second critical speeds.

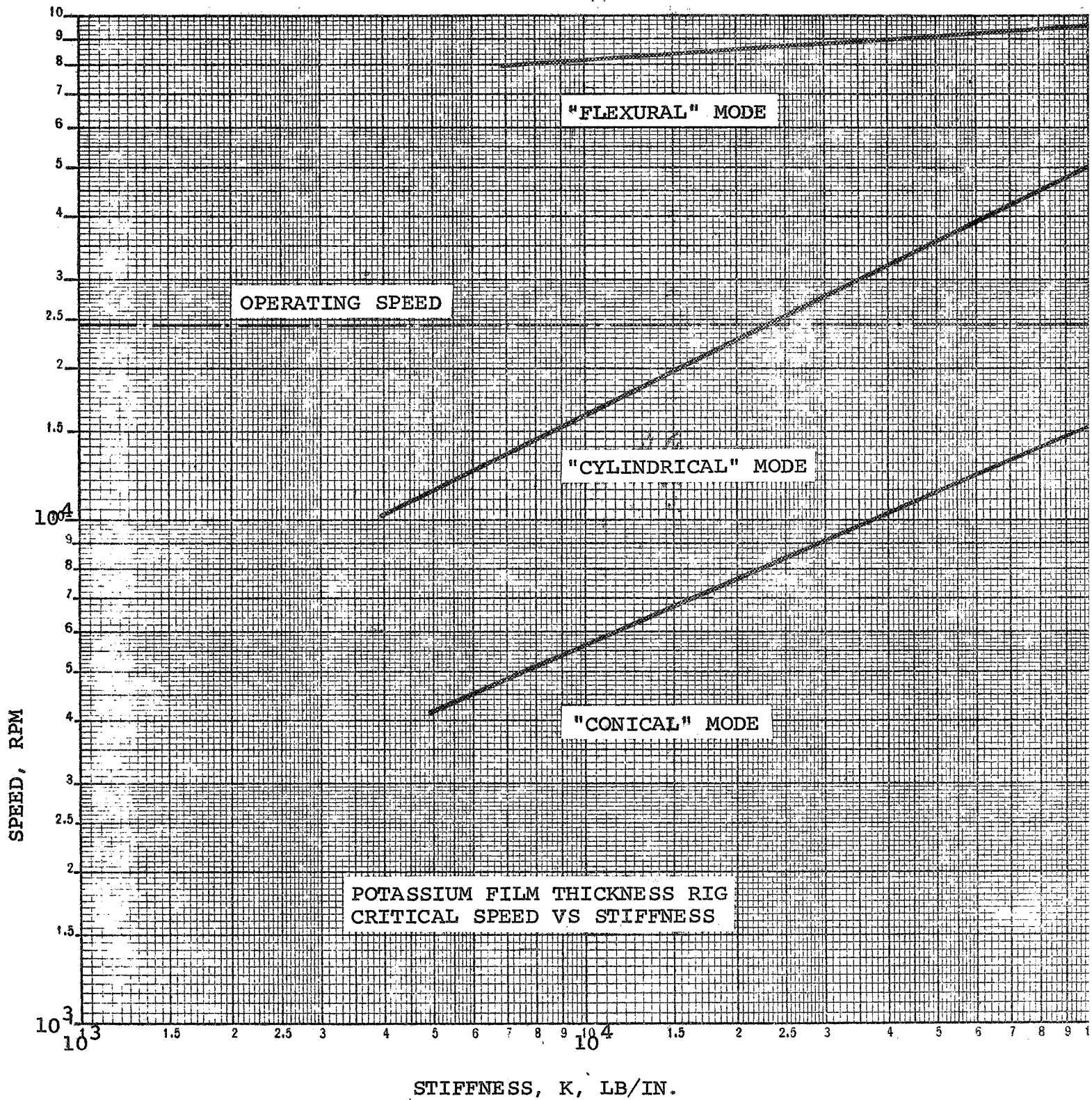


FIGURE 39.



Bearing stiffnesses of approximately 5×10^4 lb/in. were found to minimize the bearing loads at operating speed. A plot of these loads as a function of speed is shown in Figure 40, for a static unbalance of 0.0001 in. At design speed (24,000 rpm), the loads are seen to be higher than desirable, implying the need for very precise balance of the rotor.

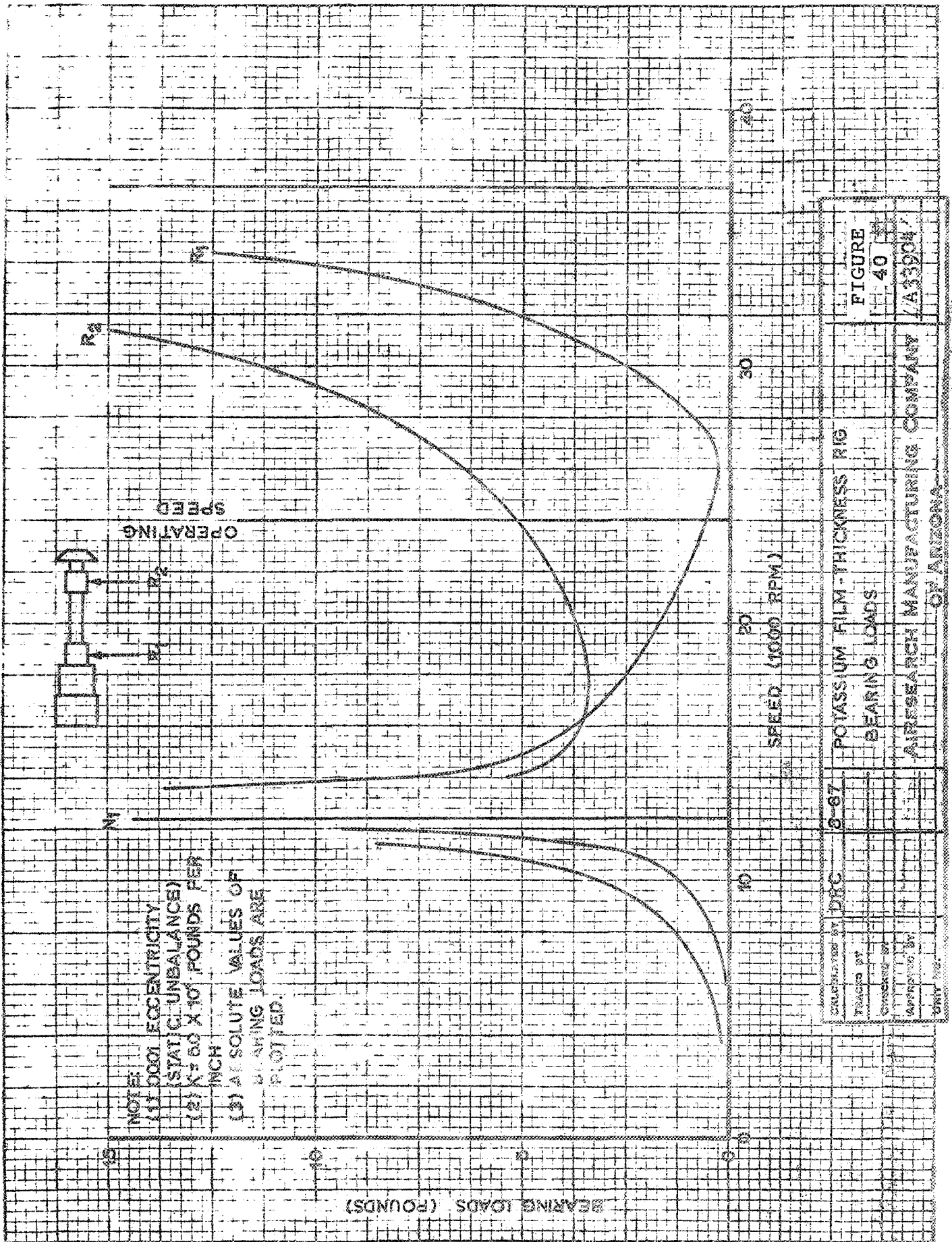
5.1.1.2 Gas Journal Bearing Design

Selection of the bearing type for support of the test rotor was based upon the following criteria:

- (a) Smoothness of operation
- (b) Ability to operate in a high-temperature environment
- (c) Minimum runout
- (d) Stability
- (e) Stiffness (as specified by the critical-speed analysis)

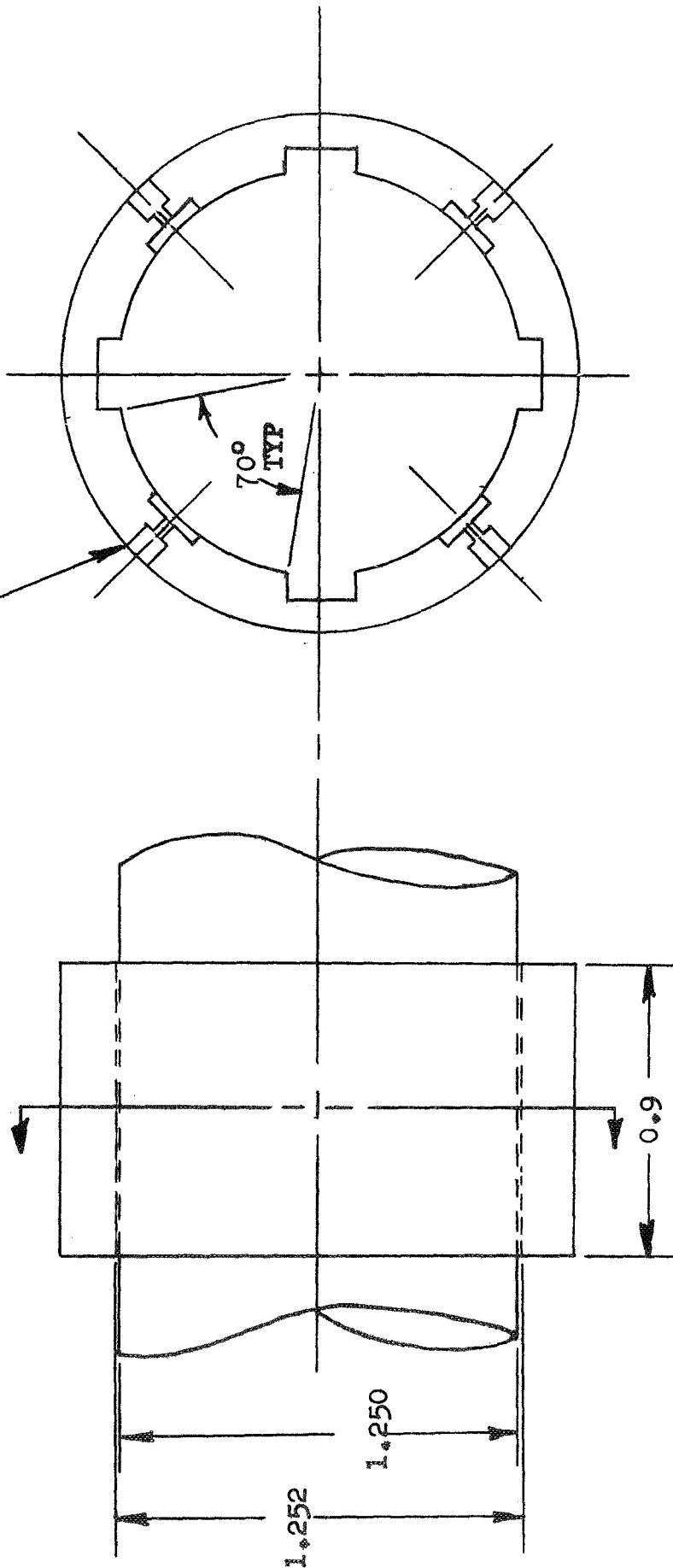
It appeared that a hydrostatic air bearing would best satisfy these requirements and the final design geometry is shown in Figure 41. Load deflection for this geometry at 150 psia supply pressure is shown in Figure 42. The single-pad stiffness is seen to be about 30,000 lb-per square inch. The four-pad bearings will therefore have a stiffness of 60,000 lb/in. (independent of direction). Stability and stiffness were the major design goals.

Two possible types of instability were considered throughout this design:



FEEDING HOLE INFORMATION:

- (1) ORIFICE DIAM = 0.018 INCH
- (2) POCKET DIAM = 0.1875 INCH
- (3) POCKET DEPTH = 0.005 INCH
- (4) MASS-FLOW RATE WILL BE LESS THAN 16.7 LB/HR (FOR THE TWO BEARINGS COMBINED)



POTASSIUM FILM-THICKNESS TEST RIG GAS BEARING GEOMETRY		FIGURE 41	
AiResearch Manufacturing Company of Arizona		A33905	
PREPARED	DRC	9/67	
WRITTEN			
APPROVED			

SINGLE PAD LOAD (POUNDS)

20

10

0

0

01

02

DEFLECTION ($\times 10^{-3}$ INCHES)

$K = 31,800$ LBS PER INCH

NOTE:

(1) PAD CONFIGURATION SHOWN
IN FIGURE 3

(2) THIS CURVE IS FOR A SINGLE
PAD ONLY

(3) DEFLECTION IS TOWARD THE
ORIFICE

(4) SUPPLY PRESSURE = 150 PSIA

CALCULATED BY

DRC

TRACED BY

CHECKED BY

APPROVED BY

UNIT NO.

POTASSIUM FILM - THICKNESS RIG
SINGLE-PAD LOAD VS DEFLECTION

FIGURE
42

AirResearch Manufacturing Company

A339064

A-5116



- (a) Hydrostatic instability ("pneumatic hammer")
- (b) Hydrodynamic instability ("self-excited" whirl)

Pneumatic hammer is dependent upon the total bearing and feeder-hole geometry, the most critical factors being bearing clearance and orifice diameter. The design presented herein has been stable in this respect. The possibility of hydrodynamic instability has been eliminated by minimizing hydrodynamic forces developed within the bearing film. This has been accomplished by the four pads separated by grooves of significant widths. Past experience indicates that the hydrodynamic flows are sufficiently broken up by the configuration such that operation at above twice the first critical speed should be no problem.

5.1.1.3 Test Rotor Gas Thrust Bearing Design

Aerodynamic analysis indicated that rotor thrust loads of 35 lb upward and 5 lb downward (largely due to the pressure differences across the drive turbine) might be encountered during unit operation. To sustain this load spectrum under all operating conditions, a double acting, air thrust bearing with hydrostatic capability was designed. The critical parameters for each side are as follows:

- (a) Outer radius = 1.0 in.
- (b) Inner radius = 0.5 in.
- (c) Orifice radius = 0.013 in.
- (d) Orifice pocket radius = 0.0625 in.
- (e) Orifice pocket depth = 0.005 in.



(f) Eight orifices equally spaced on a radius of 0.75 in. with radial slots midway between them.

(g) The mass flow rate will be less than 35.2 lb/hr.

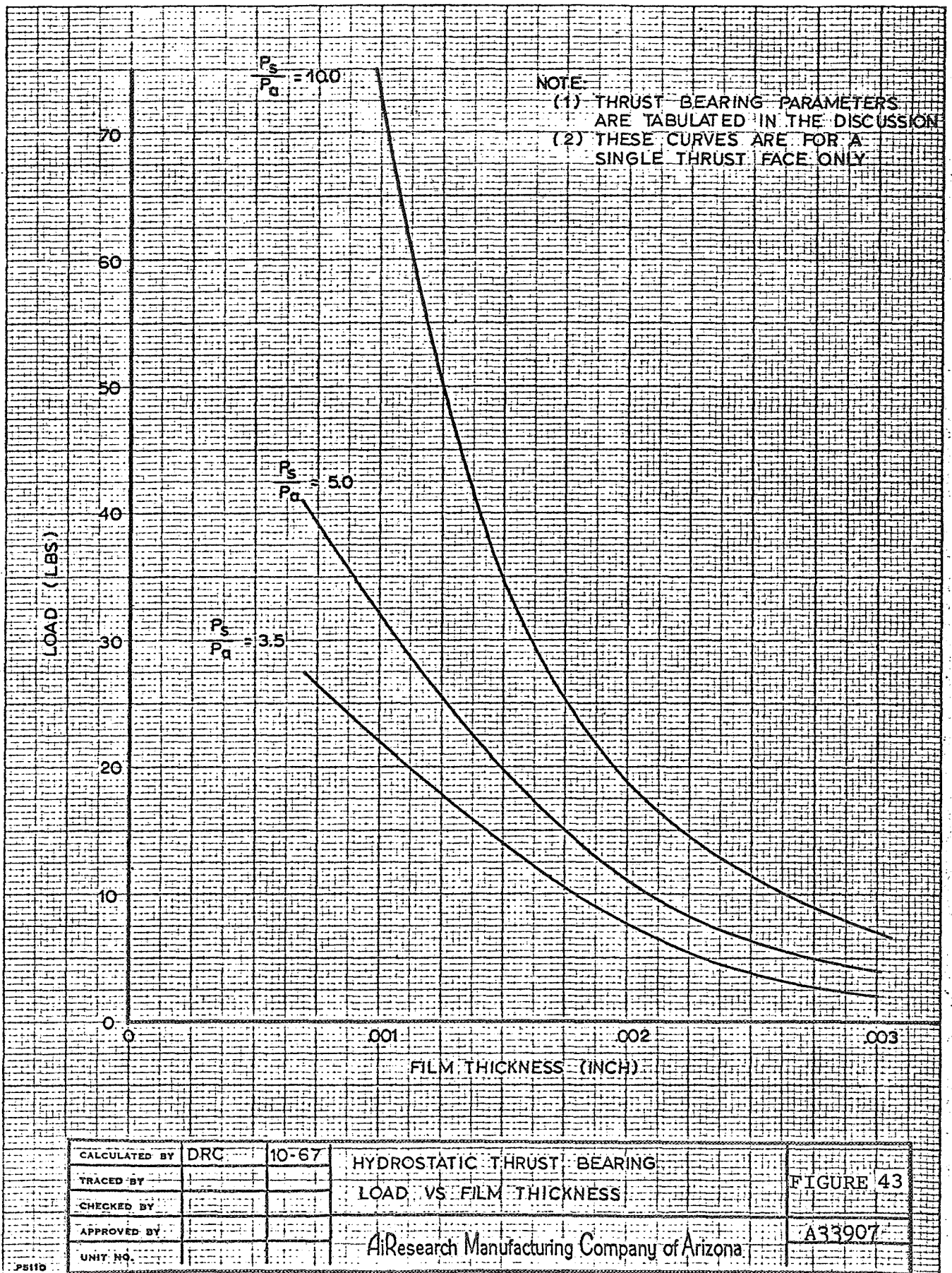
For this configuration, Figure 43 presents the load-versus film-thickness characteristics as a function of supply pressure with the total axial clearance assumed to be large enough that only one thrust face is loaded at any particular time (about 0.004 in.), either of the bearing surfaces will support the maximum required load with a film thickness of 0.0008 in. and a supply-to-ambient-pressure ratio of 5.0. The relatively large operating clearance (especially if the supply pressure ratio is greater than 5.0) will minimize problems due to thermal and elastic distortions and misalignments. Estimated elastic deflection appears to be no larger than 0.000060 in.

5.1.1.4 Potassium Test Journal Design

The instrumentation probes are to be evaluated with test journals of four different materials. Presented below are the significant material properties of each candidate journal.

JOURNAL MATERIAL PROPERTIES

<u>Material</u>	Coefficient of Thermal Expansion $\alpha \cdot 10^6 (\frac{1}{^\circ\text{F}})$	Density $\rho (\text{lb}/\text{in}^3)$	Modulus of Elasticity $E \cdot 10^{-6}$		Yield Strength σ at 1000°F (psi)
			70°F	1000°F	
TZM	3.1	0.369	46.0	38.0	60,000
WC (K-96)	2.8	0.538	91.6		200,000
H-11	7.4	0.281	30.0	22.8	90,000
T _A -111	3.5	0.603	26.0	24.4	39,500
M ₂ (Shaft Material)	6.6	0.285	31.0	23.5	250,000





Each test journal is supported on the rotor by a thermal expansion compensating mounting technique. Eight axial slots symmetrically placed are used to form eight beams. Each beam is highly flexible with respect to locally applied radial loads, but virtually rigid with respect to tangentially directed loads. This supporting method thus provides necessary freedom for differential thermal expansion between the journal and the rotor while affording an essentially rigid support with respect to externally applied transverse loads.

In order to insure the desired measurement accuracy of 5×10^{-5} in. the displacements in the test journal in the operating environment were investigated in considerable detail. Both the thermal change from room temperature to 1000°F and the operating speed of 24,000 rpm were found to significantly affect the journal deflections.

During the manufacture of the test journals, the journal is shrink-fitted on the shaft, and the journal held in place by an initial interference. The outer diameter of the journal is then ground concentric with the shaft gas bearing journals. This process also removes any initial "crowning" of the test journal that might otherwise be caused by the contact pressure between the shaft and the journal. The effects of the operating environment on the journal deflections are shown below.

JOURNAL DISPLACEMENTS
(Inches)

<u>Journal Material</u>	<u>Recommended* Initial Interference</u>	<u>Interference* at 1000°F</u>	<u>Centrifugal* Journal Growth (O.D.) $\times 10^5$</u>	<u>Journal,*,** Crowning $\times 10^5$</u>
TZM	0.001	0.00313	4.78	6.3
WC	0.001	0.0031	2.89	2.7
H-11	0.003	0.00251	6.06	7.4
T-111	0.001	0.00286	12.13	9.4

*Radial interference or growth.

**Difference between the radius at the center and of the journal due to temperature change and centrifugal force of the beams.



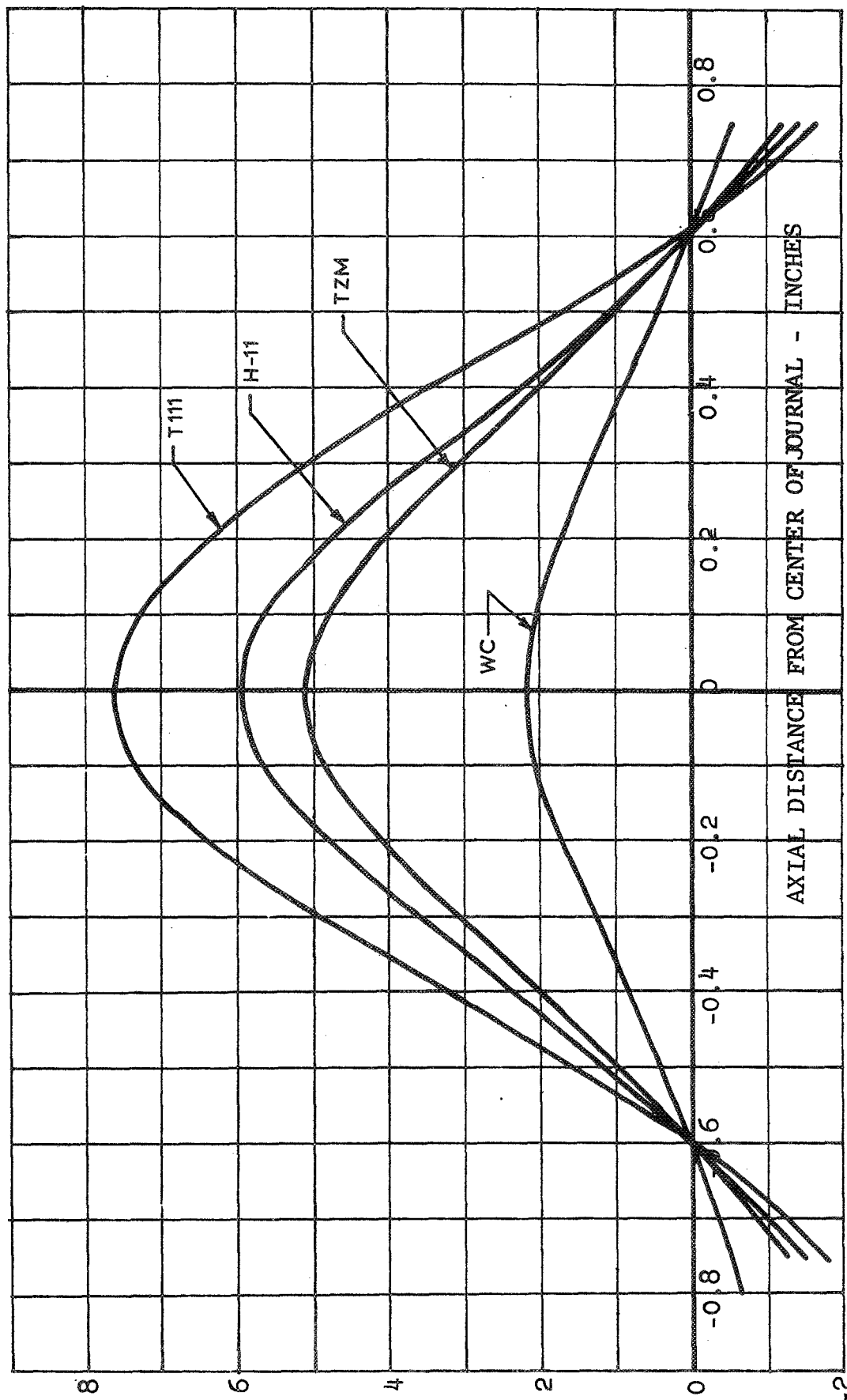
As shown above the temperature changes will reduce the contact interference and contact pressure for the H-11 journal mounted on the M-2 shaft. The other journal materials will have an increased interference at 1000°F over room temperature. At operating speed, the centrifugal force will tend to throw the beams out against the journal. Because of the radial flexibility of the beams and the stiffness of the journal, this centrifugal force is almost entirely supported by the journal. Therefore, both the temperature increase (except for the H-11 journal material) and the centrifugal force will tend to increase the contact pressure between the support beams and the test journal. The deflection curves of the test journals due to the above loads are shown in Figure 44.

The bending stresses in the journal support beams are well within the acceptable range. The greatest stress at room temperature in the journal support beam is 112,500 psi (yield point >300,000 psi). Maximum stress at elevated temperature is 93,600 psi (yield point at 1000°F >200,000 psi). The test journal itself is lightly stressed as evidenced by the maximum tangential stresses presented below for various test journal materials:

TEST JOURNAL TANGENTIAL STRESS (PSI)

<u>Material</u>	<u>Rotational Component</u>	<u>Contact Pressure Component</u>	<u>Total Tangential Stress</u>
TZM	4,120	4,340	8,460
WC	6,000	3,980	9,980
H-11	3,130	4,070	7,200
T-111	6,700	4,230	10,930

RADIAL CHANGE FROM TEMPERATURE AND CENTRIFUGAL
LOADS - INCHES $\times 10^3$



CROWNING OF JOURNAL OF VARIOUS MATERIALS
DUE TO THERMAL AND CENTRIFUGAL LOADS

FIGURE 44

A33908

AIResearch Manufacturing Company of Arizona

PREPARED JFG 10-16-67

WRITTEN

APPROVED



As mentioned previously, the journal support beams are formed from segments of the test journal. Under most of the load conditions, the beam is bent normal to the axis of minimum section modulus. The beam can be considered as a beam fixed at both ends and loaded by a uniform pressure in the center. The equivalent spring constant of this beam is $K_{eq} = 37,200 \text{ lb/in.}$ at room temperature and $28,200 \text{ lb/in.}$ at 1000°F .

The individual beams are relatively "soft" in the radial direction, as shown by the spring constants given above. However, the journal support system consists of a total of eight beams. When a single transverse load is applied to the journal, these beams will be at various orientations to the load, so that the effective bending stiffness of some beams will differ considerably from that cited. The total stiffness of the journal supports yields an effective journal spring constant of $3.9 \cdot 10^6 \text{ lb/in.}$, which is considered to be more than adequate, provided that slipping does not occur. After sufficient load is applied to overcome the static friction, however, the stiffness will progressively reduce at 24,000 rpm, contact loads between the journal and each beam are computed to be over 250 lb.

During calibration of the film-thickness transducer, the journal will be moved from the center of the bearing. Though the bearing clearance is large, a small hydrodynamic force will be generated by the rotation at this eccentricity. This transverse force of the test journal will tend to displace the shaft within its gas-lubricated journal bearings. The deflection at the test journal due to the above force depends upon the stiffness of the gas journal bearings. The effective spring constant of the gas journal bearings resisting loads at the test journal with respect to displacements at the test journal is $9,050 \text{ lb/in.}$, based upon a radial stiffness at each gas bearing of $50,000 \text{ lb/in.}$ Because hydrodynamic loads developed at the test journal



are of the order of one lb, the associated radial deflections there may be significant. The presence of capacitance probes in two axial planes allows this deflection to be calculated.

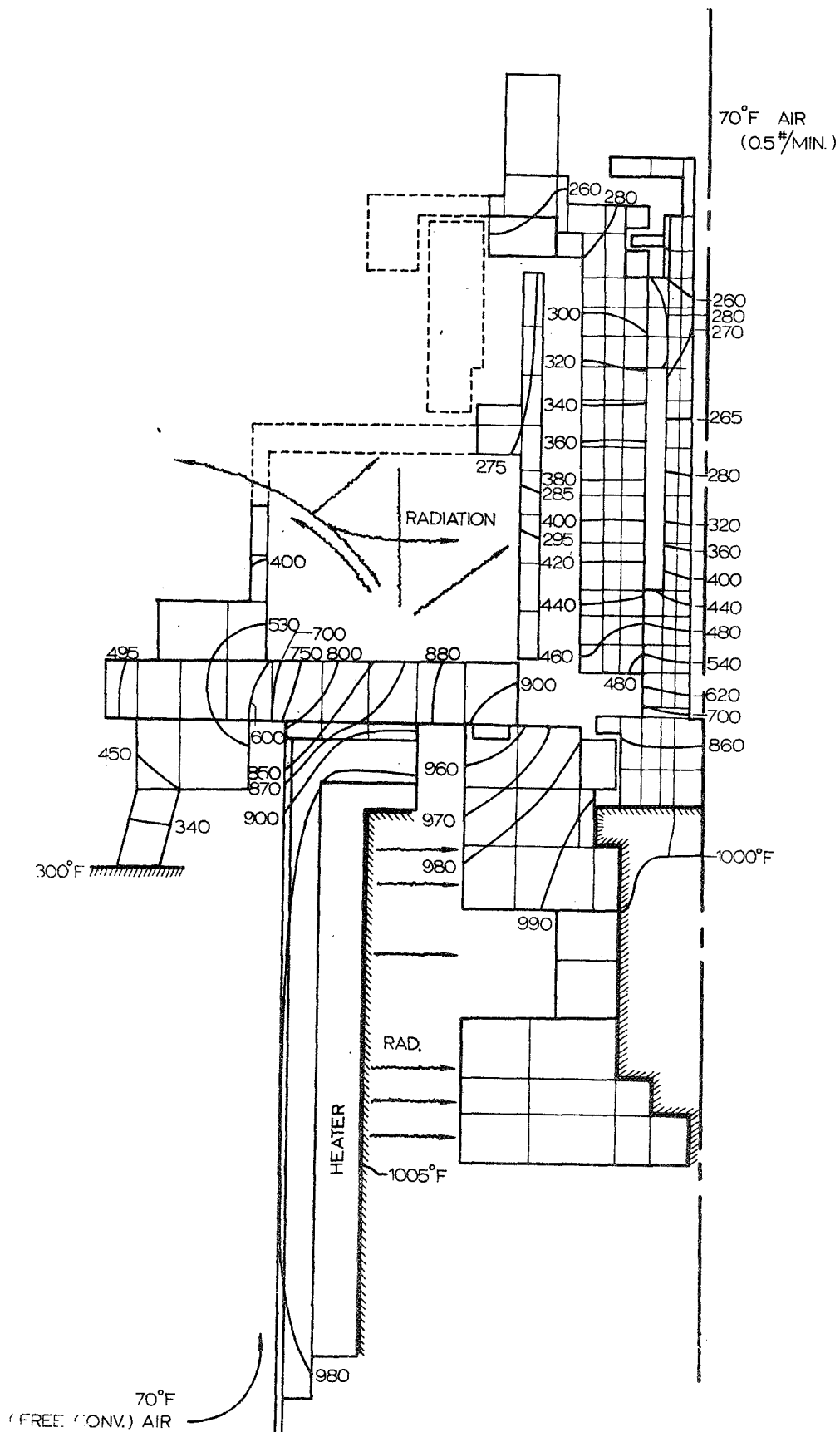
Also at the operating conditions of 24,000 rpm and 1000°F, the potassium exists as a vapor in the annular region formed by the tie-bolt and the journal inside diameter. The liquid-vapor interface will exist at a radius of approximately 0.9 in. and should have a desirable effect upon rotor apparent mass unbalance.

5.1.2 Calibration Test Rig Thermal Analysis

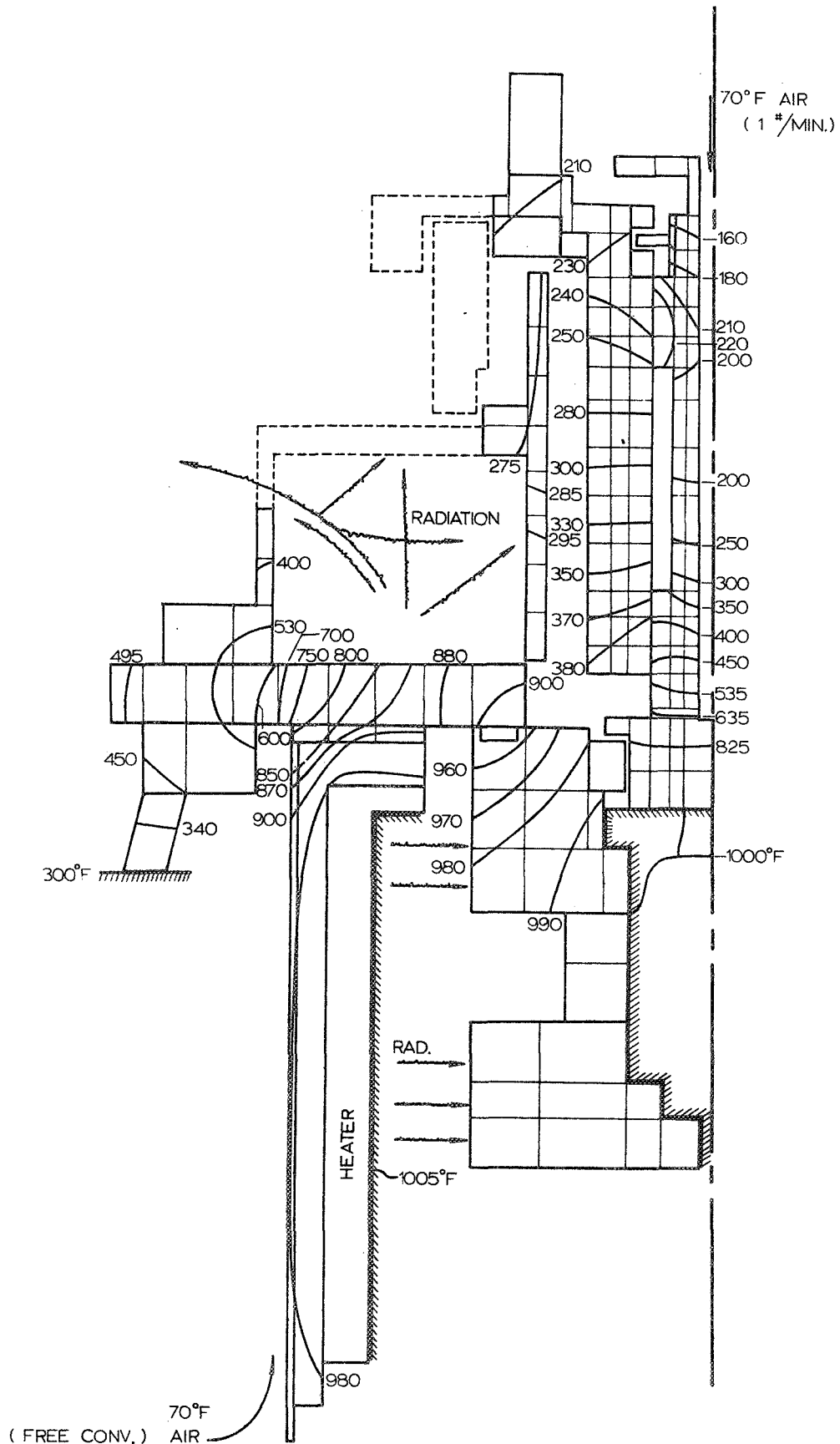
A steady-state three-dimensional heat-transfer analysis was performed on the calibration rig. This analysis served to indicate what problems would occur due to operation of the potassium journal test chamber at 1000°F.

The film-thickness calibration rig was modeled by the configuration shown in Figure 45. The areas of the calibration rig indicated in the figure by dashed lines form a transition from a round or axisymmetric geometry to rectangular forms. The true three-dimensional shape of these latter areas was used in the analysis. Besides those heat-transfer mechanisms indicated in the figures, the outer surfaces of the calibration rig were considered to be cooled by free convection to the surrounding air and by radiation to the walls of the room. The assumed boundary conditions are also shown in the figures.

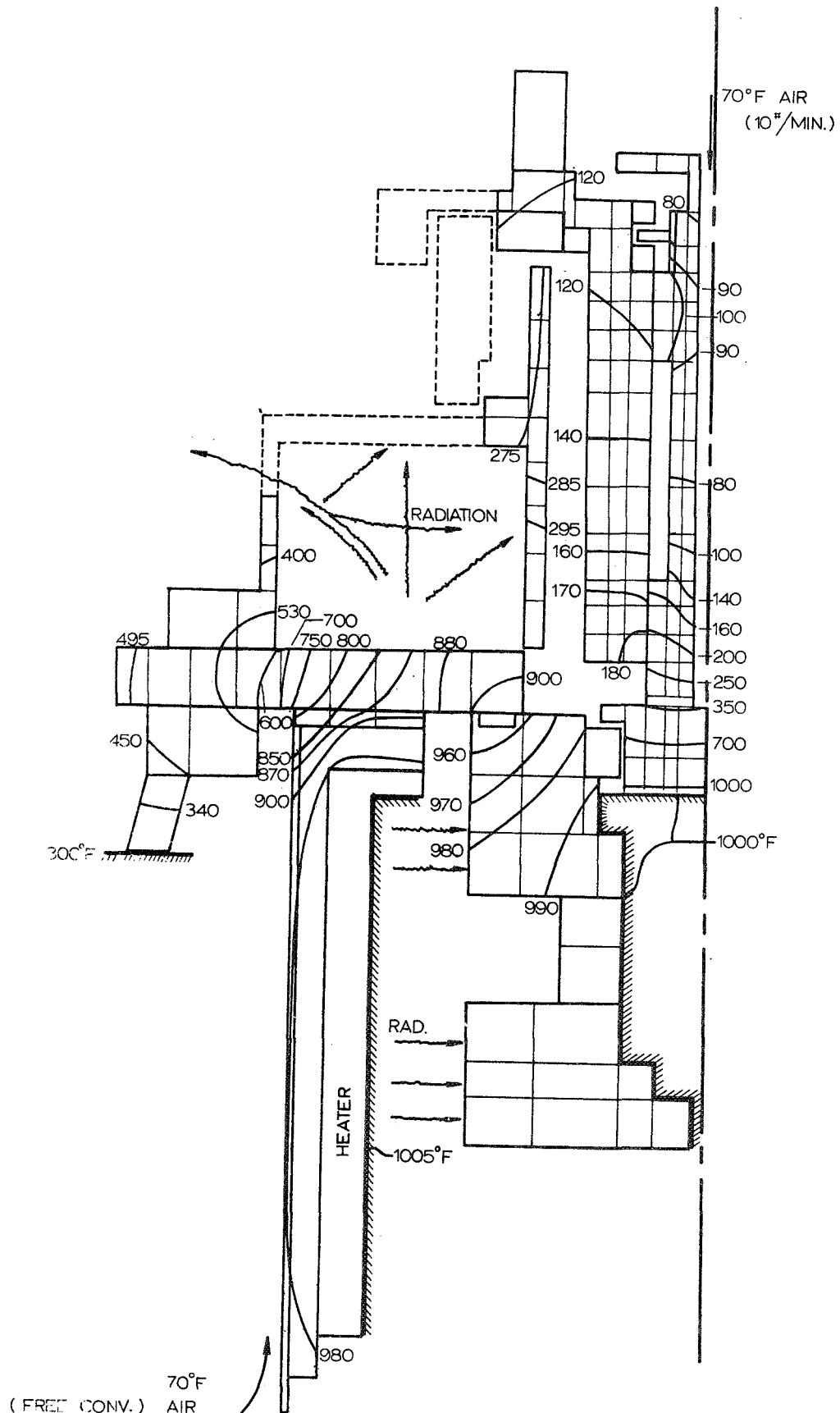
Figures 45, 46, and 47 show the isotherms in the test rig for cooling flows in the central tube of 0.5, 1, and 10 lb/min of air. The last value was taken as representative of the maximum cooling flow that could be reasonably expected with the available air supply.



PREPARED	JFG	12-67	TEMPERATURE DISTRIBUTION IN FILM THICKNESS CALIBRATION RIG - 0.5 POUND/ MINUTE COOLING FLOW	FIGURE 45
WRITTEN				
APPROVED			AirResearch Manufacturing Company of Arizona	



PREPARED	JFE	12-67	TEMPERATURE DISTRIBUTION IN FILM THICKNESS CALIBRATION RIG - 2.0 POUND/MINUTE COOLING FLOW	FIGURE 46
WRITTEN				
APPROVED			AirResearch Manufacturing Company of Arizona	



70°F
(FREE CONV.) AIR

PREPARED	JFC.	12-64	TEMPERATURE DISTRIBUTION IN FILM THICKNESS CALIBRATION RIG-10. POUND/MINUTE COOLING FLOW Air Research Manufacturing Company of Arizona	FIGURE 47
WRITTEN				
APPROVED				



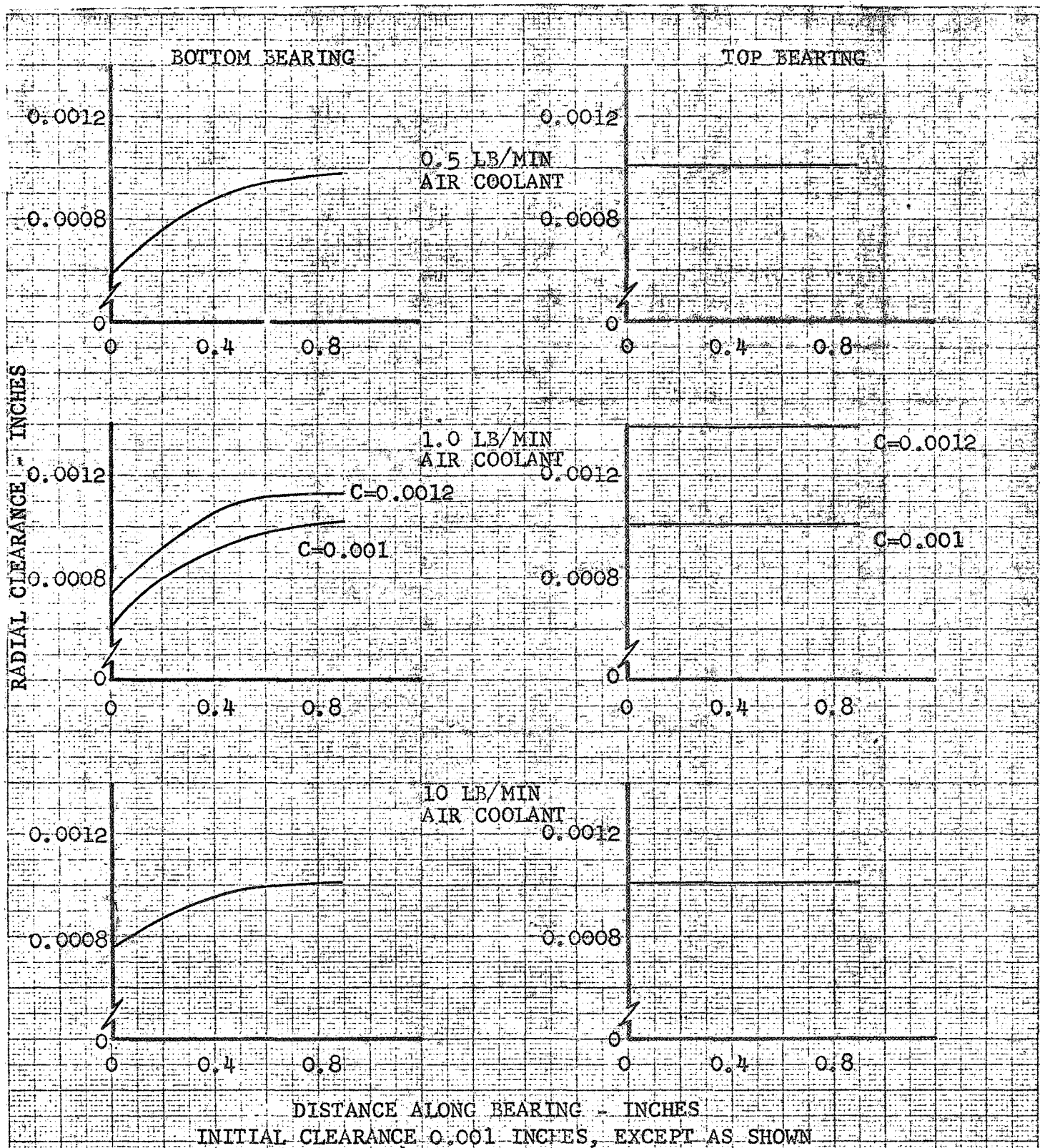
Large thermal gradients exist in the titanium base plate and the tool steel rotating shaft. By use of the temperatures shown in Figure 45, the thermal stresses in the base plate were calculated. The maximum stresses were less than one-third of the yield stress of the material at 900°F. The thermal gradients in the rotating shaft are primarily axial gradients and, thus, will not cause significant stresses because the shaft is free to expand axially.

The effect of the thermal gradients on the clearance of the gas-lubricated bearings is shown in Figure 48. The minimum clearance of the bottom bearing is decreased, and that of the top bearing is slightly increased. The middle graph (1.0 lb/min cooling flow) shows the final clearance with initial minimum clearance of 0.0010 and 0.0012 in. initial value. As might be expected, less change in the clearance occurs with the larger cooling flows in the center tube.

The temperature gradient in the adapter amount is somewhat greater than 200° initially assumed; however, the stress in the mount is sufficiently under the yield stress that no yielding should occur.

The temperature in the area of the precision dial micrometers and the linear bearings is in the range of 200°F. This temperature can cause considerable inaccuracy in the dial micrometers, depending on their materials and type of construction. The micrometers were protected by thermally insulating the mounting system.

It was concluded that no significant stress problems would occur due to thermal gradients within the test rig. However, to avoid the possibility of contact between the shaft and the gas-lubricated bearings, the cooling flow in the center tube was made as large as possible. Further, the initial clearance of the bottom bearing was increased to a minimum of 0.0012 in. due to larger journal expansion at this bearing.



CALCULATED BY	DRC	12-67	JOURNAL - BEARING CLEARANCE vs DISTANCE ALONG BEARING	FIGURE - 48
TRACED BY				
CHECKED BY			AIRESEARCH MANUFACTURING COMPANY	
APPROVED BY				
UNIT NO.				

P 5106



5.2 Calibration Rig Testing and Results

Calibration testing was done on the rig to provide additional experimental support to Task I static bench testing. First, the rig was employed to measure rotational effects on the transducer design variables empirically explored under Task I bench tests. NaK was used as the fluid film. Second, four pairs of probes were calibrated for use in the 500 hr turbodynamic endurance run utilizing potassium during calibration.

5.2.1 Calibration with NaK Film

To supplement bench tests and to evaluate rotation effect on transducer sensitivity, a standard transducer was fabricated for testing in the calibration rig.

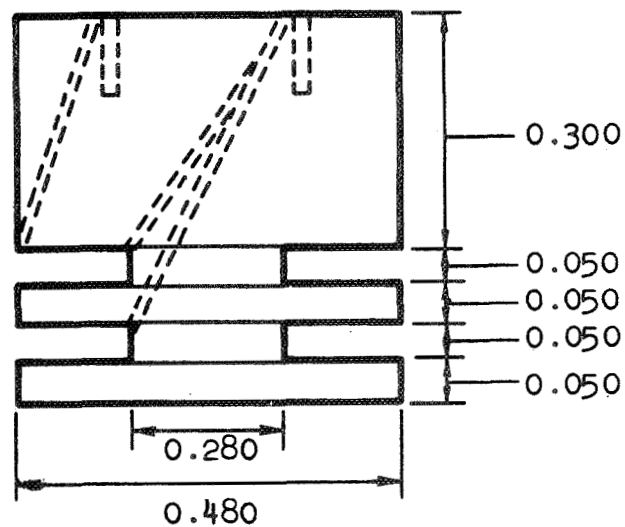
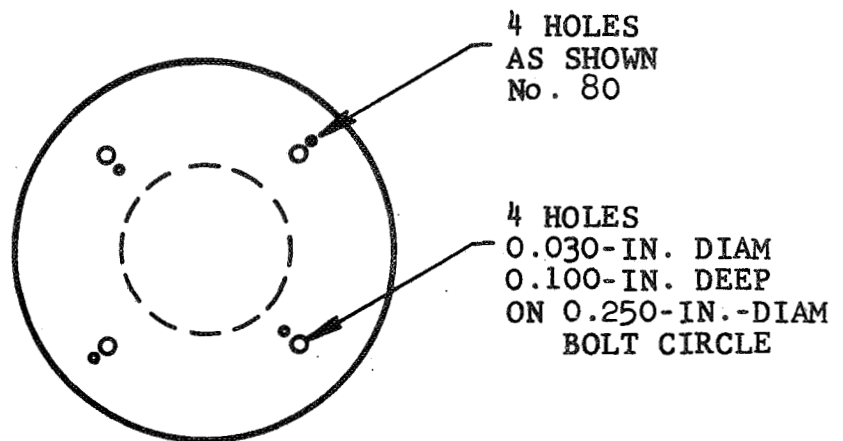
The transducer was fabricated from Grade A lava stone for the coil cores and the windings composed of No. 36 nickel-clad silver wire insulated with a Ceramicite coating. The coil form outline is shown in Figure 49. After the coils were wound with wire and electrically matched, they were placed in holders (Figure 50), which can be inserted into the instrumentation housing.

NaK was employed in the annulus between the transducer and the journal. Two sleeve materials were investigated using a 316 stainless steel housing in each case. The first test was run with a TZM sleeve on the journal--the second using an Al_2O_3 sleeve. Both tests were made with the liquid NaK film at ambient temperature. Table 3 presents a summary of data taken for each case.

A clear lucite housing was also fabricated for the calibration rig in order to fully observe the process of filling the cavity with NaK. Rotational effects on the fluid film were also observed using the clear housing.



AIRESEARCH MANUFACTURING COMPANY OF ARIZONA
A DIVISION OF THE GARRETT CORPORATION
PHOENIX, ARIZONA



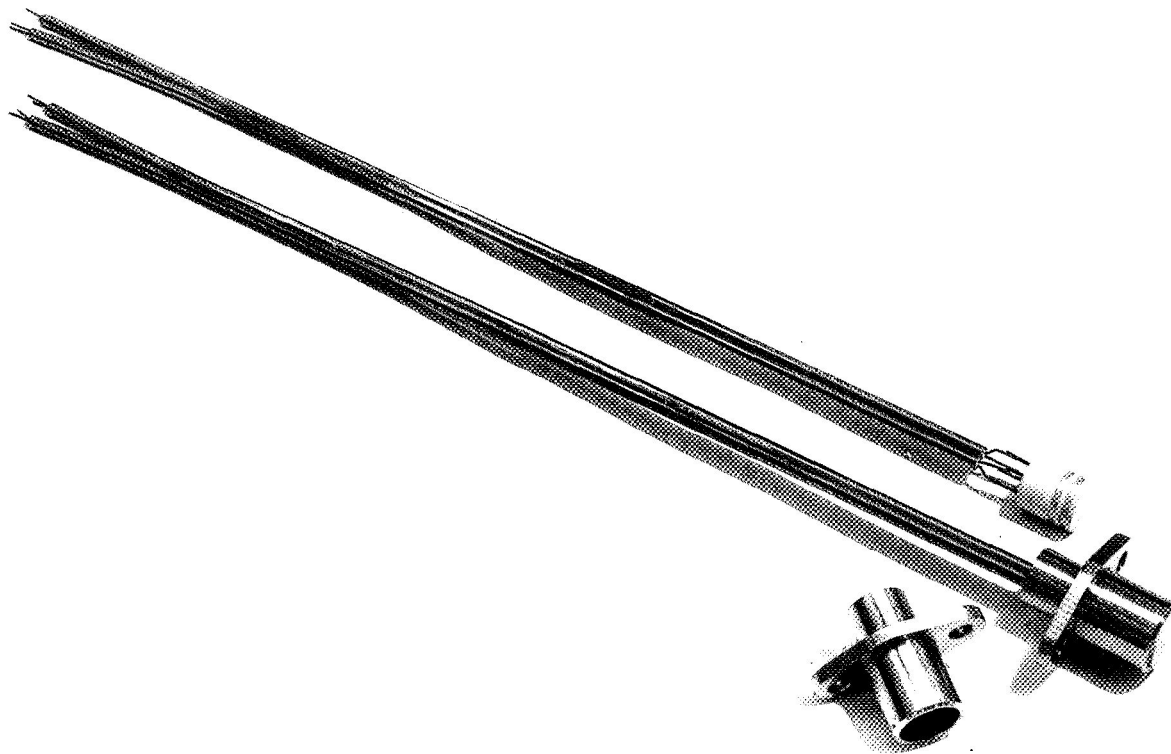
MATERIAL:
CERAMIC

COIL CONFIGURATION DRAWING

FIGURE 49



AIRESEARCH MANUFACTURING COMPANY OF ARIZONA
A DIVISION OF THE GARRETT CORPORATION



FILM THICKNESS TRANSDUCER COILS
WITH HOLDERS AND LEAD WIRES

FIGURE 50



TABLE 3
SENSITIVITY DATA FROM
SEPTEMBER 4, 1968 TO SEPTEMBER 13, 1968
Effects of Shaft Rotation on
Transducer Sensitivity
(316 Stainless Steel Housing)

TZM Sleeve Material

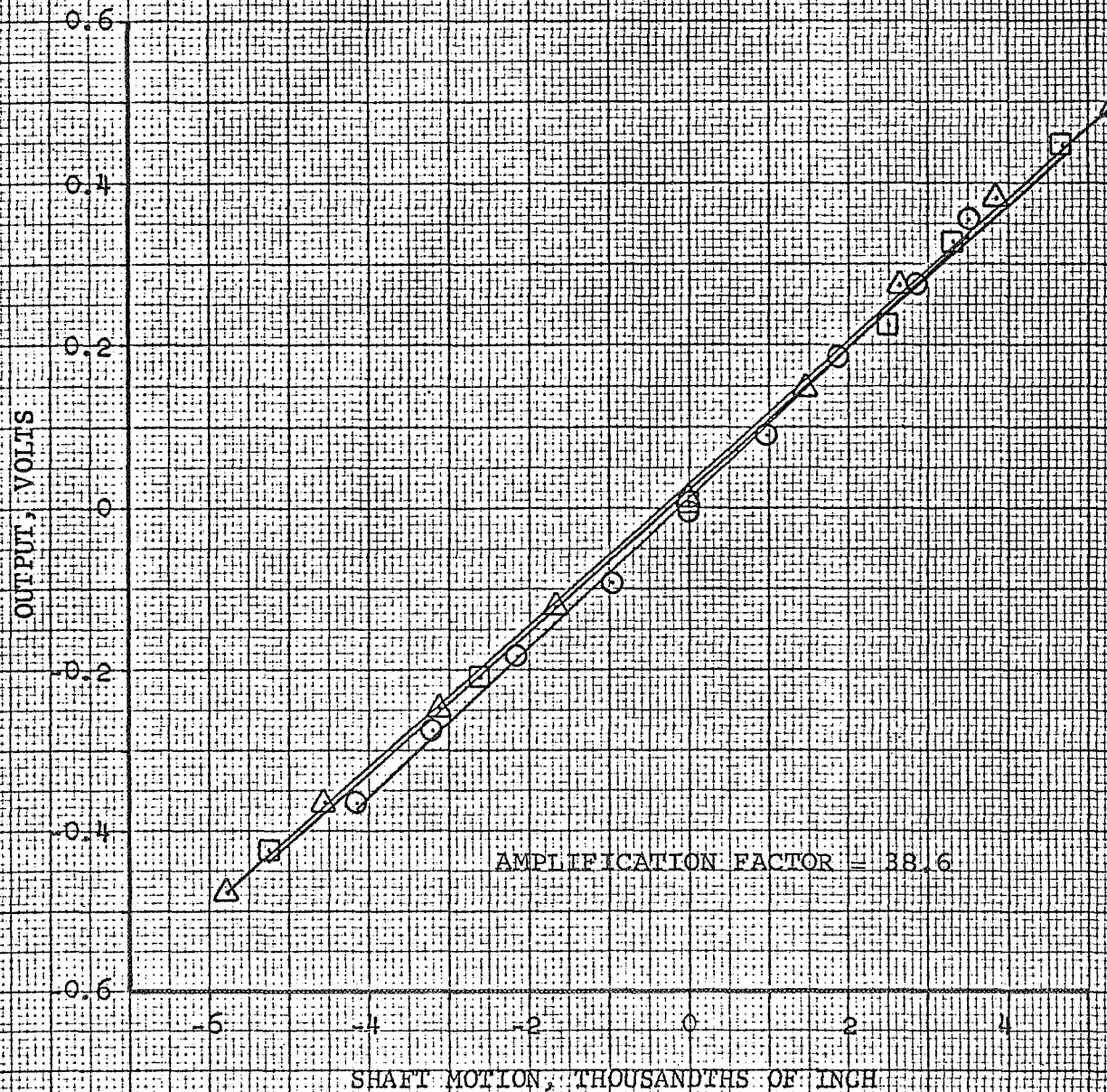
<u>Speed, rpm</u>	<u>Sensitivity, v/mil</u>
0	0.090
6,000	0.090
10,000	0.090

Al₂O₃ Sleeve Material

<u>Speed, rpm</u>	<u>Sensitivity, v/mil</u>
0	0.097
0	0.096
0	0.099
9,500	0.095
11,500	0.093
15,000	0.090

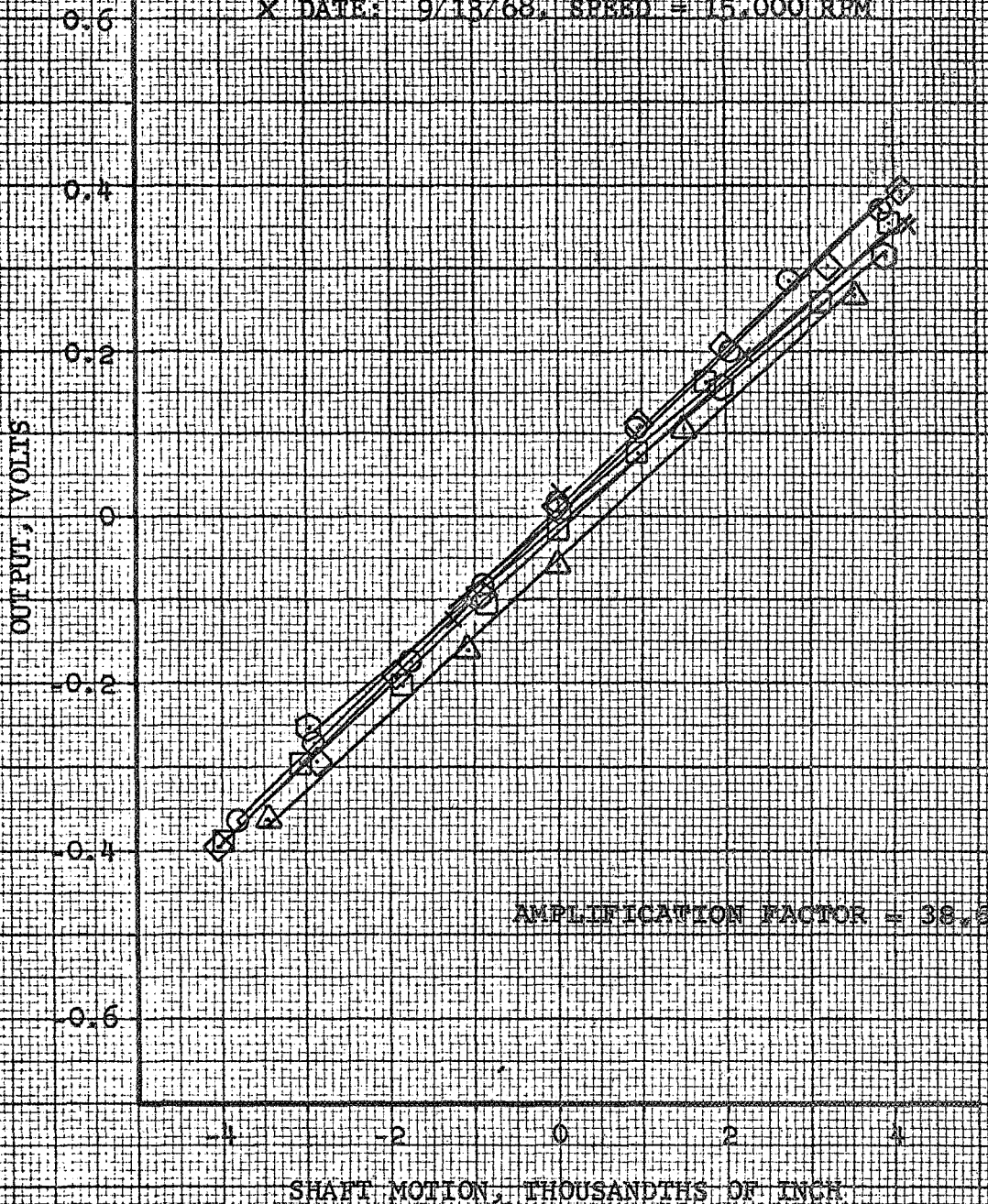
The data for the TZM and Al₂O₃ sleeves are shown on Figures 51 and 52 along with sensitivity values. It can be seen that the sensitivity as a function of speed is constant for the TZM sleeve but for the Al₂O₃ sleeve it shows a decrease as the speed is increased. This decrease may be due to a non-uniformity in the NaK film caused by the Al₂O₃ sleeve. Difficulty was experienced in filling the annulus around the Al₂O₃ sleeve because the NaK did not wet the sleeve surface.

○ DATE: 9/4/68, SPEED = 0 RPM
 □ DATE: 9/4/68, SPEED = 5000 RPM
 △ DATE: 9/4/68, SPEED = 10,000 RPM



CALCULATED BY			TZM SLEEVE		FIGURE
TRACED BY	CE	11-68	316 SS HOUSING		51
CHECKED BY			NaK FILM		
APPROVED BY			Air Research Manufacturing Company of Arizona		
UNIT NO.					

○ DATE: 9/10/68, SPEED = 0 RPM
 □ DATE: 9/11/68, SPEED = 0 RPM
 ◇ DATE: 9/13/68, SPEED = 0 RPM
 △ DATE: 9/13/68, SPEED = 9500 RPM
 ⊙ DATE: 9/13/68, SPEED = 11,500 RPM
 × DATE: 9/13/68, SPEED = 15,000 RPM



CALCULATED BY		
TRACED BY		
CHECKED BY		
APPROVED BY		
UNIT NO.		

Al₂O₃ SLEEVE
 316 SS HOUSING
 NaK FILM

FIGURE
 52

Air Research Manufacturing Company of Arizona



5.2.2 Calibration Testing with Potassium Film

Four film thickness transducer pairs were calibrated for use in the 500 hr endurance test utilizing the calibration test rig. A TZM sleeve was used on the rig shaft and the transducers were placed in a 316 stainless steel instrumentation housing. The calibration procedure was as follows: Two pairs of coils were placed in the housing. A series of measurements were made with no potassium in the rig, over a displacement range of the rig shaft of ± 0.005 in. and a temperature range to 1000°F. At the elevated temperature, random resistance increase was observed at the probe output. These failures were attributed to an increase in coil resistance with temperature and traced to the technique used to fasten the coil wires to the instrument terminal pins. This problem was remedied through techniques discussed in Section 5.2.2.1.

After the empty measurements were completed, the rig was filled with potassium and measurements performed over the temperature range of 400° to 800°F. These readings were taken in the same manner as the unfilled measurements. In all the above cases, the calibration rig was not rotating. The resulting calibrations are shown in Figure 53. Sensitivity values versus temperature are plotted for the four sets of transducers to be used in the turbine run. Only one point is shown for transducer No. 5 as higher temperature measurements were made with an incomplete potassium-fill, and unreliable sensitivity values resulted.

After static measurements were completed, rotational data were obtained on two sets of transducers over the same temperature range as the static measurements and with rotational speeds to 14,000 rpm. These data are plotted as the upper eight curves in Figure 54. In most cases the sensitivity experiences a slight decrease with both speed and temperature. This change is approximately 8 percent over the temperature range tested. Some of this change could be due to experimental error in the measurements.

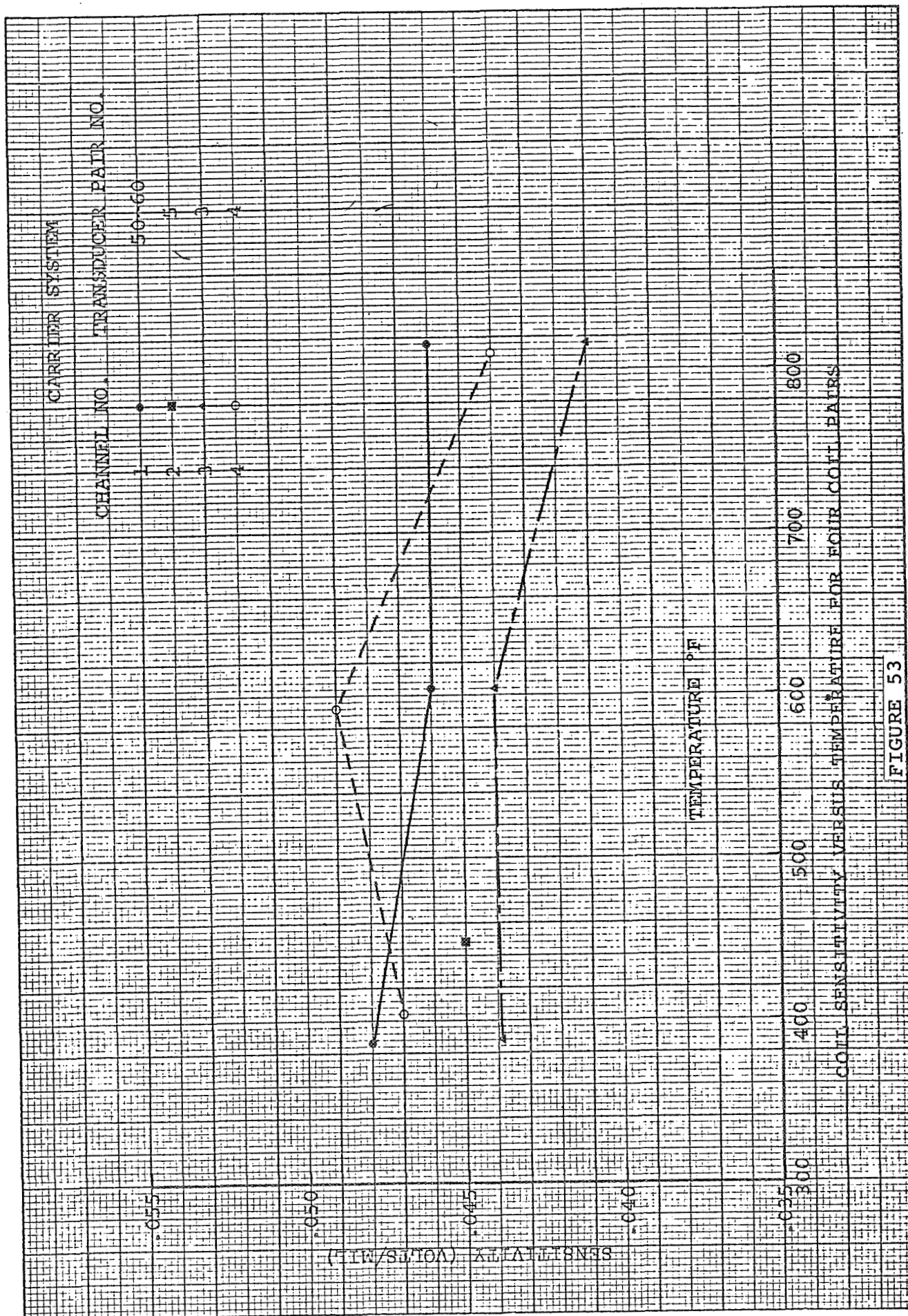


FIGURE 53

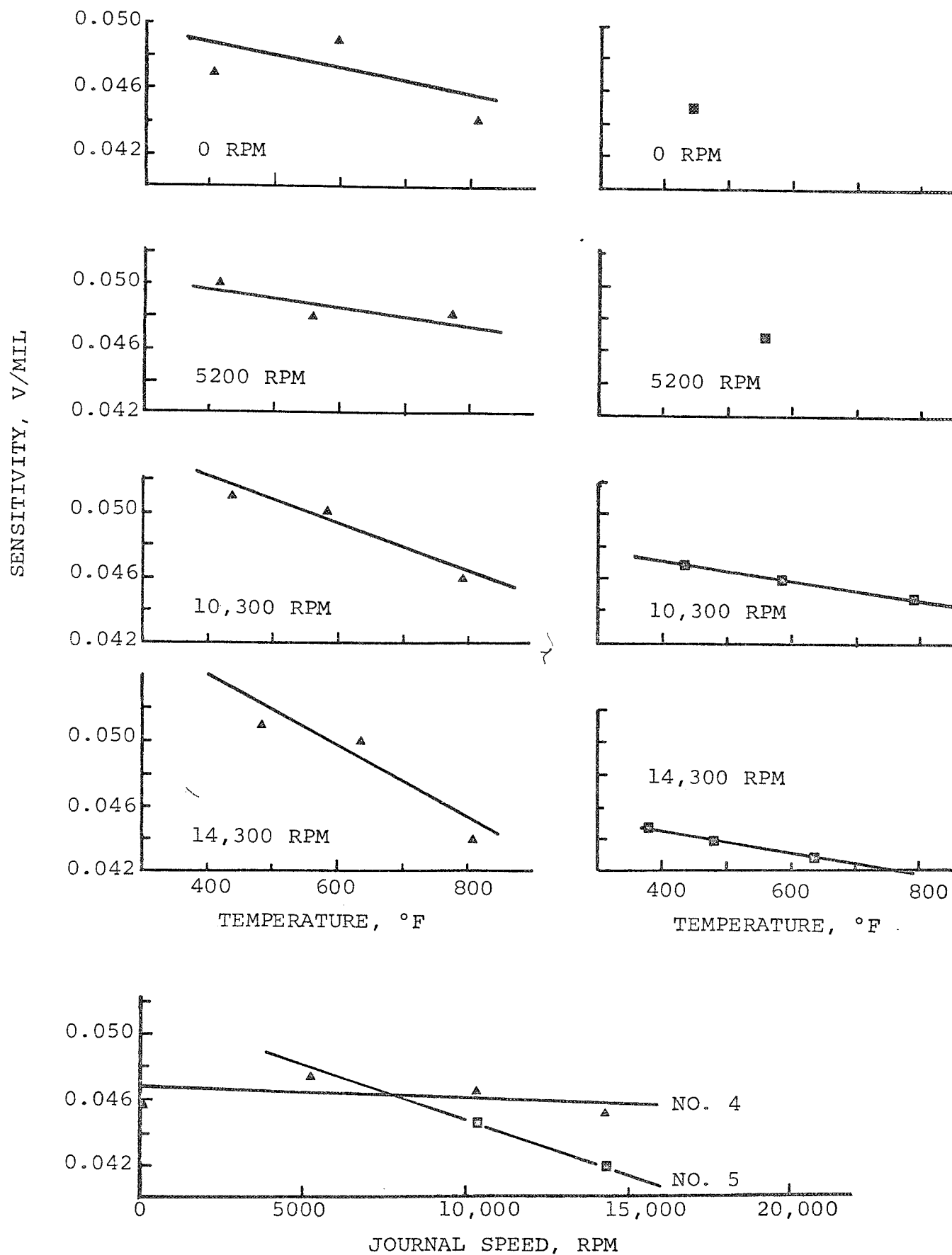


The bottom curve in Figure 54 is a cross-plot showing the change in sensitivity with speed at 800°F coil temperature for the two transducer pairs. The variation of sensitivity with speed is approximately 5 percent for transducer 4 and 15 percent for transducer 5 at 800°F. However, transducer 5 experienced a change in sensitivity during the latter stages of calibration; this may account for its large change with speed. This sensitivity change was traced to the terminal problem discussed below.

5.2.2.1 Terminal Connection Problems

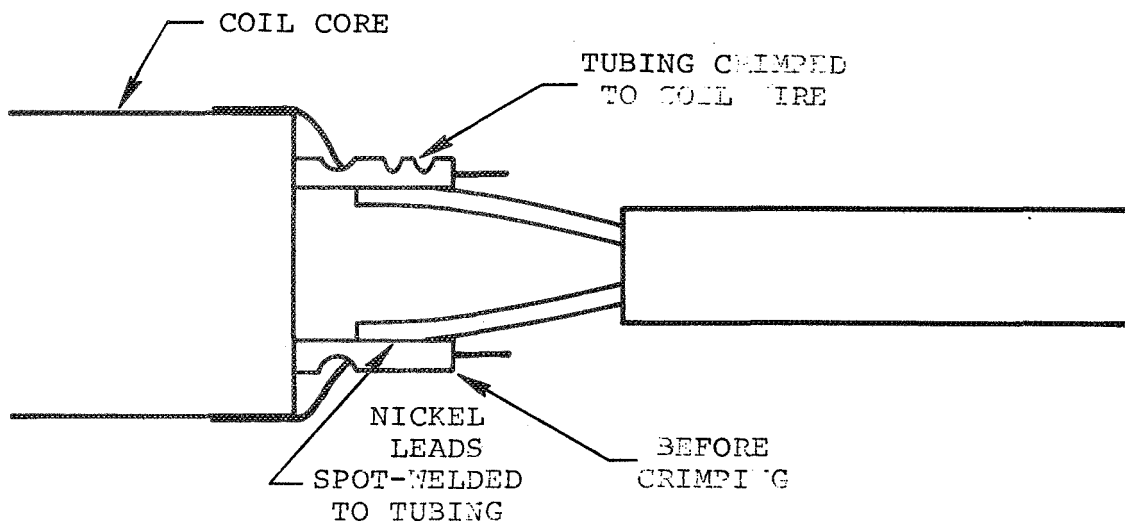
During attempts to calibrate the several sets of probes at temperatures to 1000°F, several coil failures were experienced in the temperature range from 800° to 1000°F. These failures were caused by an increase in net coil electrical resistivity. The problem has been traced to the method of making the junction between the fine (0.005-in. dia) coil wire and the relatively coarse lead wire. The technique used to fasten the coil wires to the terminal pins on the coil core is depicted in Figure 55A. After the wire is inserted into the tubing, the tubing is crimped onto the wire. During operation at temperature these joints apparently oxidize and increase the contact resistance.

Following engineering investigation of the problem and consultation with materials specialists concerning the technique, an improved method of making the wire junction was evolved. The improved method utilizes a small inert gas arc-welder to fuse the coil wire and lead wire to the terminal pin as shown in Figure 55B. The three components fuse into a compact, uniform, rounded bulb.

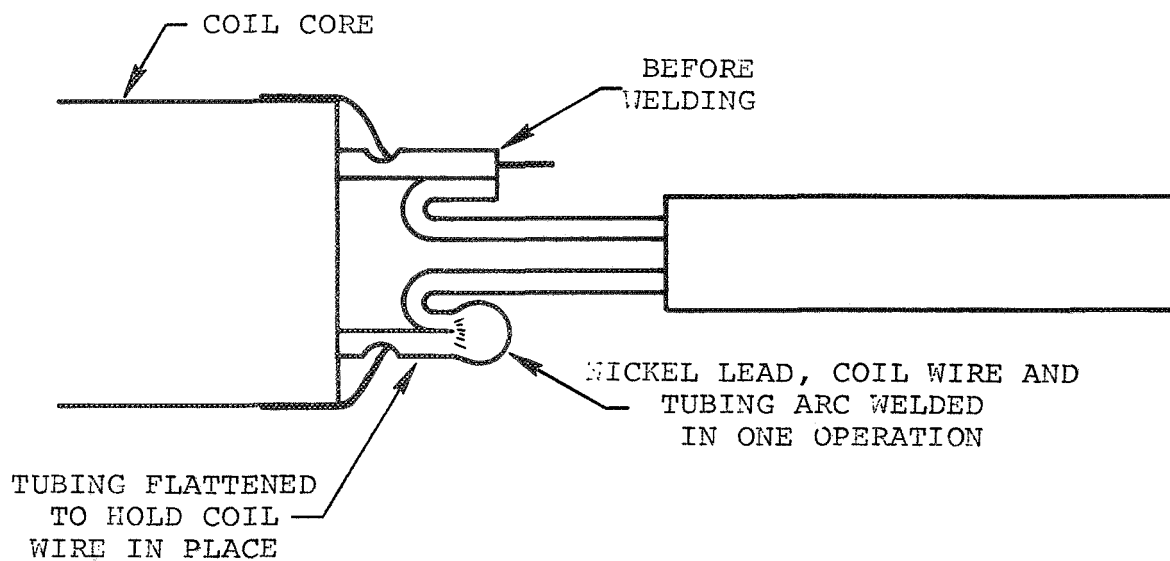


TRANSDUCER SENSITIVITY VS TEMPERATURE AND SPEED

FIGURE 54



A. OLD METHOD OF COIL WIRE TERMINATION



B. REVISED METHOD OF COIL WIRE TERMINATION

FIGURE 55



6.0 TURBODYNAMIC TESTING INCLUDING TURBINE AND LOOP MODIFICATIONS

The objective of Task IV was a 500-hour verification test of the final film-thickness-probe configuration resulting from Tasks I and II. This verification test was to be done in a potassium test loop and with use of a 24,000-rpm supersonic potassium bearing test turbine developed in 1963-1964 on the USAF/AEC SNAP 50-SPUR program. This loop had accumulated approximately 3,000 hours of operating time with vapor temperatures up to 1350°F and bearing lubricant temperatures up to 600°F. The loop was initially targeted for 1000°F bearing operation. Since all of the major loop components were in service throughout the 3,000 hours of loop operating life, any questionable loop components were refurbished as required to provide the maximum degree of reliability for the 500-hour test.

Unfortunately, the 500-hour test was not completed although transducers were fabricated, calibrated, and installed in the rig. The 500-hour test was begun, but unforeseen potassium blockages in the refurbished loop combined with a lack of funding resulted in test deferral by the program manager. The following sections detail turbine and loop modifications done to prepare for the final endurance test.

6.1 Loop Modifications

A detailed visual and past-performance inspection of the loop was made and the following components or items were identified for rework or replacement:

(a) Hot Trap

A new hot trap was fabricated.



(b) Condenser Liquid-Level Indicator

Rebuilt and reinstalled the condenser liquid-level indicator.

(c) Miscellaneous

- o All argon and vacuum lines cleaned.
- o Electrical ignition on the condenser gas burner repaired.
- o All loop sample lines (three) replaced.
- o One more layer of insulation to the emergency bearing lubricant line and tank added.
- o Checked out all trace heaters and repaired as necessary.

(d) Valves

- | | |
|-------------------------------------|---|
| 3-in. FCV-31 Turbine Outlet | - Secured in the open position |
| 2-in. FCV-1C Turbine Bypass | - Replaced the stem and bellows with available kit. |
| 2-in. FCV-1A Turbine Inlet | - New valve and actuator installed. |
| 3/4-in. FCV37 and 38 Bearing Outlet | - Procured new remotely operated valves and installed them. |



- 3/4-in. V-62 and -62 Bearing Inlet - The hand-operated valves were too big for close control of bearing flows. Therefore, procured and installed new 3/8-in. remotely operated flow-control valves.
- 3/4-in. V-60 and -61 Condenser Drain Line - Procured and installed new valves in the condenser and boiler drain lines to aid in loop drainage.

In addition, 1000°F pressure transducers were obtained to monitor potassium vapor pressure during loop operation. After incorporation of all modifications into the loop, liquid flow was established in all liquid flow circuits by a 48-hour gradual loop heating process.

On April 18, 1968, boiling was initiated, and the temperatures in the bearing feed lines were gradually increased. At approximately 2300 hours on April 18, conditions were 1390°F vapor and 950°F bearing liquid--just short of the test objective of 1390°F vapor and 1000°F bearing liquid. At approximately 2330 hours, a potassium leak was discovered that necessitated loop shutdown. The leak occurred at the tee where the bearing drain line enters the vapor line returning to the condenser. The loop was immediately blanketed with an argon cover to force drainage into the sump. The thermal shock of the cold argon entering the loop near the hot boiler discharge caused a secondary crack in the weld where those two lines join. The loop was dumped without further incident. Positive pressure was maintained on the loop at all times to prevent influx of air.

Close inspection revealed that the primary leak had occurred in the middle of the top of a forged tee. This tee was an original item of loop plumbing having been in service for about 3,000 hours of



operation prior to the leak. The secondary leak occurred at the weld where the blanketing argon supply entered the boiler discharge line.

Metallurgical examination of the failed pipe sections removed from the loop indicated the following failure modes.

- (a) Argon Inlet Tee - Failed due to excessive thermal stress resulting from shock of cool argon entering hot pipe.
- (b) Potassium Liquid-Vapor Tee - Failed due to thermal fatigue resulting from mixing of relatively cool (600° to 1000° F) potassium liquid with hot (1350° F) potassium vapor.

Both of these failed sections were replaced and presented no further problems for the duration of the program.

The argon inlet tee is used only in case of loop failure at some other point. Argon is dumped into the loop to pressurize the loop potassium into the sump and to prevent atmospheric contact with the hot potassium.

The old potassium liquid-vapor tee had been in service approximately 3000 hours with 600° F bearing discharge liquid mixing with 1350° F vapor. The present program calls for bearing lubricant temperatures above 600° F, a condition which would tend to lessen thermal fatigue on the subject tee.

Approximately 3.5 hours of boiling had taken place before the leak occurred.

Prior to the detection of the leak, no loop problems had been encountered. The bearing line flow temperatures were just short of the 1000° F objective temperature, and ample reserve heating capacity was still available to push well beyond 1000° F.



6.2 Turbine Modifications

The turbine operating in the test loop is a single-stage, impulse-bladed, partial-admission, 1350°F, saturated-vapor, supersonic turbine. A schematic cross section of the original unit is shown in Figure 56 and the unit is shown disassembled in Figure 57. The test bearings are straddle-mounted, with dynamic slinger seals separating the bearing liquid from the turbine vapor. Pivoted-pad bearings have been operated for 2,000 hours during a single run with 600°F lubricant in this unit.

The original instrumentation housings, each containing two pairs of eddy-current film-thickness-sensing coils were mounted outboard of the test bearings. Two coils mounted diametrically opposite to each other on each side of the journal shaft and two sets of coils located at 90 degrees to each other permitted detection of the change in film thickness due to motion of the shaft in any radial direction. This measurement produces the x-y coordinates of the axis of rotation of the shaft.

Unfortunately, the original design of the bearing configuration did not permit location of the film-thickness transducers in, or very close to, the bearings; therefore, the transducers were mounted several inches outboard of the bearings. The radial clearance between the journal and the transducer holder was designed to be 0.015 in. This transducer location imposed several accuracy limitations on the system. The rotating sensing surface was a piece separate from the bearing journal and required two concentricity tolerances to be included in the reading. The original housing design was such that no in-place calibration could be obtained, and failure of a coil meant test shutdown and unit disassembly.

A fundamental ground rule of the turbine modification task was to overcome these shortcomings in the original rig.



AIRESEARCH MANUFACTURING COMPANY OF ARIZONA
A DIVISION OF THE GARRETT CORPORATION

DYNAMIC BEARING RIG

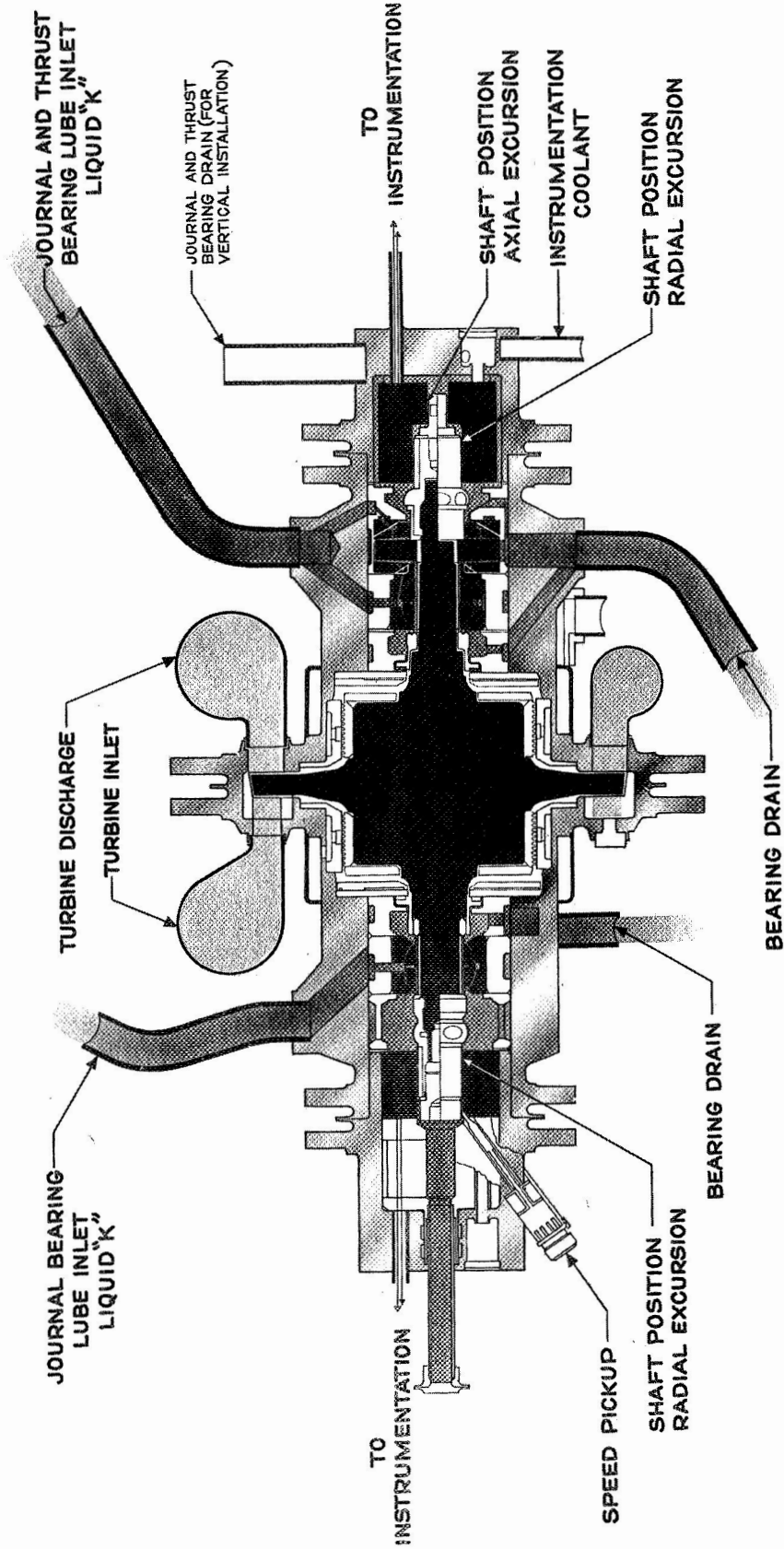
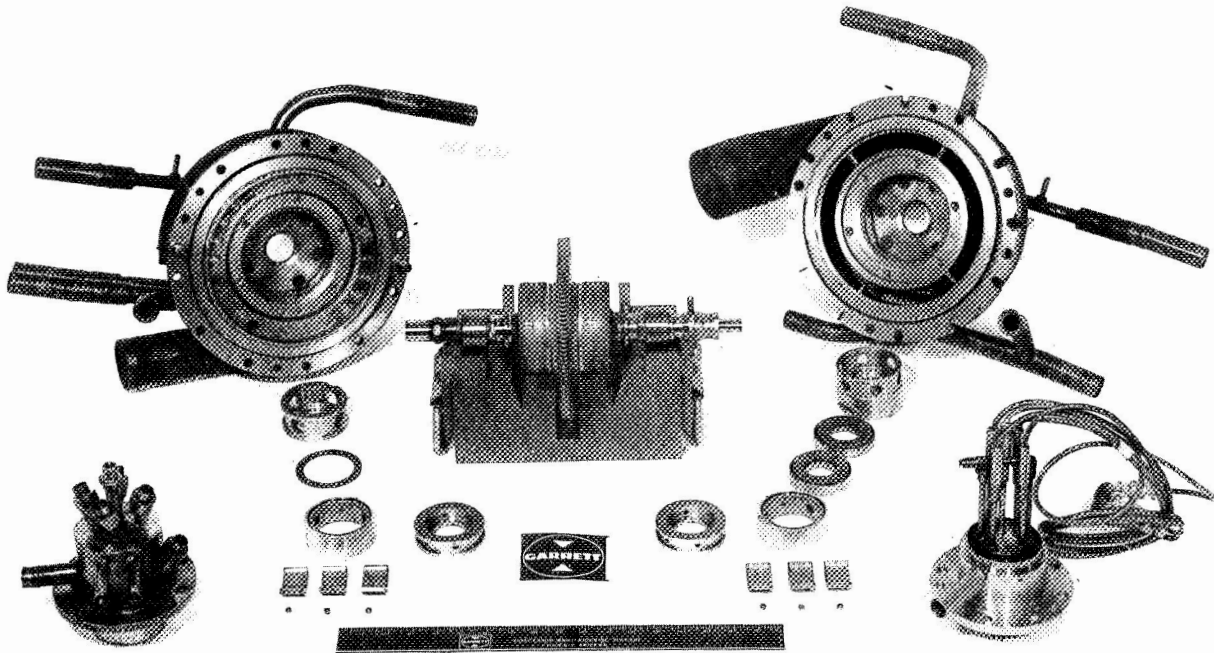


FIGURE 56



AIRESEARCH MANUFACTURING COMPANY OF ARIZONA
A DIVISION OF THE GARRETT CORPORATION



TURBODYNAMIC BEARING TEST
COMPONENTS

FIGURE 57



Initial temperature cycling from room temperature to 1200°F revealed that the original asymmetrical turbine housings changed housing bore dimension by 0.002-inch due to thermal expansion. Metallurgical investigation and thermal analysis of the required housing design revealed Haynes Stellite 31 to be a suitable material. Therefore, new housings, as symmetrical as possible, were cast and machined from this material.

6.3 Turbine Testing

6.3.1 Initial Checkout

As an initial checkout test the bearing/instrumentation test turbine was assembled and operated to 24,000 rpm using water as the bearing lubricant and plant air as the turbine working fluid. The bearings used were identical to those proven during a 2,000-hour potassium test during the earlier SNAP 50/SPUR program. No problems were encountered during this testing.

The test turbine was then disassembled, cleaned, reassembled, and hermetically sealed. The displacement and speed monitoring instrumentation may be disassembled from outside the rig. Next, the turbine was welded into the turbodynamic test loop in preparation for the 500-hour endurance test.

Following the calibration described in Section 5.2.2, the four 500-hour coil pairs were installed in the bearing/instrumentation test turbine.

On June 21, 1969, heat-up of the turbodynamic loop was initiated and soon after, potassium flow was established in the loop. It was immediately apparent that the boiler drain line was plugged. However, boiling could still be handled in the loop providing careful control was maintained in controlling flow rate into the boiler via the boiler feed pump.



AIRESEARCH MANUFACTURING COMPANY OF ARIZONA
A DIVISION OF THE GARRETT CORPORATION

On June 22, 1969, steady-state boiling conditions were established in the loop, but soon thereafter the hot trap line and one of the bearing feed lines became plugged. Repeated attempts to open these circuits met with failure and finally on June 26, 1969, further attempts were terminated and the loop was shut down.

Due to a shortage of available funding, the program was terminated at this point by the NASA program manager.

Report Distribution List

NASA-Lewis Research Center
21000 Brookpark Road
Cleveland, Ohio 44135

Attention: (See list below)

G. M. Ault (MS 3-3) - 1
R. E. English (MS 500-201) - 1
H. O. Slone (MS 500-201) - 1
J. A. Heller (MS 500-201) - 1
G. M. Kaplan (MS 500-201) - 1
V. F. Hlavin (MS 3-10) - 1
E. E. Kempke, Jr. (MS 500-201) - 10
J. E. Dilley (MS 500-309) - 1
Technology Utilization (MS 3-19) - 1
Report Control (MS 5-5) - 1
Reliability & Quality Assurance (MS 500-111) - 1
Library (MS 60-3) - 2

National Aeronautics & Space Adm.
Washington, D. C. 20546
Attention: (See list below)
NS/M. Klein - 1
RNP/P. R. Miller - 3

NASA Scientific & Technical
Information Center
P. O. Box 33
College Park, Maryland 20740
Attention: Acquisitions
Branch (SQT-34054) - 1

NASA-Marshall Space Flight Center
Huntsville, Alabama 35812
Attention: Library - 1

NASA-Flight Research Center
P. O. Box 273
Edwards, California 93523
Attention: Library - 1

U.S. Army Engineer R&D Labs
Gas Turbine Test Facility
Fort Belvoir, Virginia 22060
Attention: W. Crim - 1

NASA-Ames Research Center
Moffitt Field, California 94035
Attention: Library - 1

NASA-Goddard Space Flight Center
Greenbelt, Maryland 20771
Attention: Library - 1

NASA-Langley Research Center
Langley Station
Hampton, Virginia 23365
Attention: Library - 1

Jet Propulsion Laboratory
4800 Oak Grove Drive
Pasadena, California 91103
Attention: Library - 1
Lance Hays - 1

NASA-Manned Spacecraft Center
Houston, Texas 77058
Attention: Library - 1

AEC Headquarters
Space Nuclear Systems Division
Germantown, Maryland 20545
Attention: C. Johnson - 2

U.S. Atomic Energy Commission
Technical Information Service
Ext.
P. O. Box 62
Oak Ridge, Tennessee 37831

Air Force Systems Command
Aeronautical Systems Division
Wright-Patterson Air Force Base,
Ohio 45438
Attention: Library - 1

Brookhaven National Laboratory
Associated Universities, Inc.
Upton, Long Island, N.Y. 11973
Attention: Dr. O.E. Dwyer

Bureau of Naval Weapons
Department of the Navy
Washington, D. C. 20025
Attention: Code RAPP - 1

Institute for Defense Analyses
400 Army-Navy Drive
Arlington, Virginia 22202
Attention: Library - 1

Office of Naval Research
Department of the Navy
Washington, D. C. 20025
Attention: Dr. Ralph Roberts - 1

Naval Facilities Engineering Command
P. O. Box 610
Falls Church, Virginia 22046
Attention: Library - 1

Bureau of Ships
Department of the Navy
Washington, D. C. 20025
Attention: L. Graves - 1

University of Virginia
School of Engineering &
Applied Science
Dept. of Mechanical Engineering
Charlottesville, Virginia 22903
Attention: Dr. E.J. Gunter, Jr. - 1

University of Maryland
College of Engineering
College Park, Maryland 20740
Attention: M. E. Talast - 1

Massachusetts Institute of Tech.
Cambridge, Massachusetts 02139
Attention: Library - 1

Battelle Memorial Institute
505 King Avenue
Columbus, Ohio 43201
Attention: Library - 1

Power Information Center
University of Pennsylvania
3401 Market Street, Room 2107
Philadelphia, Pennsylvania 19104

Acrospace Corporation
2350 East ElSegundo Blvd.
ElSegundo, California 90045
Attention: H.T. Sampson - 1

AVCO-Bay State Abrasives Division
Westboro, Massachusetts 01581
Attention: George Herterick - 1

U.S. Naval Boiler and Turbine Lab.
Philadelphia, Pennsylvania 19100
Attention: Library - 1

Aerojet-General Corporation
Von Karman Center
Azusa, California 91702
Attention: Library - 1

Bendix Research Labs. Division
Detroit, Michigan 48232
Attention: Library - 1

Borg-Warner Corporation
Pesco Products Division
24700 North Miles Road
Bedford, Ohio 44014
Attention: Library - 1

Continental Aviation &
Engineering Corporation
12700 Kercheval Avenue
Detroit, Michigan 48215
Attention: Library - 1

The Boeing Company
Aero-Space Division
Box 3707
Seattle, Washington 98124
Attention: Library - 1

Curtiss-Wright Corporation
Wright Aero Division
Main and Passaic Streets
Woodridge, New Jersey 07075
Attention: Library - 1

Consolidated Controls Corp.
15 Durant Avenue
Bethel, Connecticut 06801
Attention: Library - 1

Garrett Corporation
 AiResearch Manufacturing Company
 402 South 36 Street
 Phoenix, Arizona 85034
 Attention: R. A. Rackley - 1

Garrett Corporation
 AiResearch Manufacturing Company
 9851 Sepulveda Blvd.
 Los Angeles, California 90009
 Attention: M. G. Coombs - 1

General Dynamics Corporation
 16501 Brookpark Road
 Cleveland, Ohio 44142
 Attention: Library - 1

General Electric Company
 Missile & Space Vehicle Dept.
 3198 Chestnut Street
 Philadelphia, Pennsylvania 19104
 Attention: Library - 1

General Electric Company
 Lynn, Massachusetts 01905
 Attention: Library - 1

General Electric Company
 Mechanical Technology Laboratory
 R&D Center
 Schenectady, New York 12301
 Attention: Library - 1

General Electric Company
 Flight Propulsion Laboratory Div.
 Cincinnati, Ohio 45215
 Attention: Library - 1

General Electric Company
 Large Steam Turbine-Generator Dept.
 Schenectady, New York 12301
 Attention: Mr. E. H. Miller

General Motors Corporation
 Indianapolis, Indiana 46206
 Attention: Library - 1

Franklin Institute Research
 Laboratories
 Benjamin Franklin Parkway
 at 20th Street
 Philadelphia, Pennsylvania 19103
 Attention: Library - 1

Lear Siegler, Inc.
 3171 S. Bundy Drive
 Santa Monica, California 90406
 Attention: Library - 1

Lockheed Missiles & Space Co.
 P. O. Box 504
 Sunnyvale, California 94088
 Attention: Library - 1

McDonnell-Douglas Corporation
 Space Station Office
 Huntington Beach, California
 Attention: R. Gervais - 2

McDonnell-Douglas Corporation
 Lambert Field
 St. Louis, Missouri 63166
 Attention: Library - 1

North American Rockwell Corp.
 Space Division
 12214 Lakewood Blvd.
 Downey, California
 Attention: A. Nussberger - 1
 C. Gould - 1

North American Rockwell
 Atomic International Division
 P. O. Box 309
 8900 DeSota Avenue
 Canoga Park, California 91304
 Attention: T. A. Moss - 2
 Director, Liquid Metal Informa-
 tion Center - 1

Northern Research & Engineering Co.
 219 Vassar Street
 Cambridge, Massachusetts 02139
 Attention: Library - 1

Oak Ridge National Laboratory
P. O. Box Y
Oak Ridge, Tennessee 37831
Attention: Dr. Arthur Frass.

Mechanical Technology, Inc.
968 Albany-Shaker Road
Latham, New York 12110
Attention: Library - 2

Solar Division of International
Harvester
2200 Pacific Highway
San Diego, California 92112
Attention: Library - 1

Sunstrand Denver
2480 West 70th Avenue
Denver, Colorado 80221
Attention: Library - 1

TRW Systems Division
One Space Park
Redondo Beach, California 90278
Attention: Library - 1

Union Carbide Corporation
Linde Division
P. O. Box 44
Tonawanda, New York 14152
Attention: Library - 1

United Aircraft Research Lab.
East Hartford, Connecticut 06108
Attention: Library - 1

Westinghouse Electric Corporation
Astronuclear Laboratory
P. O. Box 10864
Pittsburgh, Pennsylvania 15236
Attention: Library - 1
W. D. Pouchot - 1

Westinghouse Electric Corp.
Steam Division
Lester Branch, P. O. Box 9175
Philadelphia, Pa. 19113
Attention: W. G. Steltz

Williams Research
Walled Lake, Michigan 48088
Attention: Library - 1

General Electric Company
Nuclear Systems Programs
P. O. Box 15132
Cincinnati, Ohio 45215
Attention: D. F. Huebner - 2